



# **NUMERICAL VALIDATION OF THE FIRE RESISTANCE OF PARTITION WALLS**

**Aymen Ben Hmida**

Final report of the thesis presented to the Université libre de Tunis - ULT  
Polytechnic Institute of Bragança – IPB For the fulfilment of the requirements  
for a Master's Degree in Construction Engineering

Supervised by:

Prof. Paulo Alexandre Gonçalves Piloto

Prof. Issam Khezami

**Bragança**

**December 2022**





# **NUMERICAL VALIDATION OF THE FIRE RESISTANCE OF PARTITION WALLS**

**Aymen Ben Hmida**

Final report of the thesis presented to the Université libre de Tunis - ULT  
Polytechnic Institute of Bragança – IPB For the fulfilment of the requirements  
for a Master's Degree in Construction Engineering

Supervised by:

Prof. Paulo Alexandre Gonçalves Piloto

Prof. Issam Khezami

**Bragança**

**December 2022**



## **Acknowledgement**

First of all, I would like to thank the Université Libre de Tunis (ULT) family for their trust and allowing me to get enrolled in this double diploma program in construction engineering. As well as the Polytechnic Institute of Bragança (IPB) which welcomed me and allowed me to expand my horizons.

Special thanks to Prof. Paulo Piloto for his supervision, guidance, his valuable advice and without whom the different tracks explored in this work would never have been. Also special thanks to Prof. Iassam Khezami for his confidence and his motivation.

In closing, I would like to express my gratitude to my parents who believed in me, my sister who supported me during the master thesis and all the persons that are close to my heart for their encouragement and support.



# ABSTRACT

This work investigates the impact of fire in non-loadbearing Light Steel Frame (LSF) walls.

Numerical validation and a set of parametric analyses are carried out using ANSYS Multiphysics software in order to show the impact of structural stud's space, cavity thickness, the effect of the protective layer, and the effect of insulating material in the cavity. The results show that the cavity insulation has the greatest influence on fire resistance, followed by the increase of the number of gypsum plasterboards of the protection layer. Also the decreasing of the studs spacing has improved the time of the resistance of walls under fire.

**Keywords:** Fire resistance LSF Walls, Insulation, Finite element method, Experimental tests





# Resumé

Ce travail étudie l'impact du feu dans les murs non porteurs à ossature légère en acier (LSF). Une validation numérique et un ensemble d'analyses paramétriques sont réalisés à l'aide du logiciel ANSYS®Multiphysics afin de montrer l'impact de l'espace du montant structurel, de l'épaisseur de la cavité, de l'effet de la couche protectrice et de l'effet du matériau isolant dans la cavité. Les résultats montrent que l'isolation de la cavité a la plus grande influence sur la résistance au feu, suivie par l'augmentation du nombre de plaques de plâtre de la couche de protection et aussi la diminution de l'espacement entre les montants a amélioré la durée de la résistance des murs sous le feu.

**Mots clés :** Résistance au feu Murs LSF, Isolation, Méthode des éléments finis, Essais expérimentaux



# RESUMO

Este trabalho investiga o impacto do fogo em paredes de estrutura de aço leve não portante (LSF).

A validação numérica e um conjunto de análises paramétricas são realizadas utilizando o software ANSYS Multiphysics a fim de mostrar o impacto do espaço estrutural entre os montantes, a espessura da cavidade, o efeito da camada protetora, e o efeito do material isolante na cavidade. Os resultados mostram que o isolamento da cavidade tem a maior influência na resistência ao fogo, seguido pelo aumento do número de placas de gesso da camada de proteção, também a diminuição do espaçamento dos montantes melhorou o tempo da resistência das paredes sob fogo.

**Palavras-chave:** Paredes LSF resistentes ao fogo, Isolamento, Método dos elementos finitos, Ensaio experimentais

# Content

1	Introduction .....	19
1.1	Objectives .....	19
1.2	LSF Constructions .....	20
1.3	Thesis outline.....	21
2	State of the art .....	23
2.1	Experimental tests.....	23
2.2	Numerical tests .....	25
3	Fire and heat transfer.....	28
3.1	Origin of fire .....	28
3.2	Heat Transfer Theory.....	30
3.3	Boundary Condition .....	34
3.4	Fire rating .....	35
3.5	Behaviour of LSF Walls in Fire .....	37
4	Mathematical model.....	38
4.1	The finite element methods .....	38
4.1.1	ANSYS Multiphysics .....	39
4.1.2	Finite element type (Element type plane 55) .....	40
4.2	The materials properties .....	41
4.2.1	Gypsum Plasterboard .....	42
4.2.2	Rockwool .....	42
4.3	Numerical validation .....	43
4.3.1	Results discussion .....	48
5	Parametric study.....	51
5.1	Parameters .....	51
5.2	Results .....	53
5.3	Discussion of the Results.....	64
6	Conclusion.....	68
	References .....	69
	Appendix .....	72



# List of figures

Figure 1: LSF Construction.....	20
Figure 2: Composition of LSF wall [1].....	21
Figure 3: Standard Fire Curve [13].....	30
Figure 4: Boundary Conditions.....	34
Figure 5: Average bulk temperature versus time.....	35
Figure 6: Plane 55 [18].....	40
Figure 7: Thermal properties of steel.....	41
Figure 8: Thermal properties of gypsum.....	42
Figure 9: Thermal properties of Rockwool.....	43
Figure 10: The location of the thermocouples.....	44
Figure 11: The finite element mesh of the specimen 1.....	44
Figure 12: The finite element mesh of the zoom of the specimen 1.....	44
Figure 13: Specimen 1 - Average temperature results.....	45
Figure 14: Average and maximum temperature on the unexposed side.....	45
Figure 15: The location of the thermocouples.....	46
Figure 16: The finite element mesh of the specimen 2.....	46
Figure 17: he finite element mesh of the zoom in the specimen 2.....	47
Figure 18: Specimen 2 - Average temperature results.....	47
Figure 19: Average and maximum temperature on the unexposed side.....	48
Figure 20: Specimen 13 - Average temperature results.....	53
Figure 21: Specimen 13 - Average and maximum temperature on the unexposed side.....	54
Figure 22: Numerical results for Specimen 13, t=240min.....	54
Figure 23: Specimen 14 - Average temperature results.....	55
Figure 24: Specimen 14 - Average an maximum temperature on the unexposed side.....	55
Figure 25: Numerical results for Specimen 14, t=300min.....	56
Figure 26: Specimen 15 - Average temperature results.....	56
Figure 27: Specimen 15 - Average an maximum temperature on the unexposed side.....	57
Figure 28: Numerical results for Specimen 15, t=300min.....	57
Figure 29: Specimen 16 - Average temperature results.....	58
Figure 30: Specimen 16 - Average an maximum temperature on the unexposed side.....	59
Figure 31: Numerical results for Specimen 16, t=300min.....	59
Figure 32: Specimen 19 - Average temperature results.....	60
Figure 33: Specimen 19 - Average an maximum temperature on the unexposed side.....	60
Figure 34: Numerical results for Specimen 19, t=300min.....	61
Figure 35: Specimen 25 - Average temperature results.....	61
Figure 36: Specimen 25 - Average an maximum temperature on the unexposed side.....	62
Figure 37: Numerical results for Specimen 25, t=300min.....	62
Figure 38: Specimen 37 - Average temperature results.....	63
Figure 39: Specimen 37 - Average an maximum temperature on the unexposed side.....	63
Figure 40: Numerical results for Specimen 37, t=300min.....	64

## List of tables

Table 1: Relative error for experimental and numerical tests .....	49
Table 2: Results of the root means square error (RMS).....	50
Table 3: Configurations of all the specimens to examine .....	51
Table 4: Influence of the material and number of layer .....	65
Table 5: Influence of the thickness of gypsum layer .....	65
Table 6: Influence of stud spacing .....	66
Table 7: Influence of cavity thickness due to the dimension of the stud .....	66
Table 8: Influence of adding cavity insulation.....	67

# Notation

## Latin Lower Case Letters

$g_y$  Gravity acceleration in direction  $y$

$\dot{h}$  Heat flux [ $W/m^2$ ]

$\dot{h}_{net}$  Net heat flux [ $W/m^2$ ]

$\dot{h}_{c,x}$  One-dimensional conduction heat flux

$\dot{h}_{net,c}$  Net convection heat flux

$\dot{h}_{net,r}$  Net radiation heat flux between any two grey surfaces

$p$  Pressure [MPa]

$t$  Time [s]

$n$  direction at the surface boundary

## Latin Upper Case Letters

$C_p$  Specific heat at constant pressure [kJ/(kg K)]

$C$  Volumetric heat capacity

$E_{fi,d}$  Design effect of actions for the fire design situation [adimensional]

$K_{xx,yy,zz}$  Thermal conductivity in  $x,y,z$  directions [W/mK]

$R_{fi,d,t}$  Fire design resistance of the steel member at time  $t$



$T_y$	Viscous Loss Terms
$T_o$	Ambient temperature [ $^{\circ}C$ ]
$\vec{v}$	Velocity vector [m/s]
$T$	Temperature
$\dot{T}$	First temperature derivative with respect to time
$T_m$	Material surface temperature
$T_g$	Gas Temperature in the Vicinity of the Fire Exposed Member [ $^{\circ}C$ ]
$T_m$	Surface Temperature of the Member [ $^{\circ}C$ ]

### **Greek Letters**

$\alpha_c$	Coefficient of heat transfer by convection [W/kgK]
$\epsilon_m$	Surface Emissivity of Member [adimensional]
$\epsilon_f$	Emissivity of the fire [adimensional]
$\sigma$	Stephan Boltzmann constant = $5,67 \times 10^{-8}$ [W/m <sup>2</sup> k <sup>4</sup> ]
$\lambda$	Thermal conductivity [kW/(m $^{\circ}C$ )]
$\rho$	Density [kg/m <sup>3</sup> ]
$\rho_0$	Specific Mass [kg/m <sup>3</sup> ]

## **Acronyms**

<b>CFS</b>	Cold-formed Steel
<b>E</b>	Integrity fire resistance criterion
<b>FEM</b>	Finite Element Method
<b>FRR</b>	Fire Resistance Rating
<b>I</b>	Insulation fire resistance criterion
<b>LSF</b>	Light Steel Framing
<b>R</b>	Load-bearing fire resistance criterion
<b>AS</b>	Australian standard

# Chapter 1

## 1 Introduction

From the period of primitive humans began by constructing shelters which last only few months. Gradually as human being started residing for longer periods in one place they begin to improve their shelters and look for more durable structures. In fact, their challenge was to use more durable materials in order to have better buildings that can last for hundreds of years.

However, these constructions have a main goal to provide protection for human against animals and climate changes, little by little these goals were improved such as artistic expressions, religious representations, and now the current constructions have as a principle to be aesthetically pleasant.

### 1.1 Objectives

This work presents the numerical validation regarding the fire resistance of non-loadbearing LSF walls, using different configurations and materials. Several parameters are investigated: different panel thicknesses, characterization of their thermal behaviour and different types of steel sections. One solution method has been used in order to determine the fire resistance:

The advanced calculation method, is based on hybrid-2D finite element model to determine the temperature field of the LSF and all the other materials involved in the simulation.

Special numerical tasks aim to develop an accurate advanced calculation method for predicting fire resistance using a finite element model and ANSYS Multiphysics. The 2D finite element model validation is presented.

## 1.2 LSF Constructions

Over the last century, steel has been used in many applications around the construction industry. The growth of LSF systems is expected to increase the demand for economical solutions where specific performance is required, such as in the area of fire resistance.

Usually, when one mentions a steel framing construction one think about heavy welded rusted frames of a skyscraper or a warehouse in an industrial area.

Light steel frame (LSF) has been developed because of its lightweight characteristics see Figure 1. Steel is recycled, dimensionally stable, and easy to install, which has evolved into a modern lightweight metal framing concept that we can use in more familiar configurations in residential and commercial buildings as well.



Figure 1: LSF Construction

These walls are constructed from a cold-formed galvanized steel frame with studs, tracks, and noggings sheathed on both sides with self-drilling screws at regular intervals.

Figure 2 represents a typical LSF wall where the cavity in the wall could be empty or filled with insulation such as Rockwool, glass fiber, or cellulose fiber.

Cold-formed steel is lightweight and has a high strength-to-weight ratio.

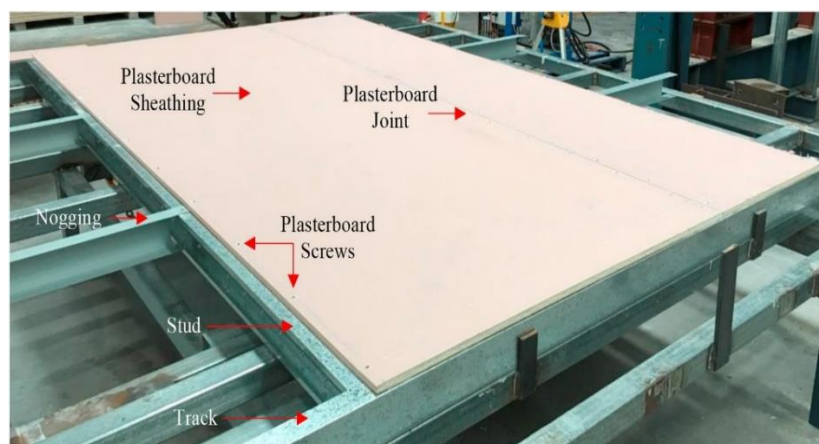


Figure 2: Composition of LSF wall [1]

### 1.3 Thesis outline

The second chapter discusses the state of the art, which is a look back at the research on the fire resistance of LSF structures.

The third chapter defines the main characteristics of the fire as well as the fire resistance structure. It also presents the most often used standard curves that measure this phenomenon and the heat transfer theory.

The fourth chapter presents the mathematical model, the material properties of various materials used in the simulation and presents the numerical models validated by the experimental tests.

The fifth chapter presents the parametric analysis, in which tests are performed by changing the number and width of layers, also with different stud spacing and cavity thickness and by adding insulation materials in the cavity followed by a result discussion.

The last chapter gives the conclusions about this work.

# Chapter 2

## 2 State of the art

In this section, recent related works on LSF wall panels under fire will be discussed on a temporal basis.

The research results will be presented, taking into account the experimental and numerical studies of the fire resistance of LSF wall panels, including the behaviour of all components.

### 2.1 Experimental tests

Sakumoto et al [2] developed an experimental study in 2003 to test the fire resistance of walls constructed with galvanized LSF. The authors concluded that protection layers made of plywood, gypsum boards, and other materials depend mostly on how well the gypsum boards protect against heat.

In 2006, Kodur et al [3] investigated the parameters influencing the fire resistance of loadbearing walls. In all, 14 wall assemblies were evaluated, with plasterboard on the exposed and sheltered sides and glass, rock, and dry brown cellulose fibre insulation in the cavity. The results demonstrated that the insulation type and quantity of plasterboards had a significant impact on fire resistance.

In 2012, Kolarkar et al [4] proposed an innovative composite stud panel based on an external insulation layer between the plasterboards instead of cavity insulation. Test results showed that their composite stud wall systems outperformed traditional stud wall systems in terms of thermal performance as well as the fire resistance is significantly higher.

In 2017 Ariyanayagam et al [5] described full-scale fire experiments using non load-bearing LSF wall panels constructed of thin-walled steel studs and coated with gypsum plasterboard and calcium silicate boards. The fire test findings were utilized to compare the fire performance of LSF walls lined with standard gypsum plasterboard, calcium silicate board, and magnesium oxide boards. They demonstrated that walls coated with calcium silicate board functioned similarly to those lined with gypsum plasterboard and better than those lined with magnesium oxide board. The 20 mm thick calcium silicate board lining exhibited no integrity degradation. This is due to the use of thicker boards and the incorporation of fibrous material throughout the thickness of the boards.

In 2018, Ariyanayagam et al [6] developed a study on the fire resistance of LSF walls to determine how factors such as the thickness of gypsum plasterboard, noggings, cavity insulation, and wall configurations affected it. The experimental investigation was done on non-load bearing LSF walls that had three meters in height. Indeed, the authors observed that the 3 m high, non-load-bearing LSF walls didn't collapse due to stiffness or strength but to the lacking of insulation. Also, they conclude that the fire resistance level (FRL) went up by 30 minutes when the thickness of the gypsum plasterboard increases from 13 mm to 16 mm. Noggings improved FRL based on structural adequacy of load-bearing walls, but not insulation. Glass fibre cavity insulation decreased the temperature of the external plasterboards but only enhanced the FRL by 12 minutes. High-melting insulating materials like Rockwool are needed for higher FRLs.

In 2020, Khetata et al [7] evaluated the fire resistance of seven LSF non-load bearing structures that were based on both experimental testing and numerical simulations, testing different types of cladding systems.

Their study shows that the increase in the number of studs, as well as, the increase in the thickness of the protective layers, both contribute to an improvement in the LSF walls insulation



fire resistance. They noted that the insulation of cavities delivers meaningful improvements to fire resistance. However, increasing the number of gypsum plates seems to compete with the LSF wall which includes insulating material in the cavity. When compared to the use of a single layer of cavity insulation material, the insulation fire performance of an LSF wall constructed with two layers of gypsum was improved.

## **2.2 Numerical tests**

In 2000, Alfawakhiri et al [8] developed an analytical thermomechanical model for LSF based on data from six standard fire resistance tests. Their TRACE (Temperature Rise Across Construction Elements) software [9] was used for the numerical simulations which could model gypsum board spalling by removing it from the simulation at a user-specified time, so the registered time of spalling based on visual test observations was used. The authors used the tool STUD to simulate the structural behavior of the load bearing LSF walls. The results were very accurate for all simulations, but the STUD software could not predict the lateral deflection at failure time so precisely.

In 2012, Keerthan et al [10] investigated a detailed numerical study on the thermal performance of non-load-bearing LSF wall panels. They developed a finite-element thermal models of both the classic light gauge cold-formed steel frame wall panels with cavity insulation and the new composite wall panels to simulate their thermal behaviour under standard and realistic fire circumstances. Gypsum plasterboard, insulation, and steel were chosen for their perceived thermal qualities. Comparisons with fire tests results were also developed. Their numerical findings indicate that the use of cavity insulation reduced the fire rating of light gauge cold-formed steel frame walls, but the use of external insulation provided improved thermal protection.

In 2017, Rusthi et al [11] focused in their study on the fire performance of LSF wall systems by using finite element (FE) models based on 3-D heat transfer FE models instead of 2-D FE models on the existing LSF wall system configurations. The authors conclude that these 3-D FE models allow parametric investigations of LSF wall designs with varying boards, cavity insulation, and stud sections. However, this research produced 3-D FE models that can directly couple heat transfer analysis to thermal-mechanical modelling of studs to include non-uniform temperature change along the height and across the stud. Their findings show that back-blocking keeps steel stud temperatures below relevant failure limits, improving fire performance. In fact, back-blocking with cavity insulation improves the wall system failure time.

In 2020, Khetata et al [7] developed a numerical study to analyze fire resistance of seven LSF non-load bearing structures and they compared it with experimental tests. They used two-dimensional numerical models based on the finite element method, the finite-volume method and hybrid finite-element method. The numerical and experimental results from fire tests were in good agreement. Both the quantity of studs and the thickness of the protective layers increase the fire resistance. They conclude that the hybrid finite-element method solution method appears to be the most accurate approximation model in order to predict fire resistance.

In 2021 Tao et al [12] presented a numerical investigation on the fire performance analysis of cold-formed steel walls constructed using steel hollow section (SHS/RHS) studs by developing simplified and sheathed stud finite element (FE) models of tested walls. The authors demonstrated through their study the benefit of employing hollow section (SHS/RHS) studs in cavity insulated walls. The hollow cavity of SHS/RHS studs helps to accelerate heat transmission between the hot and cold flanges of the stud. Compared to traditional cavity-insulated lipped-channel stud walls, this unique feature helps to prevent excessive flange temperature variations, hence reducing thermal bowing deformations. Also, they found that

FRL can be enhanced by increasing the depth of steel studs, according to fire test and FEA results. In addition, they investigate the impact of sheathing and localized plasterboard fall-off on the wall behaviour in a fire.

In this study, a parametric study was carried out using external and internal insulation in order to observe the effect of the protection layers and the effect of cavity insulation under fire and the effect of the dimension of stud and spacing between them,

# Chapter 3

## 3 Fire and heat transfer

This chapter describes the thermal behaviour of the LSF wall assembly during a fire, as well as several considerations that have been demonstrated to be necessary for performing numerical and experimental studies in this field of study.

### 3.1 Origin of fire

The fire is produced by the mixing of a combustible object with oxygen in the presence of heat which triggers the exothermic oxidation reaction of combustion. The fire starts with the burning of one object then begins to spread gradually to other objects in the vicinity and grows in size and intensity.

LSF wall fire resistance is measured in terms of Fire Resistance Level (FRL), which is the time period during which the components resist fire based on three criteria: structural adequacy, integrity, and insulation. FRLs are calculated using full-scale fire tests based on the ISO 834 [13] standard time-temperature curve.

The AS 1530.4 [14] and the European EN 1363-1 [18] define integrity (E) as the capacity to withstand flame or smoke. Large-scale testing is required for integrity evaluation since small-scale testing cannot evaluate issues such as drywall shrinkage or fractures caused by structural deformation. To determine the impact of drywall falling from the wall into the fire, high-scale experiments are also required.

The thermal insulation criteria (I) refers to the capacity to resist fire on one side while preventing excessive heat transfer and temperature elevation. This condition is reached when

the average temperature increase on the unexposed surface by  $140\text{ }^{\circ}\text{C}$  ( $T_{\text{ave}} = T_0 + 140$ ), or when the highest temperature surpasses  $180\text{ }^{\circ}\text{C}$  ( $T_{\text{Max}} = T_0 + 180$ ), above the initial average temperature, according to ISO 834 [13], AS 1530.4 [14], and EN 1363-1 [18].

The criterion (R) is a structure's ability to retain its stability and load bearing capacity during a fire, and it is used to calculate the fire resistance level ("FRL") of passive fire elements of wall. It usually tries to find the critical vertical contraction displacement or the rate of the vertical contraction displacement.

### **3.1- Fire curves**

The ISO fire curve may be traced back to fire testing on wooden furniture and cribs in the United States in the 1920s. It depicts the whole fire period while ignoring the growth and decay stages of the fire. It was then tweaked to produce a quicker temperature increase in the first few minutes. The ISO fire curve is now often utilized for building constructions.

The ISO standard fire curve is the most significant curve for fire testing and structural fire design. Informally, the curve is frequently referred to as "ISO fire" or "standard fire. Figure 3 depicts the ISO fire's time-dependent fire temperatures. The temperature never decreases, as one can see. This is in contrast to a natural fire, in which the fire load is burnt at a certain period, causing temperatures to fall. Furthermore, the ventilation conditions (amount of accessible oxygen) as well as the thermal qualities of the structure (walls, roof, and floor) impact the fire's path. As a result, so-called natural fires are far more irregular than the ISO standard fire course requires. As a result, the ISO standard fire curve is an artificial fire curve.

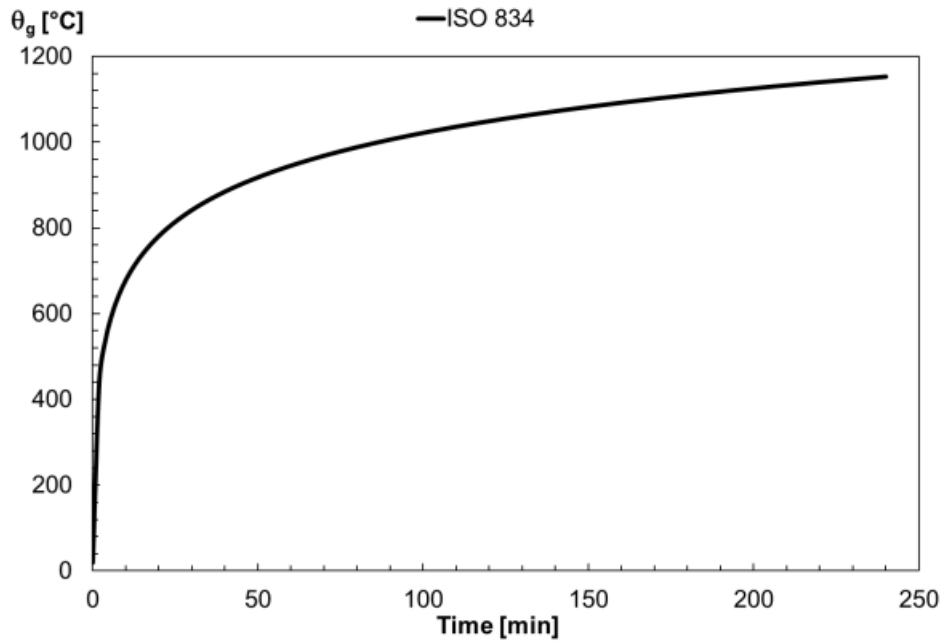


Figure 3: Standard Fire Curve [13]

The following equation, given in Eurocode EN1991-1-2 [15], describes the ISO standard fire:

$$\Theta_g = 20 + 345 \log_{10}(8t + 1) \quad (3.1)$$

The term in this equation is the gas temperature (°C), while the variable  $t$  is the time (min).

### 3.2 Heat Transfer Theory

A heat transfer is a transit of energy in a disordered microscopic form due to temperature differences. The hotter body gives energy to the colder body

When two objects have different temperatures, heat is transferred. The colder object gets hotter until both objects have the same temperature. Heat energy always flows from the warmer object to the colder object.

Heat transfer occurs through the three processes of conduction, convection and radiation, which can occur separately or simultaneously depending on the conditions.

The thermal actions for temperature analysis were given by The Eurocode 1 - Part 1-2 [15], which are represented by the net heat flux ( $\text{W/m}^2$ ) to the element's boundary surface. On fire-exposed surfaces, the net heat flux is separated into two components: the first examines heat transfer by convection ( $\dot{h}_{net,c}$ ) and the second considers heat transfer by radiation ( $\dot{h}_{net,r}$ ), as shown below.

$$\dot{h}_{net} = \dot{h}_{net,c} + \dot{h}_{net,r} \quad (3.2)$$

The subsections that follow contain the formulation used to derive each component of the above equation as well as a short overview of the three mechanisms of heat transport. The process of conduction is the heat transmission process in solid materials. Heat is conveyed via interactions involving free electrons in materials that are excellent conductors of heat; hence, materials that are good electrical conductors are generally also good conductors of heat. Heat is carried through mechanical vibrations of the molecular lattice in other materials that are poor conductors. Heat conduction is a critical aspect in the igniting of solid surfaces as well as the fire resistance of barriers and structural parts.

For heat transfer calculations in solid materials which is conduction, many material parameters are required. These are the density, specific heat and thermal conductivity. The density of a substance is its mass per unit volume (in kg/m<sup>3</sup>).

$$\dot{h}_x = -\lambda dT/dx \quad (3.3)$$

The convection is the transmission of heat through the movement of fluids, which may be gases or liquids. Convective heat transfer is an essential feature in flame propagation and the upward movement of smoke and hot gases from a room fire to the ceiling or out the window. Convective heat transfer calculations often include heat transfer between a solid's surface and a surrounding fluid that warms or cools the solid. The rate of heating or cooling is determined by various elements, the most important of which is the velocity of the fluid at the surface. [16] Heat transfer is commonly assumed to be directly proportional to the temperature differential between the two materials under certain circumstances, therefore the heat flow per unit area  $h_{net,c}$  (W/m<sup>2</sup>) is given by:

$$\dot{h}_{net,c} = \alpha_c \cdot (\theta_g - \theta_m) \quad (3.4)$$

Where  $\theta_g$  is the gas temperature, the  $\theta_m$  is the surface temperature and  $\alpha_c$  Coefficient of heat transfer by convection

The radiation is the transmission of energy by electromagnetic waves that may pass through a vacuum or a transparent material or liquid. Radiation is critical in fires because it is the primary heat transmission method from hot flames to fuel surfaces, hot smoke to building items, and a



burning structure to a neighbouring building. At a location on a receiving surface, the radiant heat flux. [16].

The  $\dot{h}_{net,r}$  (W/m<sup>2</sup>) is given by:

$$\dot{h}_{net,r} = \Phi \cdot \varepsilon_c \cdot \varepsilon_f \cdot \sigma \cdot [(\theta_r + 273)^4 - (\theta_m + 273)^4] \quad (3.5)$$

Where the view factor equals  $\Phi = 1.0$ , however lower values may be used to take into account shadow effects. The surface emissivity of the member, m, is to be employed at a value of  $\varepsilon_m = 0.8$  unless otherwise specified in the design standard. The value of fire emissivity,  $\varepsilon_f$ , should be considered as  $\varepsilon_f = 1$ . The Stephan Boltzmann constant  $\sigma$  is  $5.67 \cdot 10^{-8}$  (W/m<sup>2</sup>K<sup>4</sup>) the effective radiation temperature of the fire environment is  $\theta_r$  [°C] and the surface temperature of the member is  $\theta_m$  [°C].

The second order partial differential equation for the heat transfer by conduction in ANSYS was evaluated using the Fourier law of heat transfer as following [17]:

$$\rho C \frac{\partial T}{\partial t} = \frac{\partial}{\partial x} \left( k_x \frac{\partial T}{\partial x} \right) + \frac{\partial}{\partial y} \left( k_y \frac{\partial T}{\partial y} \right) \quad (3.6)$$

where T is the temperature,  $k_x$  and  $k_y$ , are the thermal conductivities in the x and y directions, C is the specific heat capacity, and t is the time.

### 3.3 Boundary Condition

The boundary conditions are specified based on EN1991-1-2[15]. The wall is exposed to fire from a one side and the other side is exposed on the ambient temperature. Assuming warm exchange by radiation (emissivity of fire  $\epsilon = 1$ ) and convection (convection coefficient  $\alpha = 25\text{W/m}^2\text{C}$ ) in the fire side and heat exchange by convection (convection coefficient  $\alpha = 9\text{W/m}^2\text{C}$ ) in the unexposed side to include the radiation effect. The gas temperature in the fire side follows the ISO834 standard [13]. The temperature of the unexposed is equal to the initial temperature ( $T = 20^\circ\text{C}$ ), during all the simulation time.

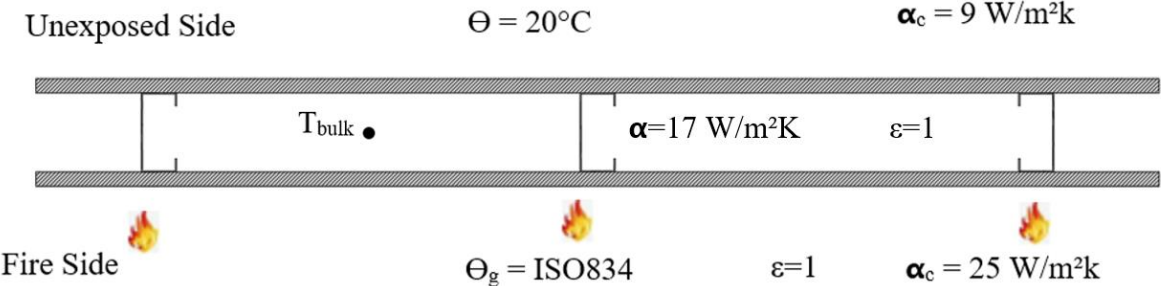


Figure 4: Boundary Conditions

The bulk temperature is given as an average of the hot and cold flanges and is intended to reflect any damage during the test. A different Bulk temperature value was chosen in this investigation for each wall structure the blue curve for the single gypsum layer, the orange curve double gypsum layer and the grey curve composite wall of Rockwool and gypsum) as shown in Figure 5.

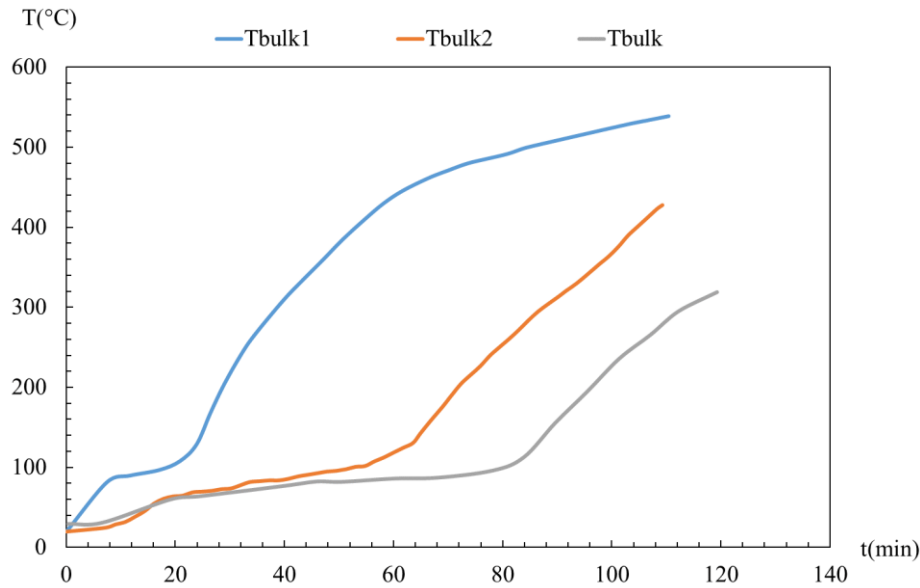


Figure 5: Average bulk temperature versus time

### 3.4 Fire rating

This section will present the standards used to determine the fire resistance of non-loadbearing LSF walls besides we will present our work.

The common standards which are used in this investigation are EN 1363-1[18] (fire test - general requirements) and EN 1364-1[19] (Specific information to perform the fire test of non-loadbearing walls).

EN 1363-1 standard [18] specifies the main principles for assessing the fire resistance of various structural elements when exposed to standard fire exposure circumstances.

To submit the test specimen to the test conditions, a specifically built furnace is necessary.

The system for controlling the furnace's temperature, the equipment for controlling and monitoring the pressure of the hot gases inside the furnace, the frame into which the element may be put and subjected to suitable heating, pressure, and support conditions.

The arrangement for loading and restraint of the test specimen should be suitable, including control and monitoring of the load apparatus for determining temperature in the furnace and in the test specimen. The system for measuring the deflection of the test specimen is necessary in some cases. In certain circumstances, specialized instruments are also necessary to assess the integrity and ensure compliance with the performance criteria.

For very special cases, the equipment for measuring the oxygen concentration of furnace gases is also required. This testing standard also defines the design and tolerances of systems, as well as certain sketches of sensors such as disk thermocouples and plate thermocouples.

The insulation criteria (I) is the performance criteria used to verify the fire resistance tests of non-load bearing walls. By definition, this is the time, in completed minutes, during which the test specimen maintains its separating function without developing temperatures on its unexposed surface that raise the average temperature above the initial average temperature by more than 140 °C or raise the temperature at any location (including the roving thermocouple) by more than 180 °C. When the "integrity" criterion is no longer satisfied, the "insulation" performance criteria are presumed not to be satisfied. The integrity criteria (E), in this situation, relate to the time of passage of flame or smoke through the face not exposed by some cracks.

EN 1364-1 is the protocols for performing experimental tests to determine the fire resistance of a non-loadbearing wall to prevent fire propagation from one side to another are included in EN 1364-1[19].

More details on the prerequisites are provided for this experiment. To secure the specimen, a strong frame with high rigidity and minimal thermal expansion is required.

The specimen's dimensions should be determined as follows: if the width or height of the construction element is less than 3 m, the specimen shall be tested in its real size. If one of the dimensions of the construction element is more than 3m, the dimension in the test shall not be

less than 3m. In any event, the wall dimensions in this experiment were limited by the furnace aperture, and it is strongly advised that the maximum size of the wall match with this size, in this case, the specimens used were 1280 mm in width and 1015 mm in height.

### **3.5 Behaviour of LSF Walls in Fire**

The heat flow is transferred by three ways that contribute to the increase in temperature of structural materials during the fire, first the heat flow begins to spread from the fire by radiation in which it is transferred by electromagnetic waves, at the same time by convection which is an important factor in the spread of the flame and in the upward transport of smoke and hot gases to the wall at the exposed side so the heat flow propagates in the layers of the wall by conduction until reaching the cavity where the phenomenon of convection and radiation occurs. The same process is repeated in the other layers, generating a hot layer that heats the unexposed side.

# Chapter 4

## 4 Mathematical model

This chapter presents the mathematical model, the material properties and the numerical validation of the experimental tests.

### 4.1 The finite element methods

The finite element method is a numerical technique for engineering and mathematical physics problem solving. This approach may be used to solve typical engineering and mathematics problems including heat transfer, fluid dynamics, mass transport, and electromagnetic potential. These analytical solutions often need the solution of ordinary or partial differential equations, because to the complex geometries, loads, and material characteristics, are generally unavailable. Therefore, we must use numerical methods, such as the finite element approach.

The Finite Element Analysis (FEA) method, was first developed by Turner et al. in 1956 [17]. It is a powerful computer tool for approximating solutions to a wide range of "real-world" engineering problems involving complicated domains subject to generic boundary conditions. This method is included as one solution method in the European standards such as the Eurocodes according to prEN1192-1-2[20]

“Advanced design methods shall be based on fundamental physical behaviour, employing local equilibrium equations which are satisfied at every point in the structure.

Any potential failure mode not covered by the advanced design method (e.g. local failure in shear) shall be prevented by appropriate means.

Advanced design methods may include separate calculation models for the determination of:

- The development and temperature distribution within structural members (thermal response model).
- The mechanical behaviour of the structure or of any part of it (mechanical response model).

Advanced design methods may be used in association with any thermal action, provided the material properties are known for the relevant temperature history. «The fundamental notion of FEM involves dividing the computing domain into tiny patches and finding local solutions that satisfy the differential equation inside the patch's boundary. By reassembling the individual solutions on these patches, it is possible to generate a global solution. There are many softwares which algorithms are based on FEM such as ANSYS®Multiphysics.

#### **4.1.1 ANSYS Multiphysics**

ANSYS Multiphysics is a FEM-based software program capable of performing geometric design and thermal analysis on steady or transient linear and non-linear heat transfer issues (including 1D, 2D or 3D domains). The software provides a set of elements with finite lines, surfaces or volumes. Depending on the target of study, these elements have a variable number of nodes with distinct degrees of freedom and interpolation functions. Depending on the temperature, the complex boundary conditions of the material and the associated thermal characteristics may be represented as tables or functional quantities [18]. The ANSYS solver controls three primary modes of heat transfer during transient analysis. The outward surface charge of a solid element or conductive shell is referred to as convection. The film coefficient may be specified as a temperature-dependent parameter if required. The generalized radiation interaction between two or more surfaces within the enclosure may be considered as 2D or 3D elements with degree of freedom temperature when considering radiation effects, with the

change in temperature in each enclosure being specified as a Space Function node. Multiple gray diffuse radiating surfaces with known emissivity may be used to construct the enclosure, with the emissivity of each material pattern varying with temperature. To determine the view factor between 3D shell surfaces, use the hemicube approach. The calculated heat flow will serve as the boundary condition for the whole finite element model's conduction analysis. Determine the new surface heat flux condition for each node temperature and calculate the next node temperature for the overall model.

**4.1.2 Finite element type (Element type plane 55)**

PLANE55 is an element in Ansys Mechanical APDL that is shown in Figure 6 and will be used in this study due to its 2D heat conduction capability.

The element has four nodes with a single degree of freedom, temperature, at each node.

This element is using linear interpolating functions and full gauss integration.

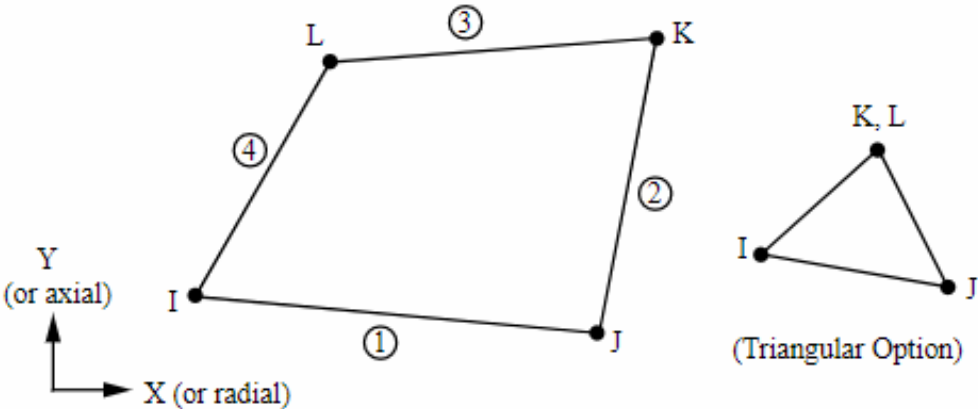


Figure 6: Plane 55 [18]



It is applicable to steady-state or transient 2D thermal analysis and may also account for mass transport heat flux from a constant velocity field [18].

### 4.2 The materials properties

The materials employed in this investigation were steel as described by Eurocode 3 Part 1.2[21], gypsum as presented bay EN1995-1-2 [22] and the Rockwool used in the cavity insulation. These materials have an important impact in the numerical results.

For carbon CFS elements, their thermophysical properties are given by EN 1993-1-2 [21]. Figure presents the specific heat of the carbon steels and it reaches 5000 [J/kgK] as maximum heat, its specific mass is considered constant, stated by EN 1991-1-2 [15] as shown in the Figure 7.

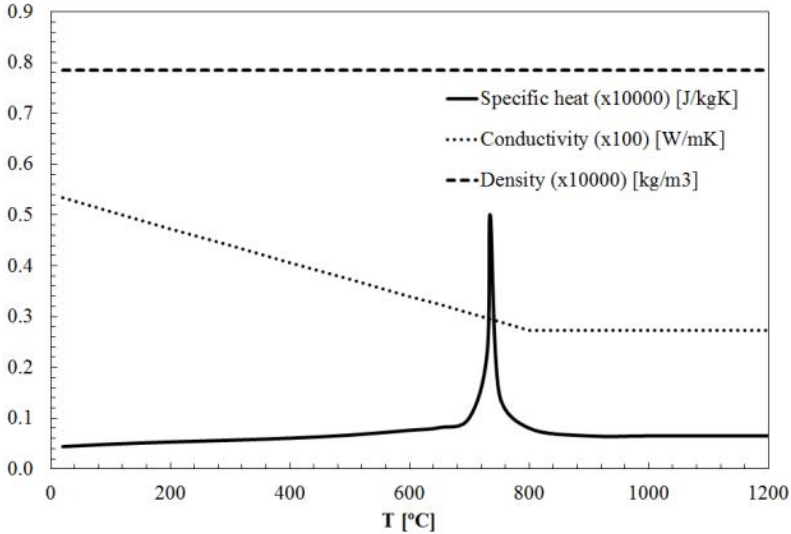


Figure 7: Thermal properties of steel

### 4.2.1 Gypsum Plasterboard

The thermal properties of the gypsum used in this study are presented according to the prEN1995-1-2 [22]. The specific heat of the plasterboard gypsum is presented in figure 8 and it reaches 25000 [J/kgK] as maximum heat. Its Conductivity and its Density are also depicted.

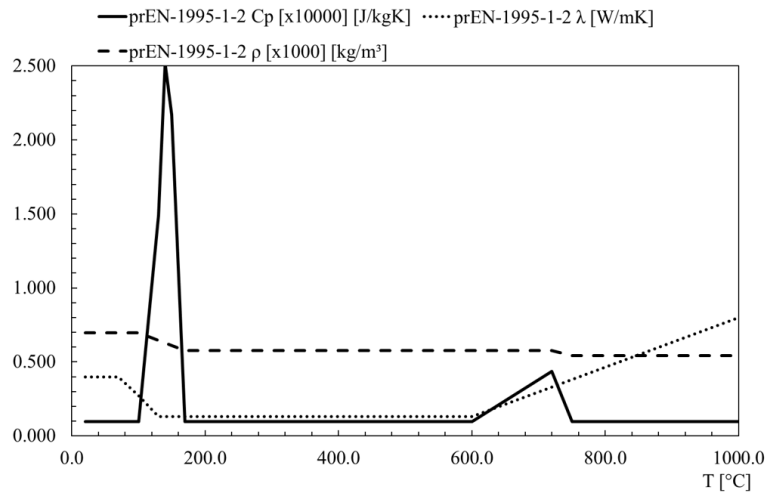


Figure 8: Thermal properties of gypsum

### 4.2.2 Rockwool

The Rockwool [23] is the material used for the cavity and external insulation with density of 75 (kg/m<sup>3</sup>). The thermal properties of the Rockwool are presented in the Figure 9.

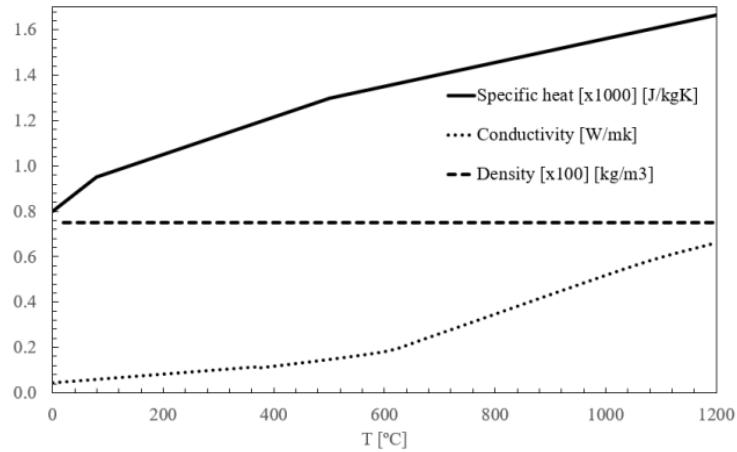


Figure 9: Thermal properties of Rockwool

### 4.3 Numerical validation

The test specimen geometry was taken from the investigation of Prakash Kolarkar and Mahen Mahendran [24] in 2012.

#### Validation of Specimen 1

The studs that were used are C90x40x15x1.15, with steel grade G500 and the tracks are 92x50x1.15, with steel grade G500. A 3 studs per track was adopted to examine the effects of the different material for plates in the wall.

The wall's material composition is a single gypsum plasterboard for each side. This constructive solution was utilized to evaluate the performance of the wall under fire.

The average temperature values obtained from the numerical simulation on several places of the non-load bearing wall are shown in Figure 10, the data were gathered at chosen nodes across the finite element mesh.

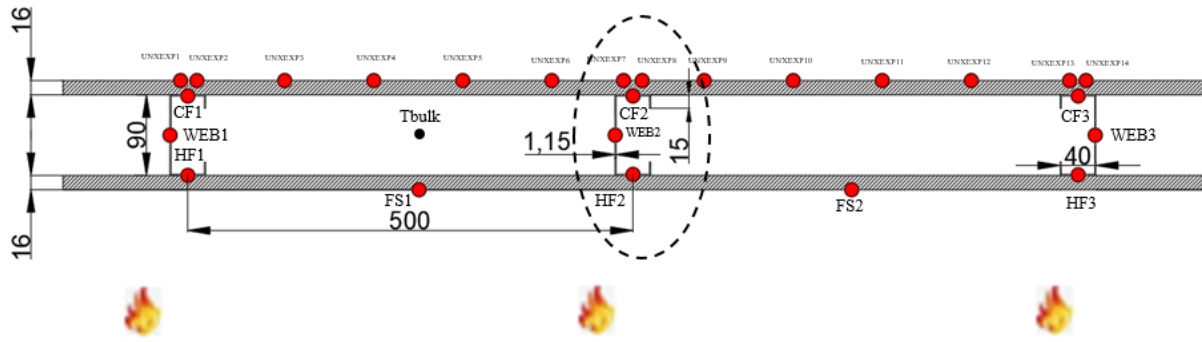


Figure 10: The location of the thermocouples

The Figure 11 presents the finite element mesh of the specimen 1

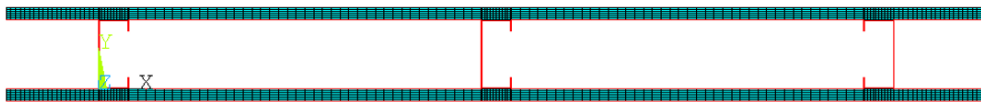


Figure 11: The finite element mesh of the specimen 1

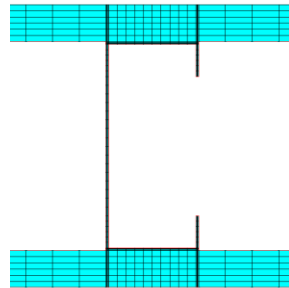


Figure 12: The finite element mesh of the zoom of the specimen 1

Figure 13 presents the comparison between the experimental and numerical results for the temperature development in specimen 1.

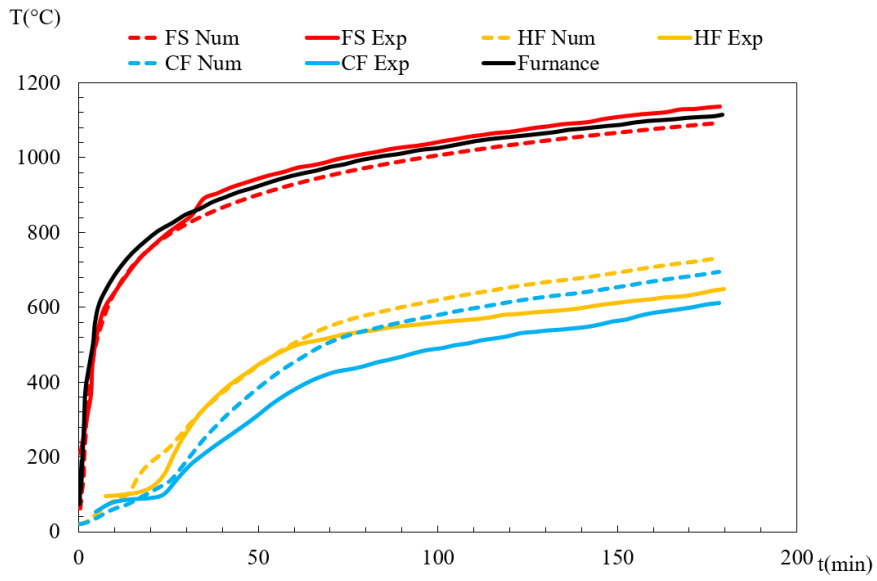


Figure 13: Specimen 1 - Average temperature results

Figure 14 presents average and maximum temperature on the unexposed side in specimen 1.

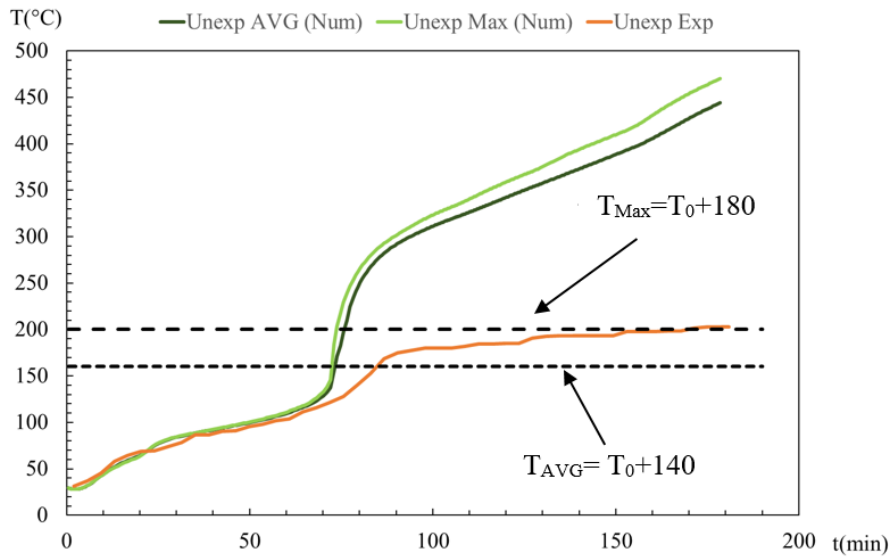


Figure 14: Average and maximum temperature on the unexposed side

### Validation of specimen 2

The same wall configuration was used in this simulation but with double gypsum plasterboards as presented in the figure 15

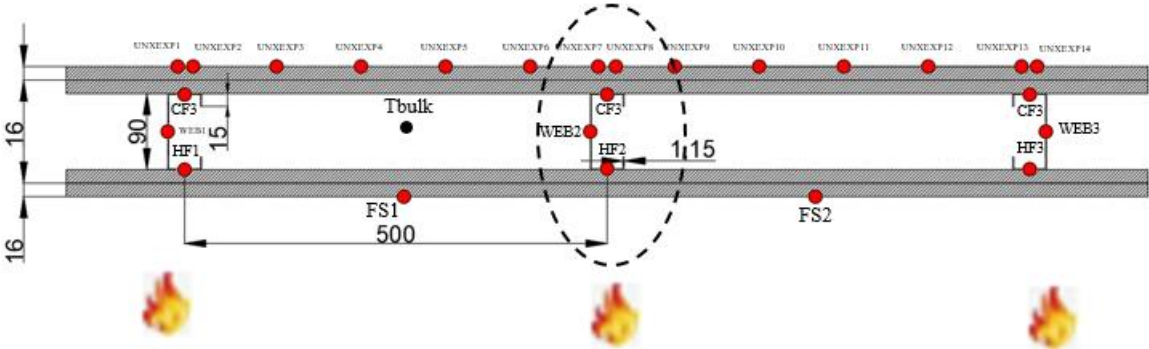


Figure 15: The location of the thermocouples

The figure 16 presents the finite element mesh of the specimen 2

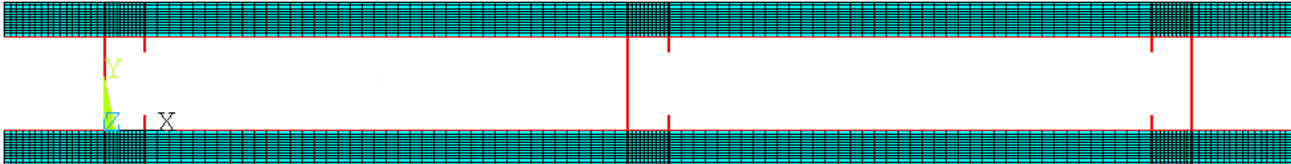


Figure 16: The finite element mesh of the specimen 2

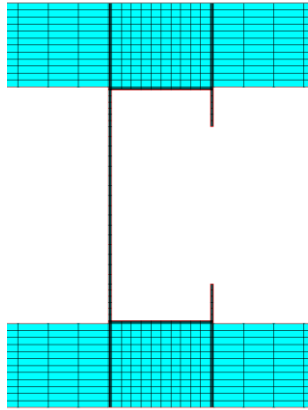


Figure 17: he finite element mesh of the zoom in the specimen 2

Figure 18 presents the comparison between the experimental and numerical results for the temperature development in specimen 2.

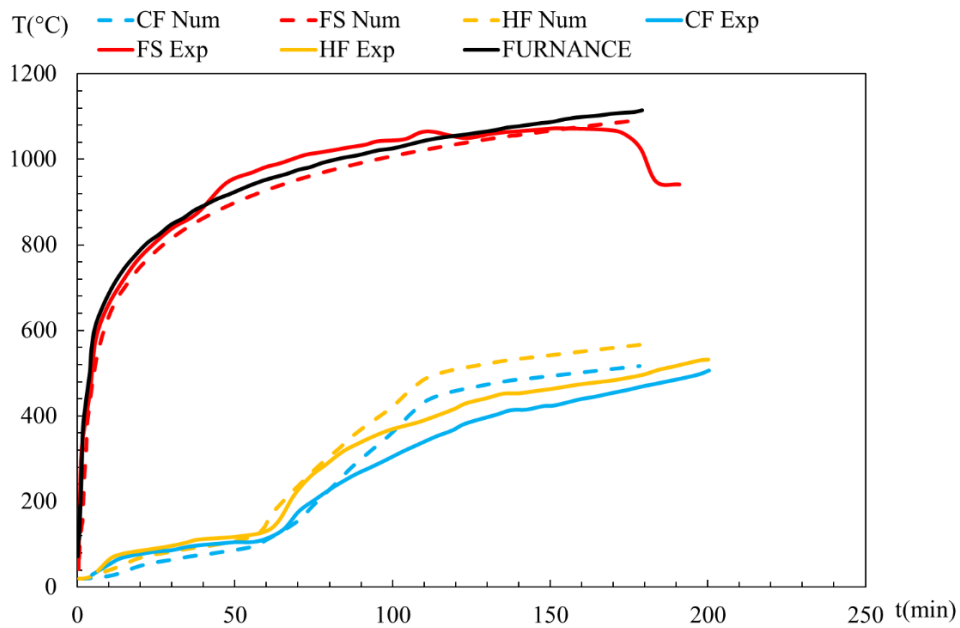


Figure 18: Specimen 2 - Average temperature results

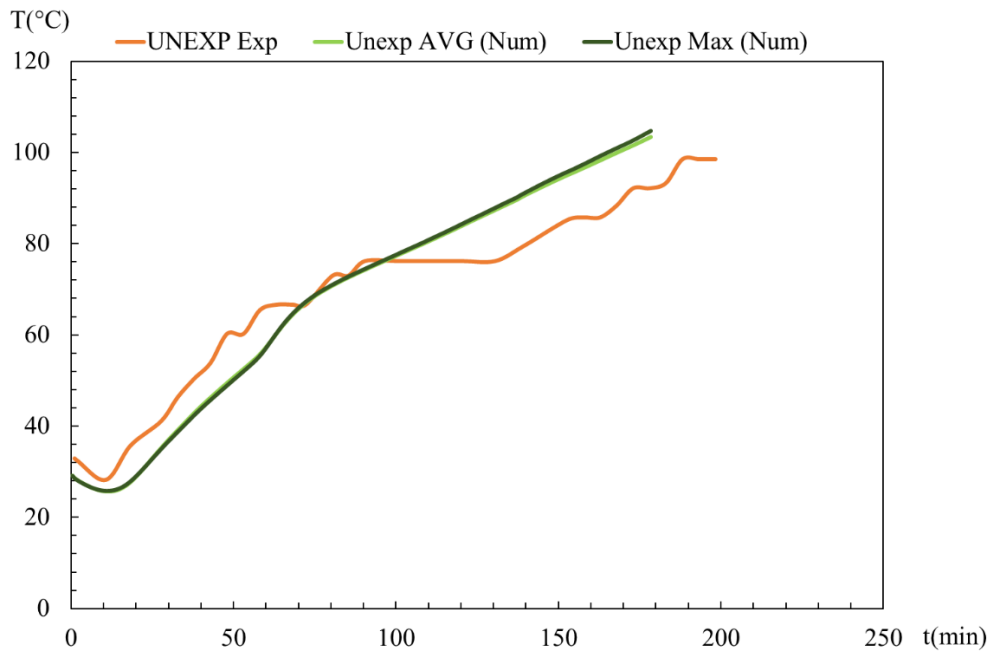


Figure 19: Average and maximum temperature on the unexposed side

The temperatures are largely below the criteria ( $T_{ave}$  and  $T_{max}$ )

#### 4.3.1 Results discussion

The thermal properties employed in this numerical simulation such as the steel were taken from EN 1993-1-2 [21] and the gypsum were taken from prEN1995-1-2 [22].

From the figure 13, 14, 18 and 19 it can be observed that the numerical results are higher than the experimental ones, this difference can be justified by the poor contact between the thermocouples and the surfaces that are measured also by the bad contact between the elements of the wall and by the amount of the gypsum moisture. The comparison of the experimental and numerical fire resistance for the LSF walls regarding  $T_{AVG}$  and  $T_{MAX}$ . The numerical models were validated using the specimens evaluated in the paper of Prakash Kolarkar and Mahen Mahendran [24] in 2012. The approach used to compare the fire resistance is called the relative error.



## The relative error

$$RE = \frac{T_{exp} - T_{num}}{T_{exp}} (\%) \quad (4.1)$$

Table 1: Relative error for experimental and numerical tests

Specimen n°:	Experimental	Numerical	Relative Error (%)
	Fire resistance ( <i>Tave</i> ) (min)	Fire resistance ( <i>Tave</i> ) (min)	
Specimen 1	85	73	16.44

The Root mean square (RMS) method was used to compare the time history temperature error measured at various locations on the wall.

The perfect RMS representation when it is equal to 0, which means that as closer as 0 is, the better the finite element results are.

## The root means square error (RMS%)

$$RMS = \sqrt{\frac{1}{n} \times \sum_i^n (T_{exp} - T_{num})^2} \times 100 (\text{°C}) \quad (4.2)$$

n: The number data points.

Table 2: Results of the root means square error (RMS)

Specimens	EXP – PB1 (°C)	PB - CAV (°C)	CAV – PB2 (°C)
Specimen 1	36.3	57.9	77.0
Specimen 2	32.9	56.1	51.6

EXP – PB1: FS (fire side)

PB – CAV : HF (hot flange)

CAV – PB2: CF (cold flange)

To compare the numerical and experimental average temperature results, the RMS equation is employed. The values reflect a good approximation, considering that, at any time, after the first 10 minutes of any standard fire test, the thermocouple temperature recorded by any furnace should not exceed by more than 100 °C from the corresponding temperature of the standard temperature/time curve, EN1363-1[18].

# Chapter 5

## 5 Parametric study

In this study five analyses will be investigated: one to investigate the variation of the structure's protection layer, another to compare the effect of variation of the thickness of the structure protection layer, a third to investigate the performance of the wall with cavity insulation, fourth to investigate the effect of variation of the stud spacing and fifth to investigate the variation of cavity thickness.

The parametric analysis and testing were suggested to get information about the impact of changing various parameters to improve fire resistance in LSF walls.

### 5.1 Parameters

The table 6 shows all the possible configurations of all the specimens to examine in the study.

Table 3: Configurations of all the specimens to examine

N° of specimen	Steel Section	Spacing between the studs (mm)	N° Layers gyps	Cavity insulation	Fire resistance (min)
1	C90x40x15x1.15	600	1Gypsum12.5	/	55
2	C90x40x15x1.15	600	2Gypsum12.5	/	168
3	C90x40x15x1.15	600	1Gypsum12.5 1Rockwool25 1Gypsum12.5	/	-
4	C90x40x15x1.15	600	1Gypsum16	/	73
5	C90x40x15x1.15	600	2Gypsum16	/	211
6	C90x40x15x1.15	600	1Gypsum16 1Rockwool25 1Gypsum16	/	-
7	C90x40x15x1.15	600	1Gypsum12.5	Rockwool	243
8	C90x40x15x1.15	600	2Gypsum12.5	Rockwool	218
9	C90x40x15x1.15	600	1Gypsum12.5 1Rockwool25 1Gypsum12.5	Rockwool	-
10	C90x40x15x1.15	600	1Gypsum16	Rockwool	133
11	C90x40x15x1.15	600	2Gypsum16	Rockwool	288
12	C90x40x15x1.15	600	1Gypsum16 1Rockwool25 1Gypsum16	Rockwool	-
13	C90x40x15x1.15	400	1Gypsum12.5	/	55
14	C90x40x15x1.15	400	2Gypsum12.5	/	129
15	C90x40x15x1.15	400	1Gypsum12.5 1Rockwool25 1Gypsum12.5	/	-
16	C90x40x15x1.15	400	1Gypsum16	/	74

17	C90x40x15x1.15	400	2Gypsum16	/	264
18	C90x40x15x1.15	400	1Gypsum16 1Rockwool25 1Gypsum16	/	-
19	C90x40x15x1.15	400	1Gypsum12.5	Rockwool	136
20	C90x40x15x1.15	400	2Gypsum12.5	Rockwool	218
21	C90x40x15x1.15	400	1Gypsum12.5 1Rockwool25 1Gypsum12.5	Rockwool	-
22	C90x40x15x1.15	400	1Gypsum16	Rockwool	129
23	C90x40x15x1.15	400	2Gypsum16	Rockwool	289
24	C90x40x15x1.15	400	1Gypsum16 1Rockwool25 1Gypsum16	Rockwool	-
25	C150x50x20x2.0	600	1Gypsum12.5	/	49
26	C150x50x20x2.0	600	2Gypsum12.5	/	178
27	C150x50x20x2.0	600	1Gypsum12.5 1Rockwool25 1Gypsum12.5	/	-
28	C150x50x20x2.0	600	1Gypsum16	/	79
29	C150x50x20x2.0	600	2Gypsum16	/	192
30	C150x50x20x2.0	600	1Gypsum16 1Rockwool25 1Gypsum16	/	-
31	C150x50x20x2.0	600	1Gypsum12.5	Rockwool	145
32	C150x50x20x2.0	600	2Gypsum12.5	Rockwool	300
33	C150x50x20x2.0	600	1Gypsum12.5 1Rockwool25 1Gypsum12.5	Rockwool	-
34	C150x50x20x2.0	600	1Gypsum16	Rockwool	197
35	C150x50x20x2.0	600	2Gypsum16	Rockwool	-
36	C150x50x20x2.0	600	1Gypsum16 1Rockwool25 1Gypsum16	Rockwool	-
37	C150x50x20x2.0	400	1Gypsum12.5	/	75
38	C150x50x20x2.0	400	2Gypsum12.5	/	177
39	C150x50x20x2.0	400	1Gypsum12.5 1Rockwool25 1Gypsum12.5	/	-
40	C150x50x20x2.0	400	1Gypsum16	/	74
41	C150x50x20x2.0	400	2Gypsum16	/	254
42	C150x50x20x2.0	400	1Gypsum16 1Rockwool25 1Gypsum16	/	-
43	C150x50x20x2.0	400	1Gypsum12.5	Rockwool	139
44	C150x50x20x2.0	400	2Gypsum12.5	Rockwool	-
45	C150x50x20x2.0	400	1Gypsum12.5 1Rockwool25 1Gypsum12.5	Rockwool	-
46	C150x50x20x2.0	400	1Gypsum16	Rockwool	178
47	C150x50x20x2.0	400	2Gypsum16	Rockwool	-
48	C150x50x20x2.0	400	1Gypsum16 1Rockwool25 1Gypsum16	Rockwool	-

## 5.2 Results

The fire resistance of non-load-bearing walls is dependent on the calculation of the surface temperature of non-exposed walls. These structural components' performance criteria account for both the average temperature  $T_{ave}$  and the greatest temperature  $T_{max}$ . The maximum temperature and average temperature are calculated based on the distribution of nodes throughout the whole length of the unexposed surface.

Figure 20 presents the average temperature results for the temperature development in specimen 13.

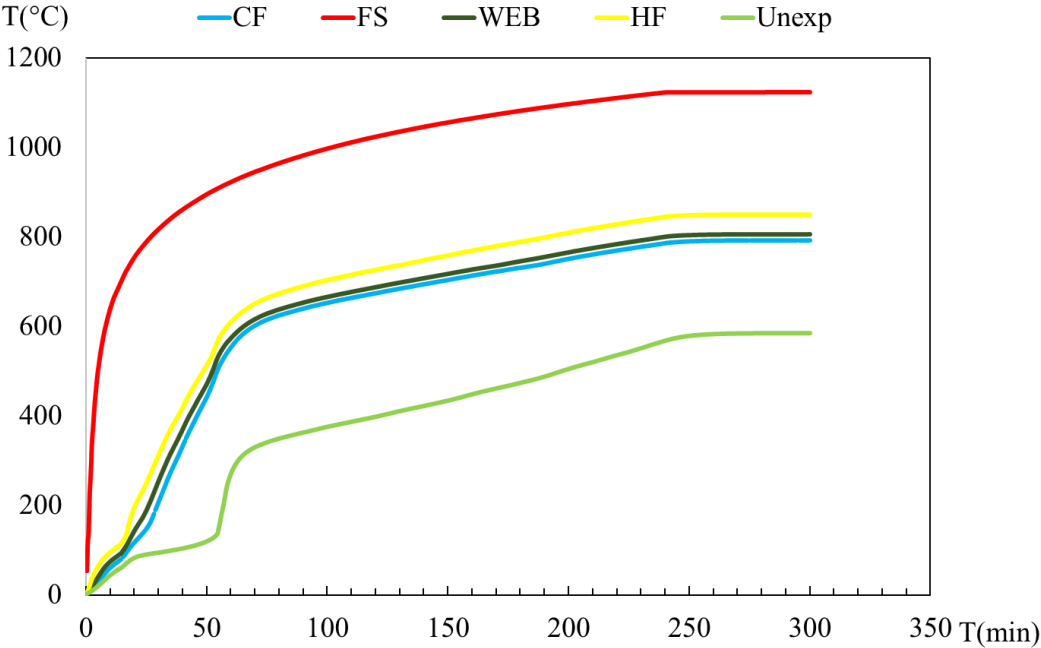


Figure 20: Specimen 13 - Average temperature results

Figure 21 presents the comparison between the average and the maximum temperature on the unexposed side for specimen 13.

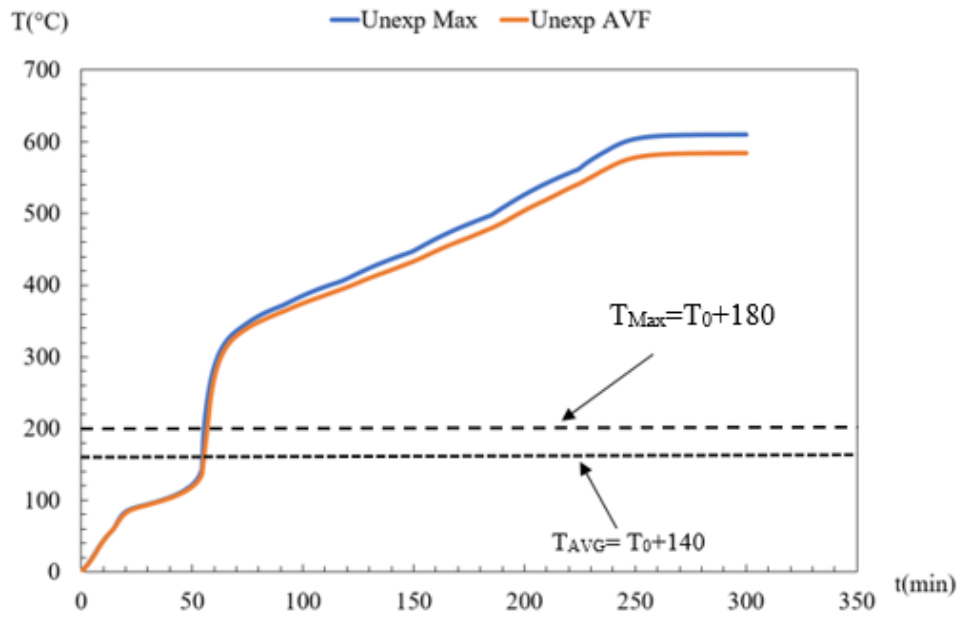


Figure 21: Specimen 13 - Average and maximum temperature on the unexposed side

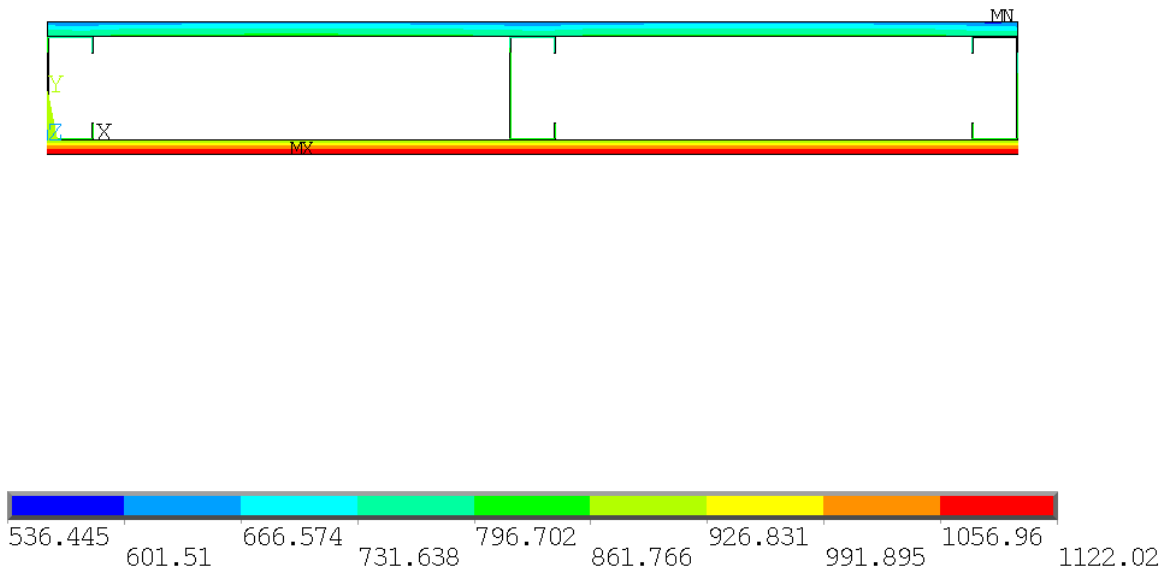


Figure 22: Numerical results for Specimen 13,  $t=240$ min

Figure 23 presents the average temperature results for the temperature development in specimen 14.

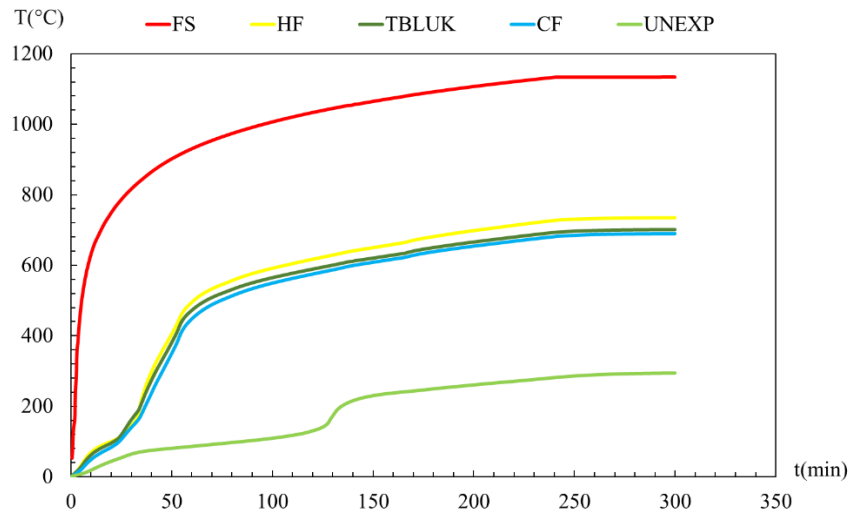


Figure 23: Specimen 14 - Average temperature results

Figure 24 presents the comparison between average and maximum temperature on the unexposed side for the specimen 14.

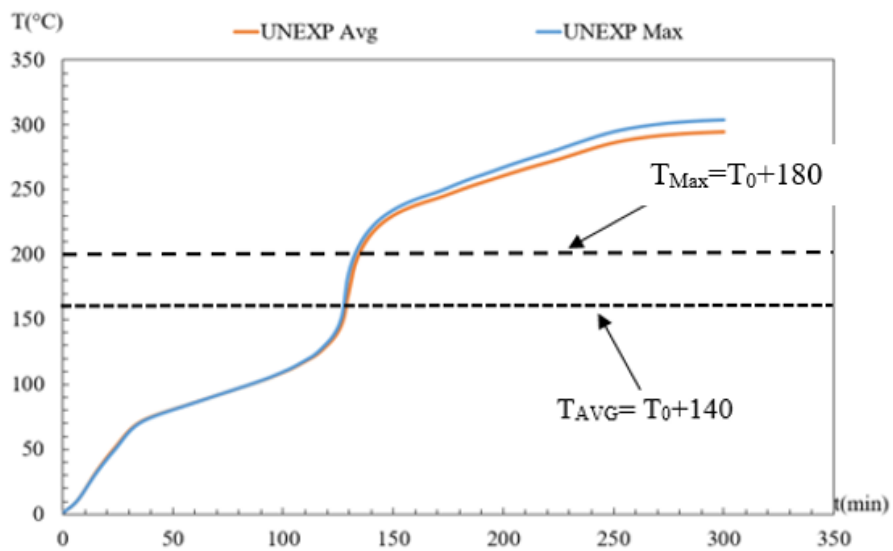


Figure 24: Specimen 14 - Average and maximum temperature on the unexposed side

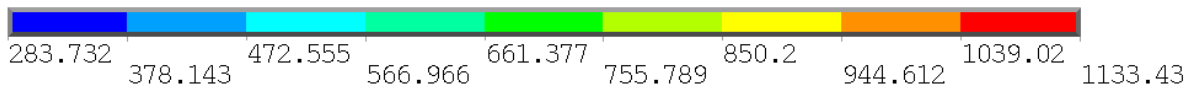
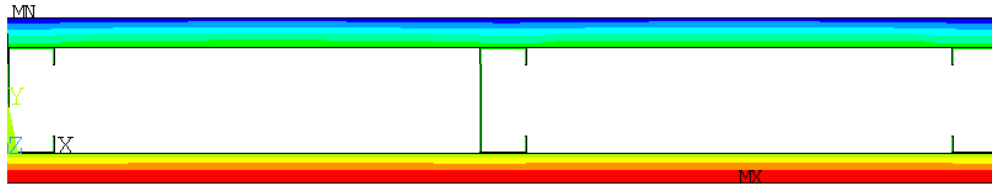


Figure 25: Numerical results for Specimen 14, t=300min

Figure 26 presents the average temperature results for the temperature development in specimen 15.

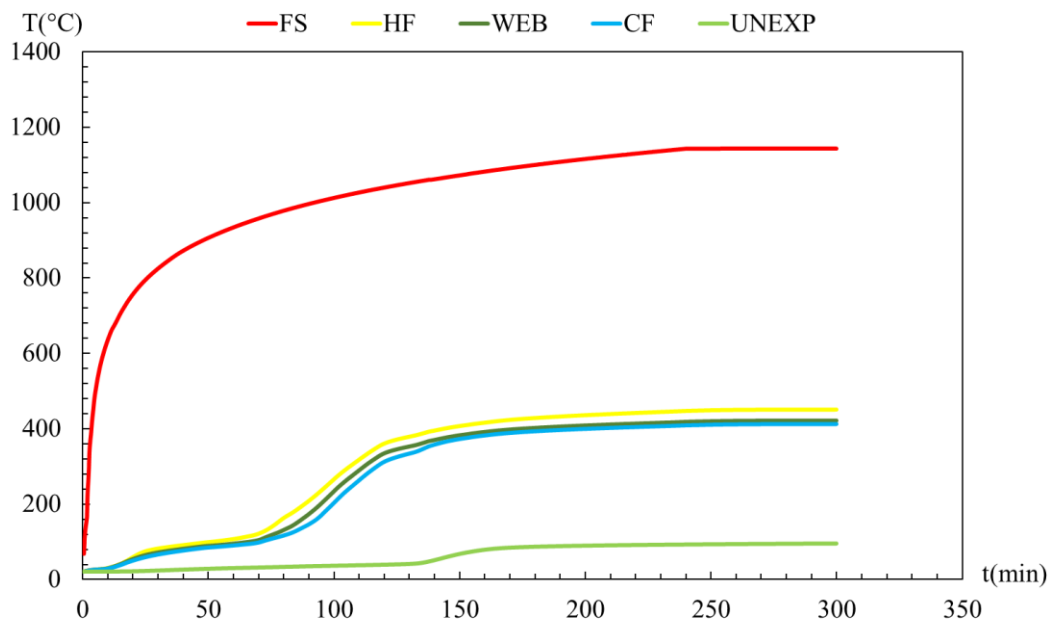


Figure 26: Specimen 15 - Average temperature results



Figure 27 presents the comparison between average and maximum temperature on the unexposed side for the specimen 15.

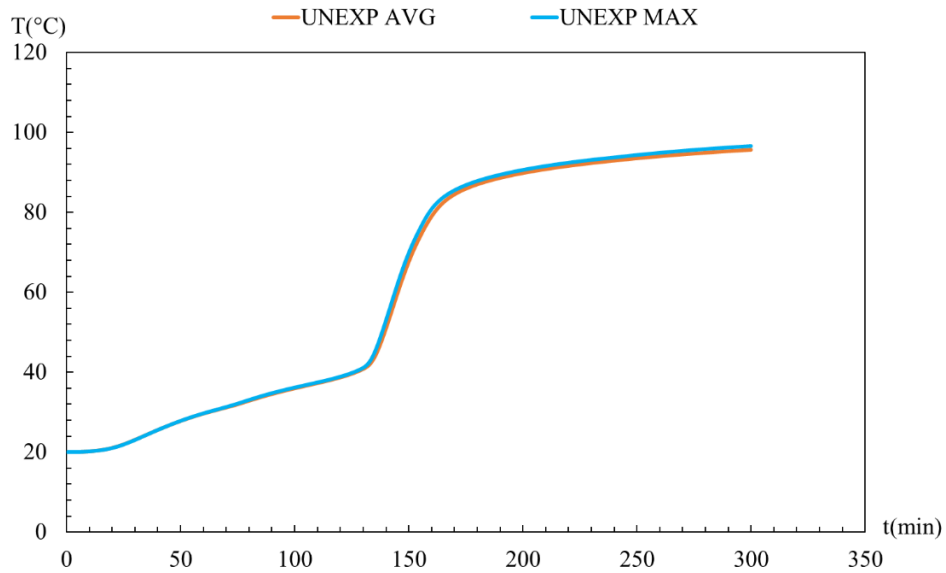


Figure 27: Specimen 15 - Average an maximum temperature on the unexposed side

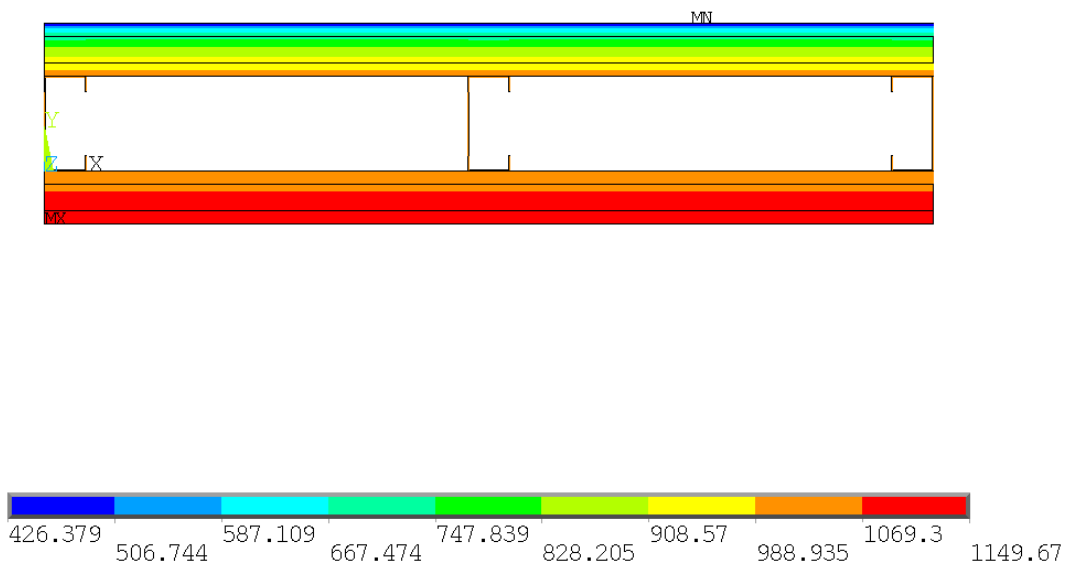


Figure 28: Numerical results for Specimen 15, t=300min

Figure 29 presents the average temperature results for the temperature development in specimen 16.

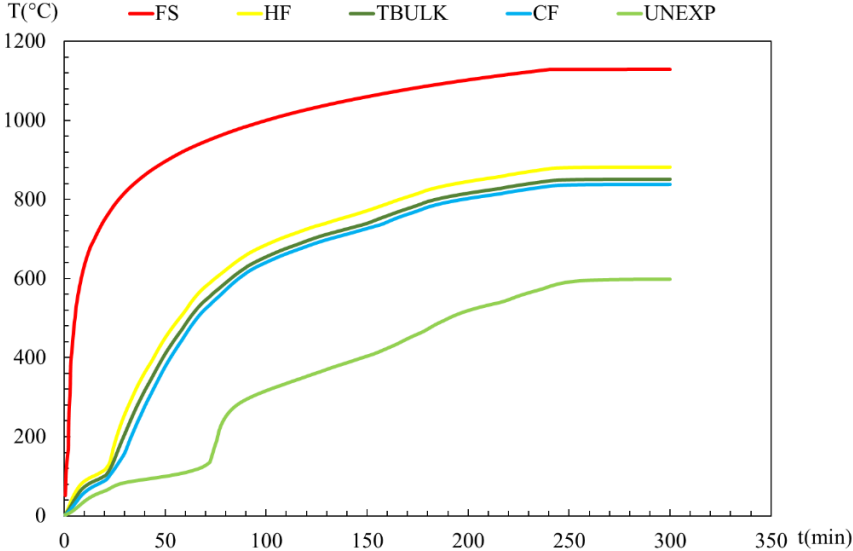


Figure 29: Specimen 16 - Average temperature results

Figure 30 presents the comparison between average and maximum temperature on the unexposed side for the specimen 16.

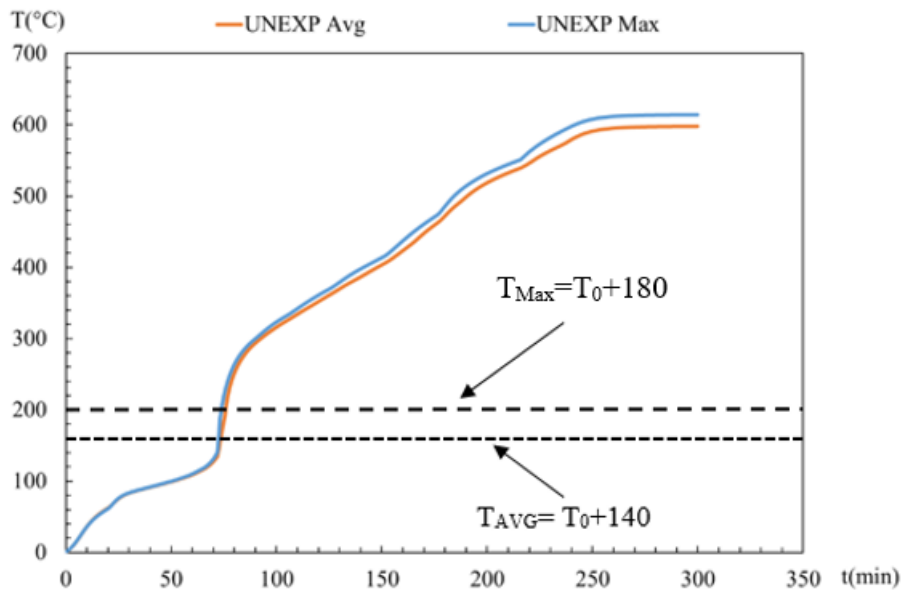


Figure 30: Specimen 16 - Average and maximum temperature on the unexposed side

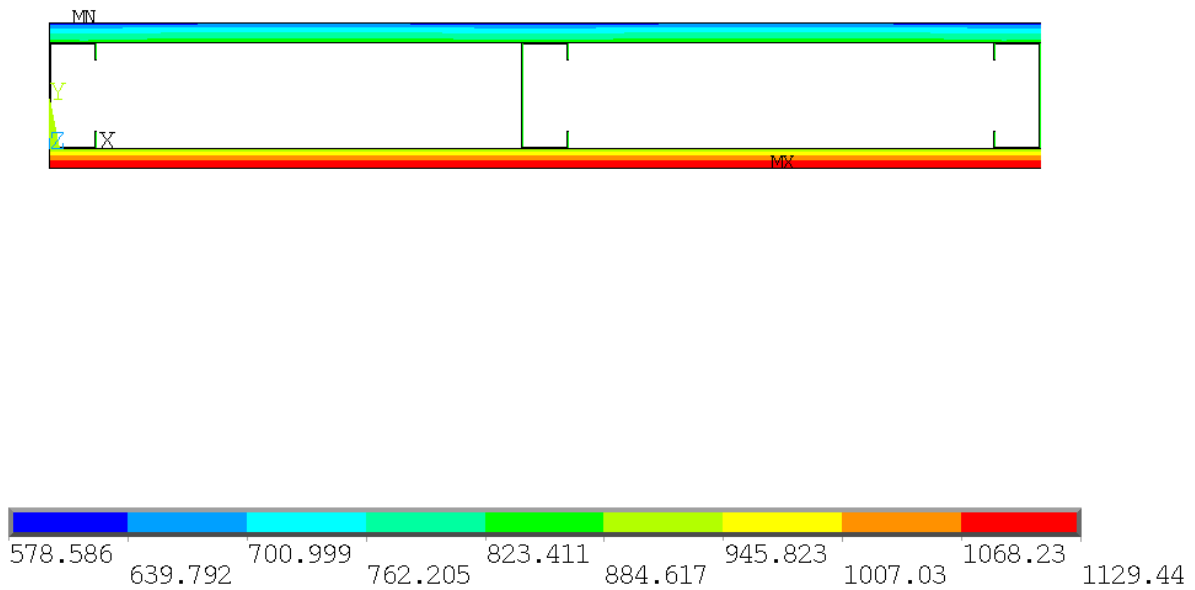


Figure 31: Numerical results for Specimen 16,  $t=300\text{min}$

Figure 32 presents the average temperature results for the temperature development in specimen 19.

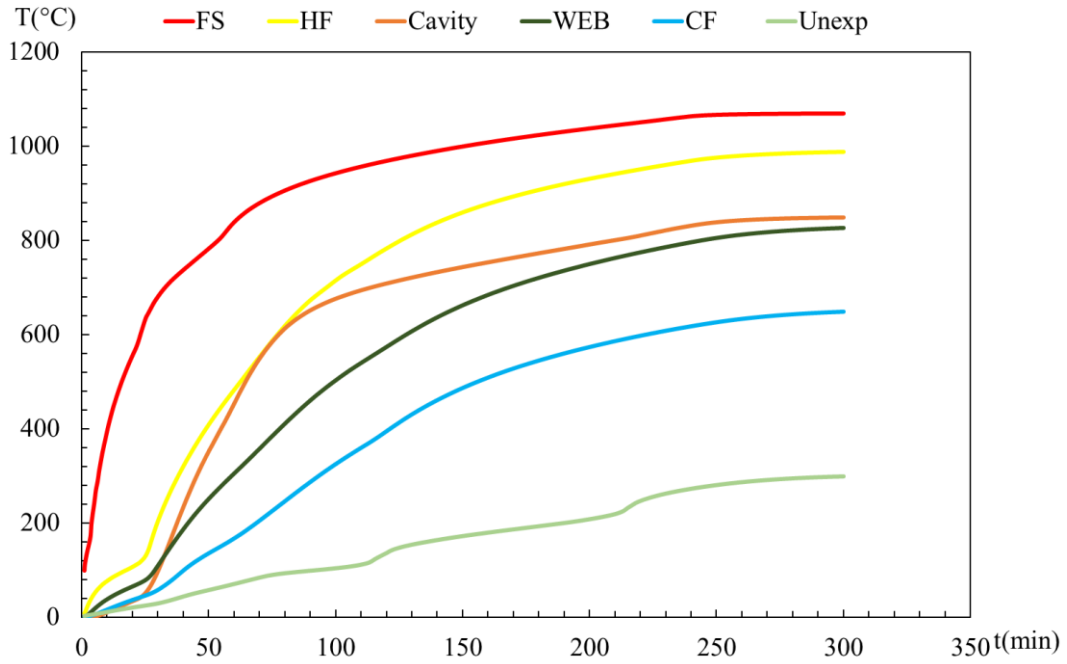


Figure 32: Specimen 19 - Average temperature results

Figure 33 presents the comparison between the average and the maximum temperature on the unexposed side for specimen 19.

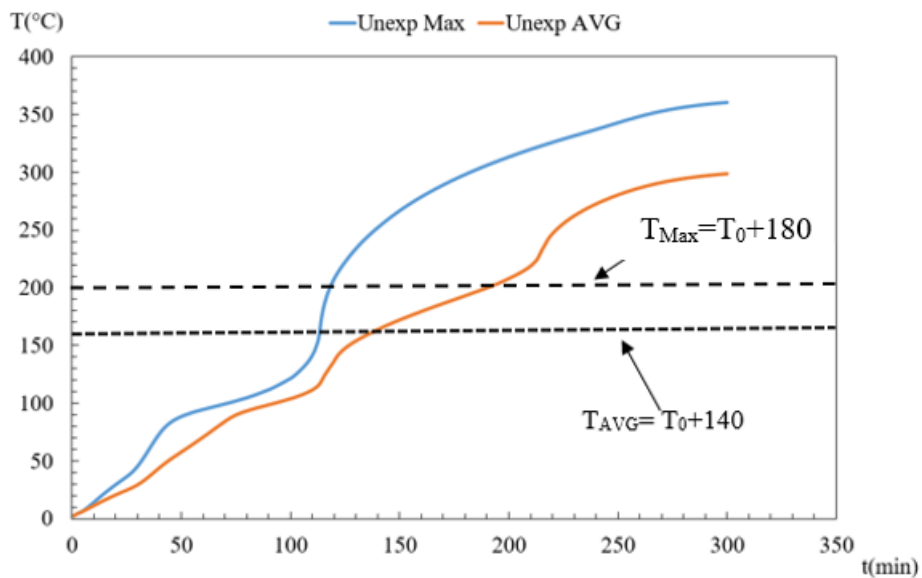


Figure 33: Specimen 19 - Average and maximum temperature on the unexposed side

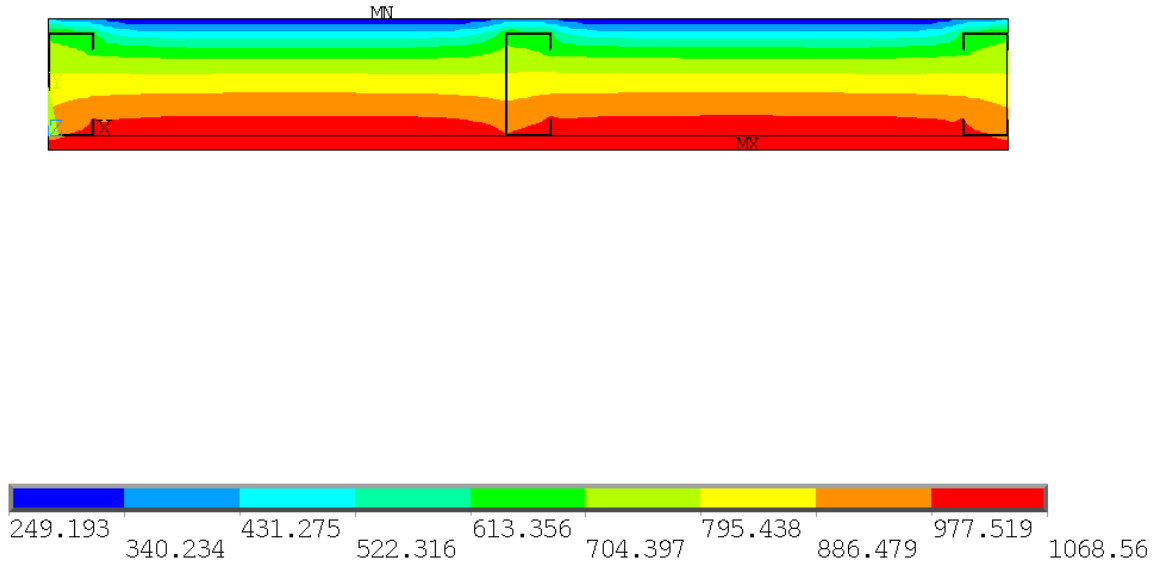


Figure 34: Numerical results for Specimen 19, t=300min

Figure 35 presents the average temperature results for the temperature development in specimen 25.

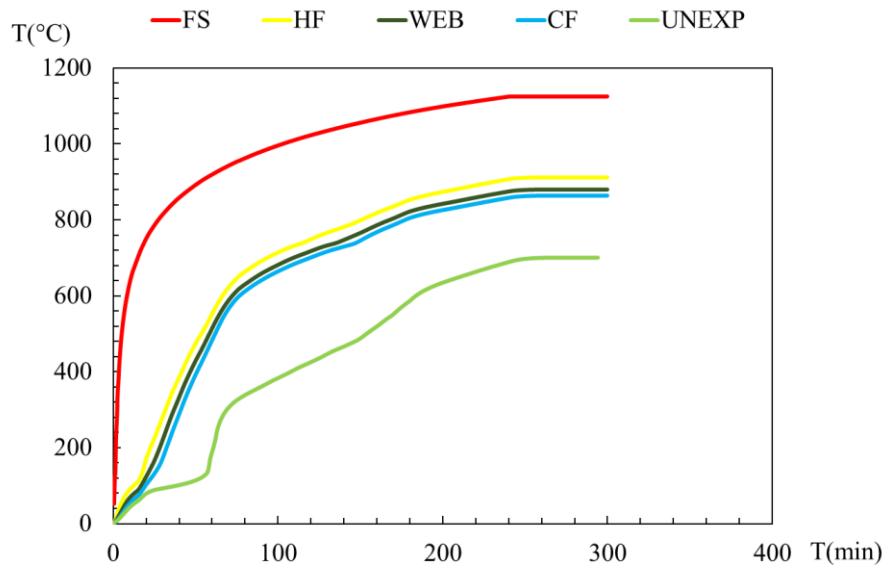


Figure 35: Specimen 25 - Average temperature results

Figure 36 presents the comparison between the average and the maximum temperature on the unexposed side for specimen 25.

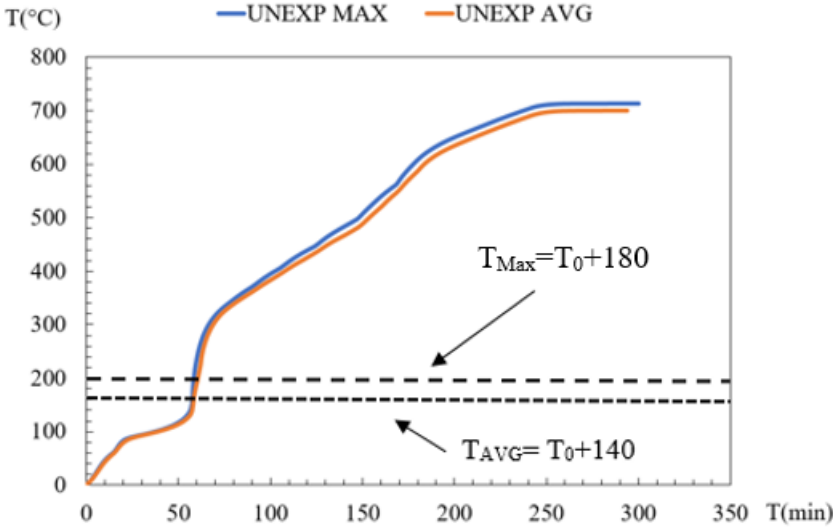


Figure 36: Specimen 25 - Average an maximum temperature on the unexposed side

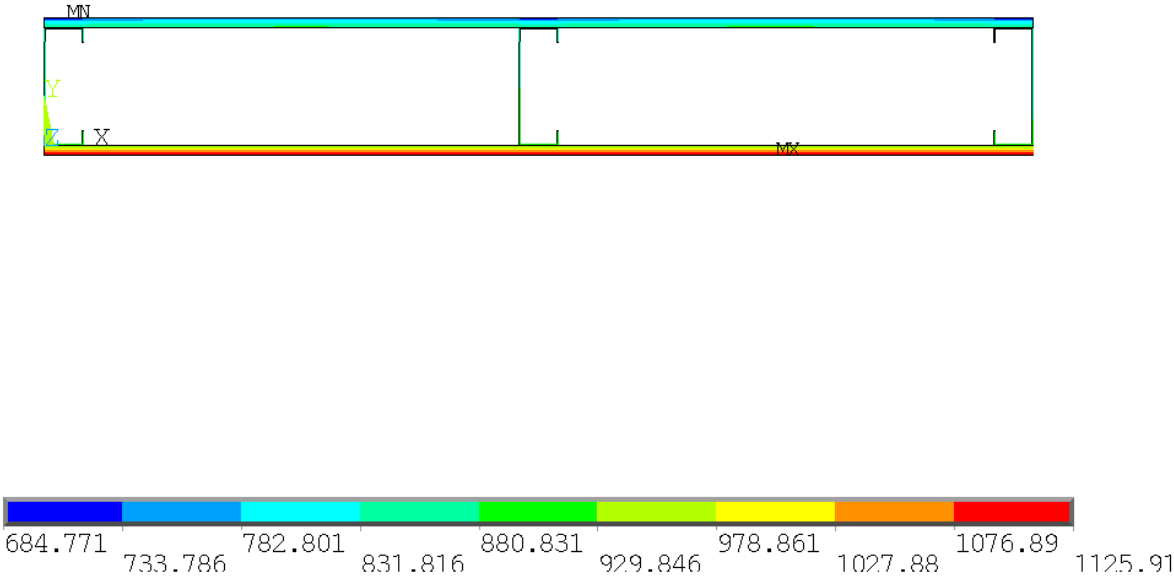


Figure 37: Numerical results for Specimen 25, t=300min

Figure 38 presents the average temperature results for the temperature development in specimen 37.

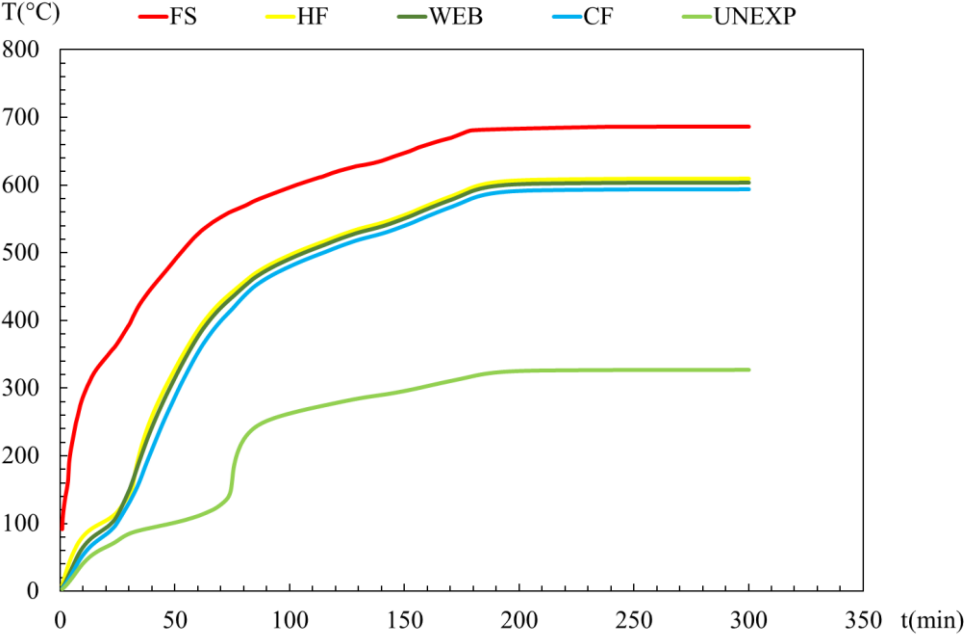


Figure 38: Specimen 37 - Average temperature results

Figure 39 presents the comparison between average and maximum temperature on the unexposed side for the specimen 37.

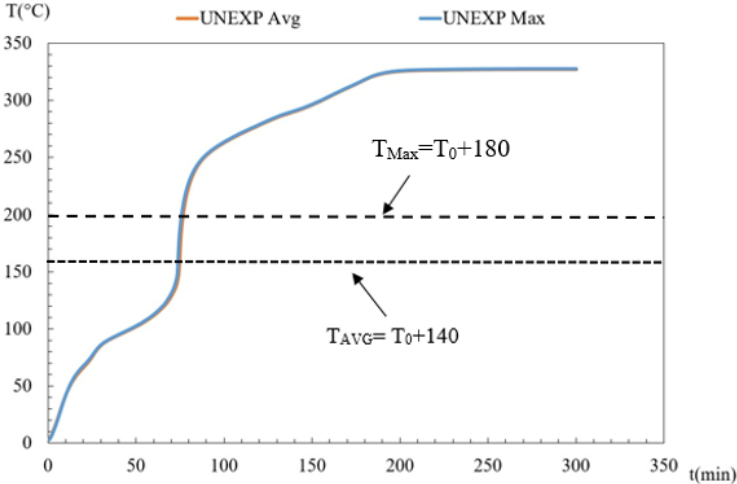
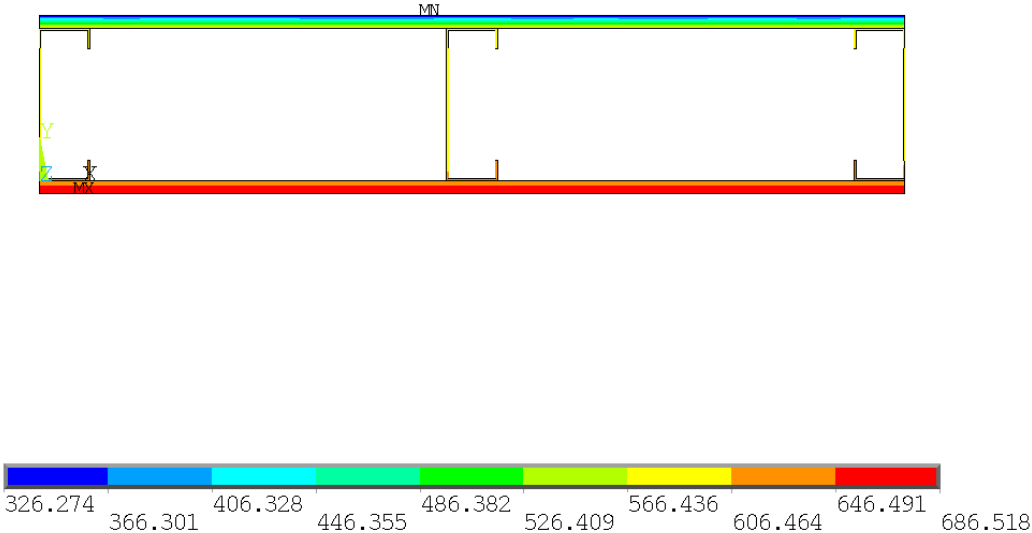


Figure 39: Specimen 37 - Average an maximum temperature on the unexposed side

The average and maximum curves are superposed because the temperature is uniform and there is no effect of the steel.



### 5.3 Discussion of the Results

#### Effect of the material and number of layers

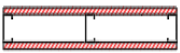


The LSF configurations of specimens 13, 14, and 15 are the same, with three studs and empty cavities, but with various protective layers, including single gypsum plasterboard, double gypsum plasterboard, and Rockwool and gypsum plasterboard composite.

The specimen 15 with the composite wall of Rockwool and plasterboard has the greatest fire resistance, as can be seen from the table 4, followed by the configuration when the gypsum layer was doubled.

The single plasterboard wall had the worst fire resistance (specimen13) and the double plasterboard wall (specimen14)



Table 4: Influence of the material and number of layer

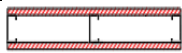
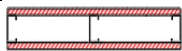
Specimen n°:	Drawing	Plate Layer (mm)	Fire resistance ( $T_{ave}$ )	Fire resistance ( $T_{max}$ )
13		1x12.5	55	56
14		2x12.5	129	133
15		1xGypsum(12.5mm) 1xRockwool(25mm) 1xGypsum (12.5mm)	-	-

### Effect of thickness of gypsum layer

In this parametric analysis we will analyse the effect of the thickness of the gypsum plasterboard.

For the same thickness of the steel and thickness of the cavity, increasing the plate thickness from 12.5 mm to 16 mm will result in an increase in the fire resistance by 19 min.


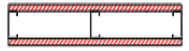
Table 5: Influence of the thickness of gypsum layer

Specimen n°:	Drawing	Plate Layer (mm)	Fire resistance ( $T_{ave}$ ) (min)	Fire resistance ( $T_{max}$ ) (min)
13		1x12.5	55	56
16		1x16	74	74

### Effect of stud spacing

This parametric analysis considers different spacing between studs to see their influence in the fire resistance. The geometry considered was the same as Specimen 13 but with increasing the studs spacing from 400 mm to 600mm.

Table 6: Influence of stud spacing

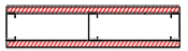

Specimen n°:	Drawing	stud spacing (mm)	Fire resistance ( $T_{ave}$ ) (min)	Fire resistance ( $T_{max}$ ) (min)
25		600	59	59
37		400	75	76

The decreasing of the studs spacing has improved the time of the fire resistance by 16 min.

### Effect of cavity thickness due to the dimension of the stud

This parametric analysis is based on various stud dimensions for the same wall configurations. The table 7 shows the fire resistance of the cases for cavity thicknesses from 90mm and 150mm. It is observed that by increasing the thickness of the cavity insulation the time of the fire resistance improved by 20 min.

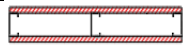

Table 7: Influence of cavity thickness due to the dimension of the stud

Specimen n°:	Drawing	Dimension of the stud (mm)	Fire resistance ( $T_{ave}$ ) (min)	Fire resistance ( $T_{max}$ ) (min)
13		C90x40x15x1.15	55	56
37		C150x50x20x2.0	75	76

### Effect of adding cavity insulation

The configuration of the specimen is maintained for the whole of this parametric analysis, however, an insulating material has been added to the cavity.

Table 8: Influence of adding cavity insulation

Specimen n°:	Drawing	Cavity insulation	Fire resistance ( $T_{ave}$ ) (min)	Fire resistance ( $T_{max}$ ) (min)
13		No	55	56
19		Rockwool	136	118

The failure occurs for the specimen 13 with no cavity insulation after 55 min, however when the Rockwool is added to the cavity (specimen 19), the failure occurs after 136 min.

As conclusion the cavity insulation significantly improves the fire resistance of LSF walls.

# Chapter 6

## 6 Conclusion

This work investigates the fire impacts on non-loadbearing walls using a Light Steel Frame (LSF) structure. The study includes a numerical validation of 2 specimens taken from the investigation developed by [24]. Various configurations and 48 parametric analysis were performed in order to assess the influence of different parameters of the fire resistance according to the thermal insulation criterion (I), to show the influence of structural stud space, cavity thickness, effect of the number protective layer, effect of thickness of gypsum of the protective layer, and the effect of insulating material in the cavity.

This investigation was evaluated using a two-dimensional Finite Element (FE) model created in ANSYS® Multiphysics software. The results explain that the most relevant parameter in the fire resistance of the LSF non-loadbearing walls is the cavity insulation. However, this parameter depends on the thickness of the cavity.

Also the results show that the increase of number of the protection layers has a significant improvement on the fire resistance of the walls but less good than the performance of wall with cavity insulation.

For future works, other parameters should be tested such as materials for the cavity insulation and its thickness, various spacing between the studs also a different stud's dimensions.

# References

- [1] Y. Dias, P. Keerthan, and M. Mahendran, "Fire performance of steel and plasterboard sheathed non-load bearing LSF walls." *Fire Safety Journal*, pp. 1-18, 2019.
- [2] Y. Sakumoto, T. Hirakawa, H. Masuda, and K. Nakamura, "Fire Resistance of Walls and Floors Using Light-Gauge Steel Shapes." *Journal of Structural Engineering*, pp. 1522-1530, 2003.
- [3] V. K. R. Kodur and M. A. Sultan, "Factors Influencing Fire Resistance of Load-bearing Steel Stud Walls." *Fire Technology*, pp. 5-26, 2006.
- [4] P. Kolarkar and M. Mahendran, "Experimental studies of non-load bearing steel wall systems under fire conditions." *Fire Safety Journal*, pp. 85-104, 2012.
- [5] A. D. Ariyanayagam and M. Mahendran, "Fire tests of non-load bearing light gauge steel frame walls lined with calcium silicate boards and gypsum plasterboards." *Thin-Walled Structures*, pp. 86-99, 2017.
- [6] A. D. Ariyanayagam and M. Mahendran, "Fire performance of load bearing LSF wall systems made of low strength steel studs." *Thin-Walled Structures*, pp. 487-504, 2018.
- [7] S. M. Khetata, P. A. Piloto, and A. B. Gavilán, "Fire resistance of composite non-load bearing light steel framing walls." *Journal of Fire Sciences*, pp. 136-155, 2020.
- [8] F. Alfawakhiri, M. A. Sultan, and D. H. MacKinnon, *Fire Technology*, pp. 308-335, 2000
- [9] "Proceedings of the 13th international conference on Supercomputing - ICS ." 1999, doi: 10.1145/305138
- [10] P. Keerthan and M. Mahendran, "Numerical modelling of non-load-bearing light gauge cold-formed steel frame walls under fire conditions." *Journal of Fire Sciences*, pp. 375-403, 2012.

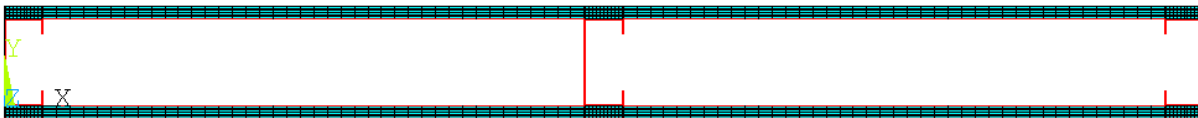
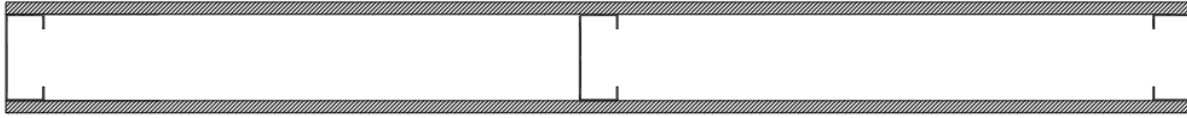
- [11] M. Rusthi, P. Keerthan, M. Mahendran, and A. Ariyanayagam, "Investigating the fire performance of LSF wall systems using finite element analyses." *Journal of Structural Fire Engineering*, pp. 354-376, 2017.
- [12] Y. Tao, M. Mahendran, and A. Ariyanayagam, "Numerical study of LSF walls made of cold-formed steel hollow section studs in fire." *Thin-Walled Structures*, p. 108181, 2021.
- [13] International Organization for Standardization, ISO 834-1 Fire-Resistance Tests - Elements of Building Construction Part 1: General Requirements, (1999).
- [14] Standards Australia, AS 1530.4 - Methods for Fire Tests on Building Materials, Components and Structures, (2005) 151.
- [15] EN (Belgium). 1991-1-2, Eurocode 1: Actions on structures - part 1-2: General actions - actions on structures exposed to fire. Brussels: European Committee for Standardization, 2002.
- [16] M. K. Thompson and J. M. Thompson, ANSYS Mechanical APDL for Finite Element Analysis. Butterworth-Heinemann, 2017.
- [17] APDL, ANSYS Mechanical. Mechanical applications Theory reference. ANSYS Release, 2010, vol. 13, no 010.
- [18] EN (Belgium) 1363-1, Fire resistance tests - part 1: General requirements. Brussels: European Committee for Standardization, 2020.
- [19] EN (Belgium) 1364-1, Fire resistance tests for non-loadbearing elements. part 1: Walls. Brussels: European Committee for Standardization, 1999.
- [20] E. Madenci and I. Guven, The Finite Element Method and Applications in Engineering Using ANSYS®. Springer, 2015.
- [21] EN (Belgium) 1993-1-2, Eurocode 3: Design of steel structures. part 1-2: General rules - structural fire design. Brussels: European Committee for Standardization, 2005.

- [22] EN (Belguim) 1995-1-2, Eurocode 5 – design of timber structures. part 1-2: General – structural fire design. Brussels: European Committee for Standardization, 2004.
- [23] Rockwool aislamiento de lana de roca. ROCKWOOL aislamiento de lana de roca. (n.d.). Retrieved December 20, 2022, from <https://www.rockwool.com/es/>
- [24] P. Kolarkar and M. Mahendran, “Experimental studies of non-load bearing steel wall systems under fire conditions.” Fire Safety Journal, vol. 53, pp. 85-104, 2012, doi: 10.1016/j.firesaf.2012.06.009.

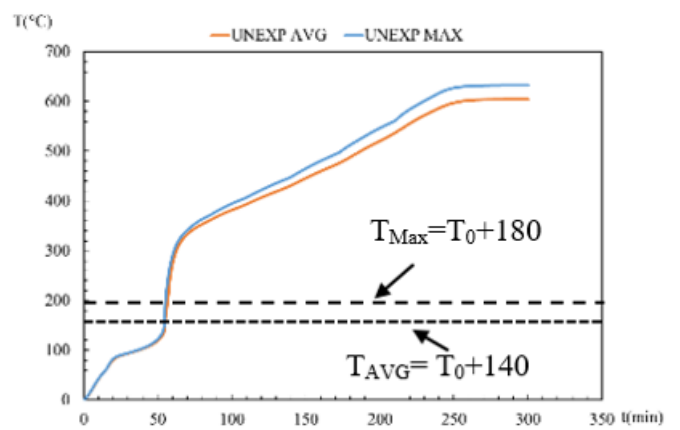
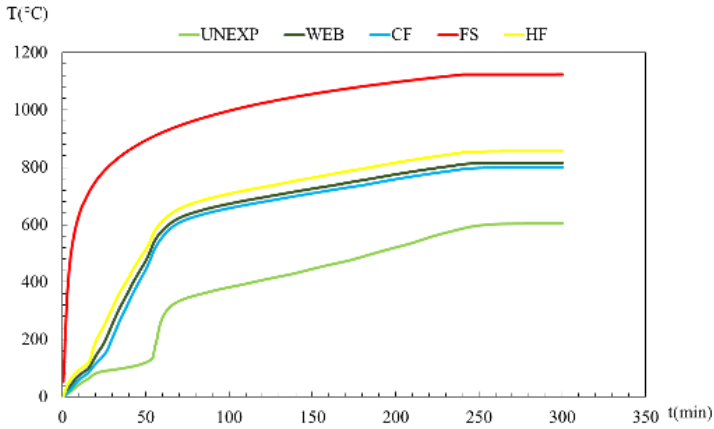
# Appendix



Specimen n°	Steel Section	Spacing between the studs (mm)	N° Layers gyps	Cavity insulation
1	C90x40x15x1.15	600	1Gypsum12.5	/



Mesh from Ansys



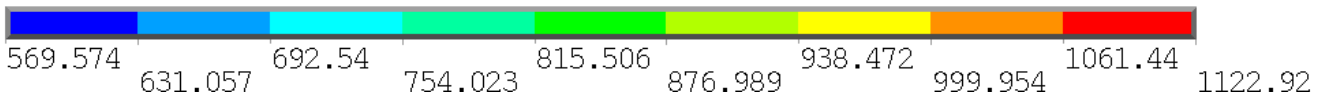
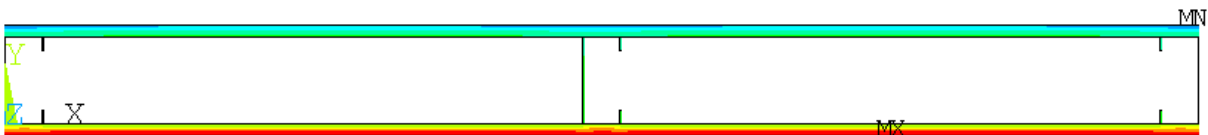
Average temperature results

Unexposed curves

Ansys Fire Resistance(min)

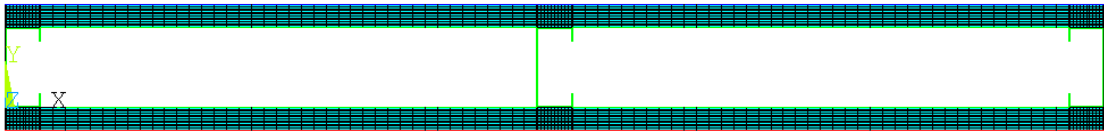
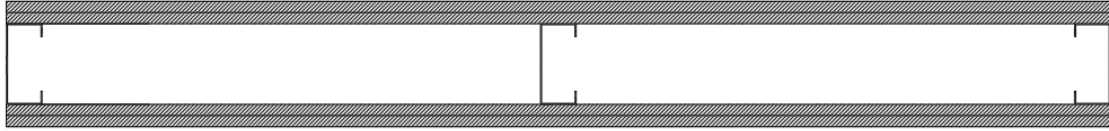
Avg : 55

Max : 55

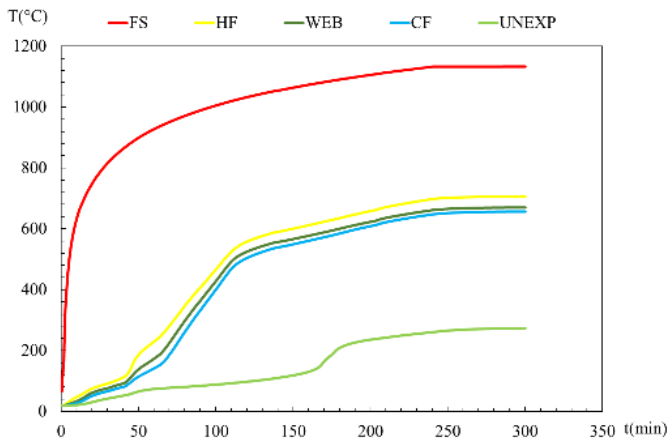


Ansys result in t= 300 min

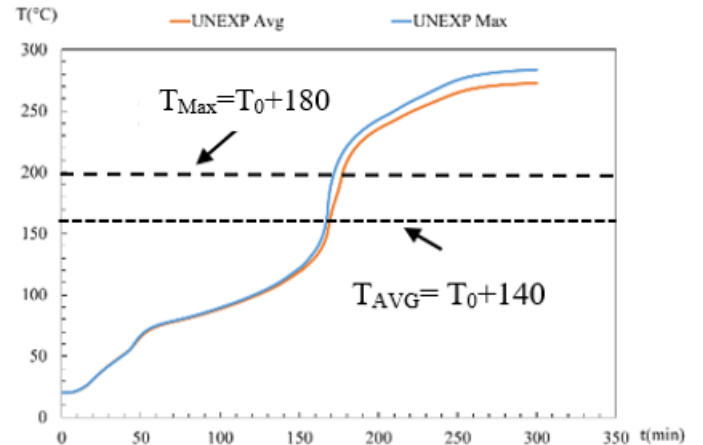
Specimen n°	Steel Section	Spacing between the studs (mm)	N° Layers gyps	Cavity insulation
2	C90x40x15x1.15	600	2Gypsum12.5	/



Mesh from Ansys



Average temperature results

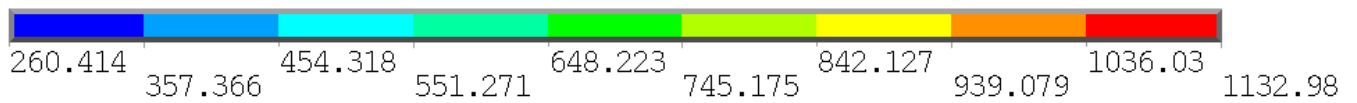
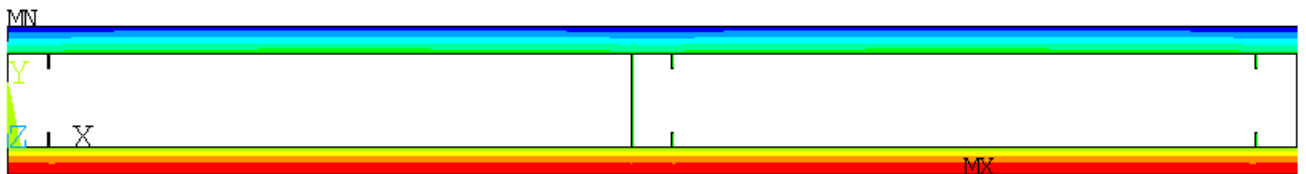


Unexposed curves

Ansys Fire Resistance(min)

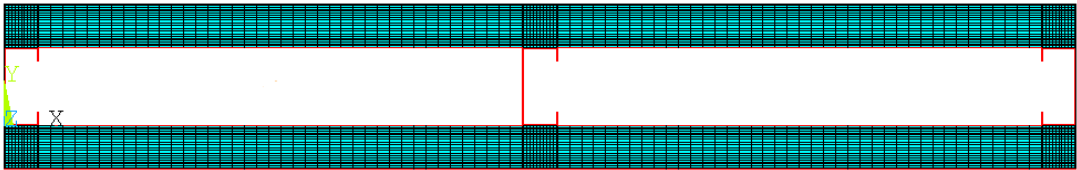
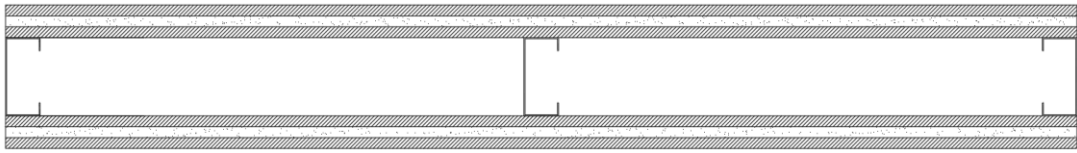
Avg : 168

Max : 170

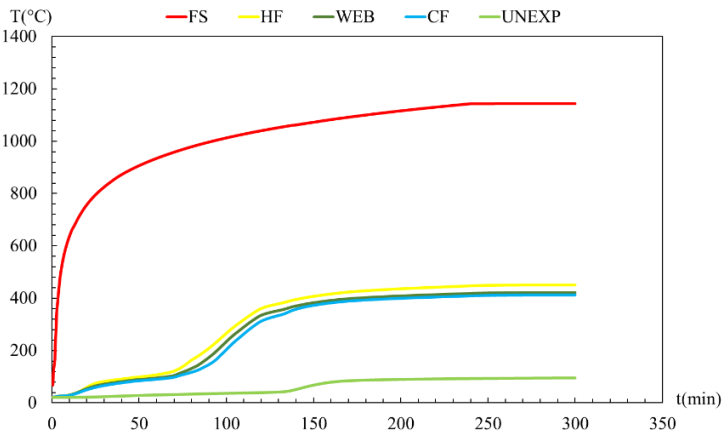


Ansys result in t= 300 min

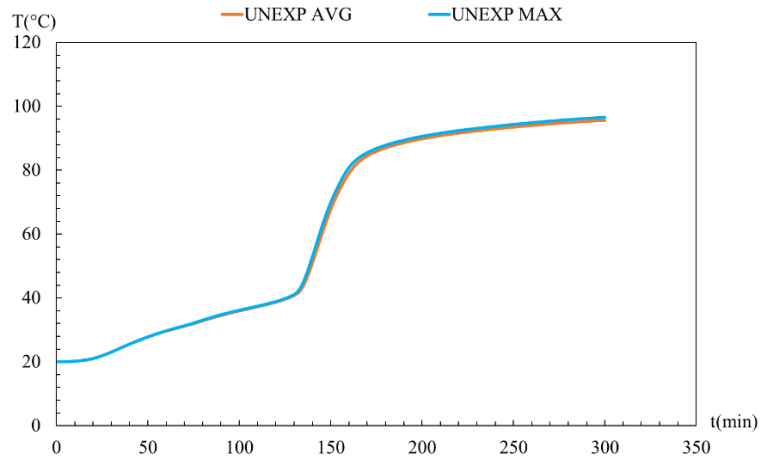
Specimen n°	Steel Section	Spacing between the studs (mm)	N° Layers gyps	Cavity insulation
3	C90x40x15x1.15	600	1Gypsum12.5 1Rockwool25 1Gypsum12.5	/



Mesh from Ansys

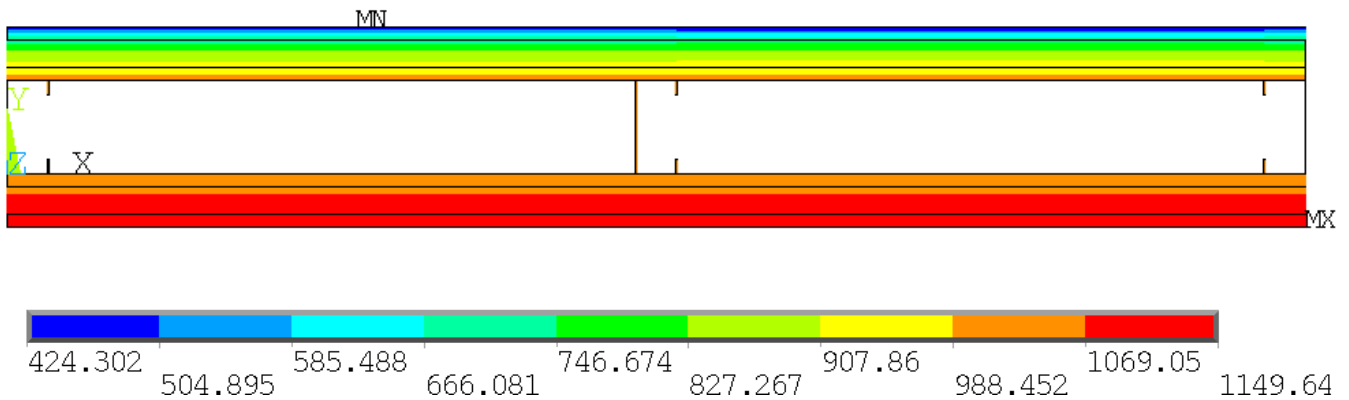


Average temperature results



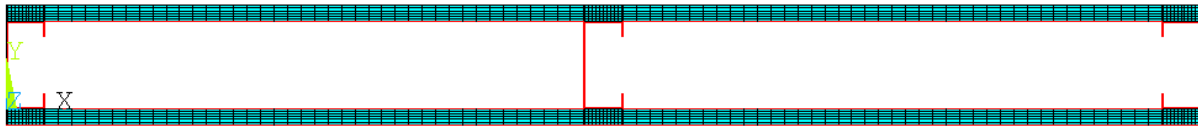
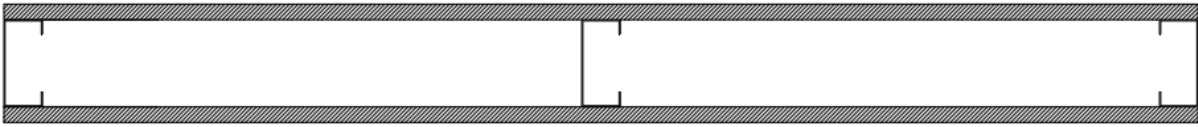
Unexposed curves

Ansys Fire Resistance(min)

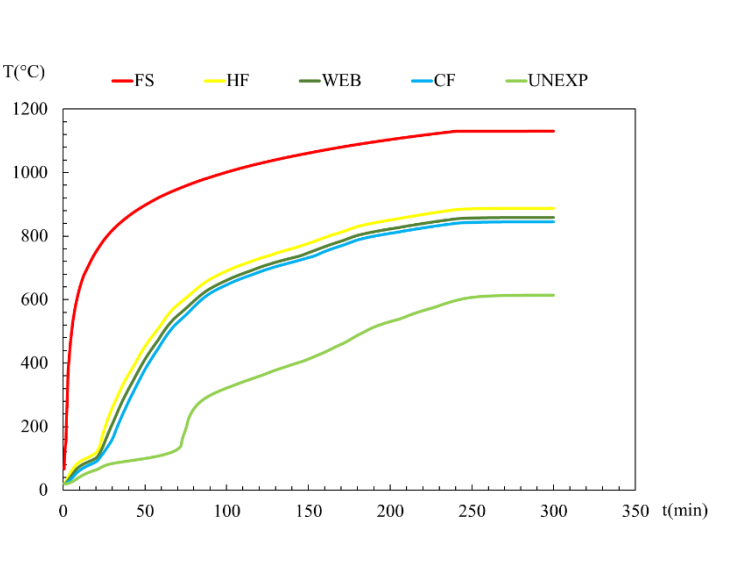


Ansys result in t= 300 min

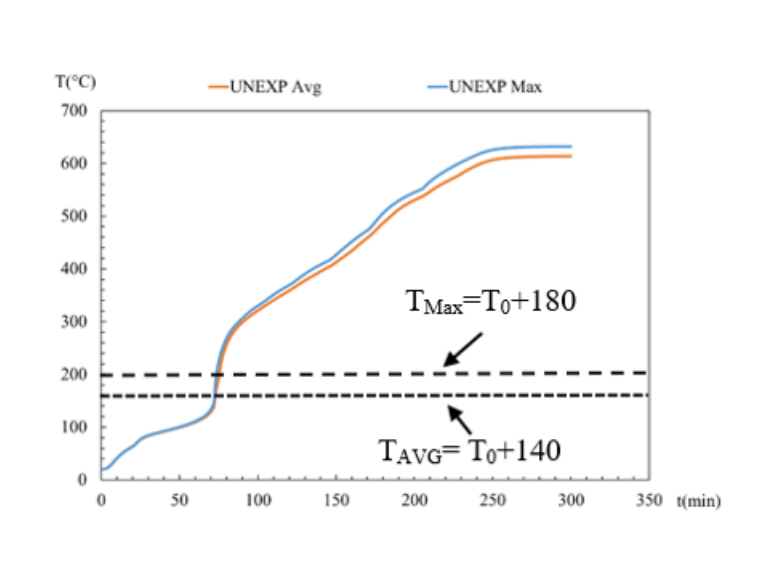
Specimen n°	Steel Section	Spacing between the studs (mm)	N° Layers gyps	Cavity insulation
4	C90x40x15x1.15	600	1Gypsum16	/



Mesh from Ansys

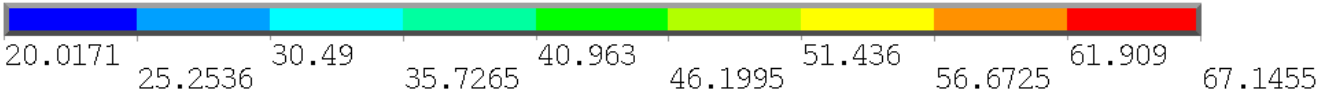
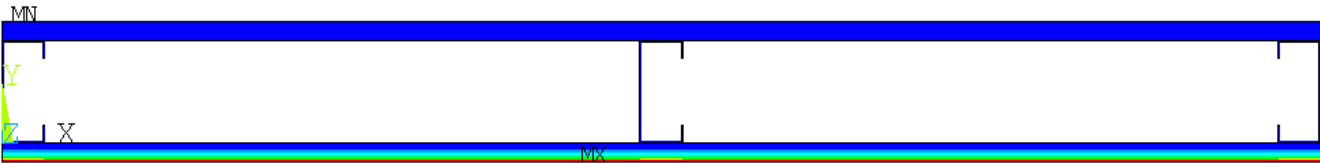


Average temperature results



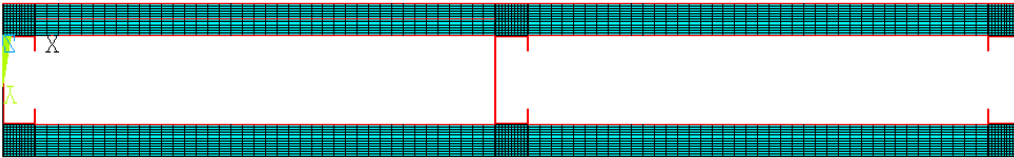
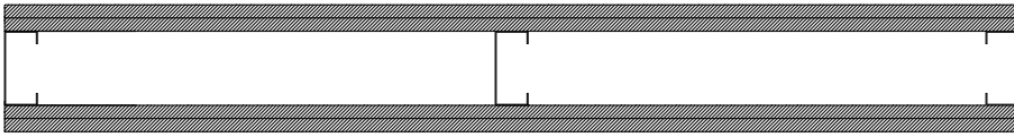
Unexposed curves

Ansys Fire Resistance(min)	Avg :73	Max :73
----------------------------	---------	---------

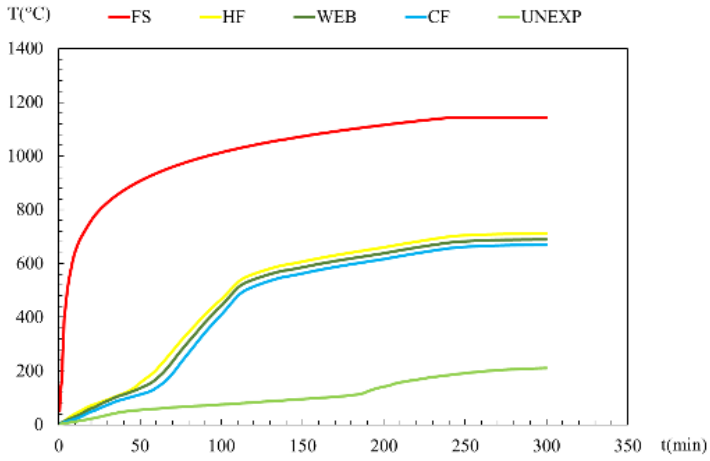


Ansys result tt= 1 min

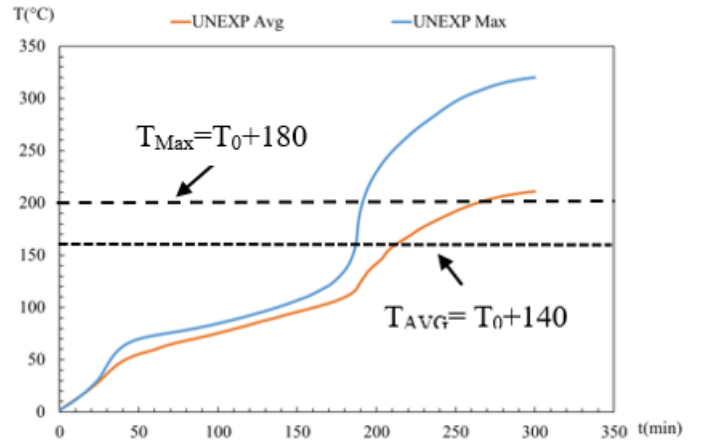
Specimen n°	Steel Section	Spacing between the studs (mm)	N° Layers gyps	Cavity insulation
5	C90x40x15x1.15	600	2Gypsum16	/



Mesh from Ansys



Average temperature results

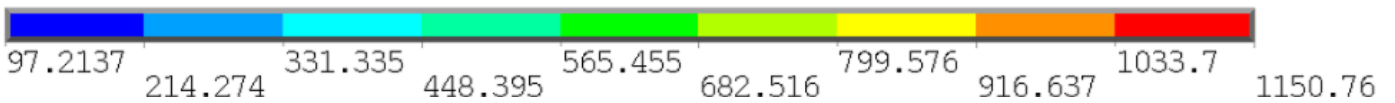
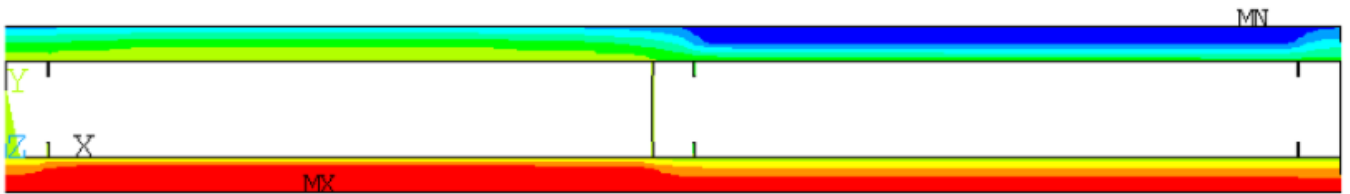


Unexposed curves

Ansys Fire Resistance(min)

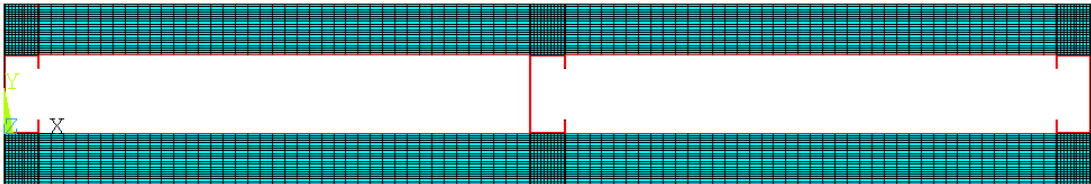
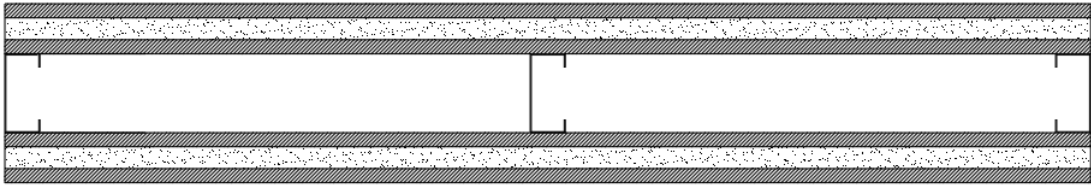
Avg : 209

Max : 192

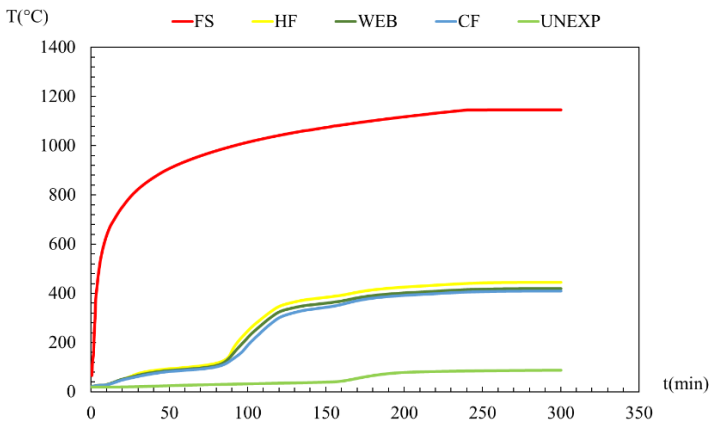


Ansys result in t= 300 min

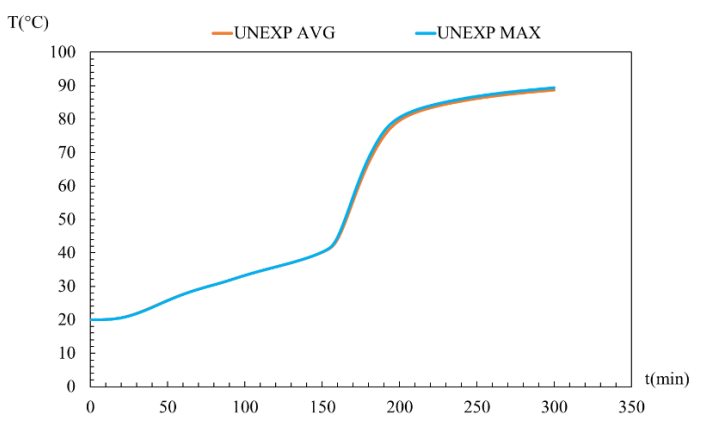
Specimen n°	Steel Section	Spacing between the studs (mm)	N° Layers gyps	Cavity insulation
6	C90x40x15x1.15	600	1Gypsum16 1Rockwool25 1Gypsum16	/



Mesh from Ansys

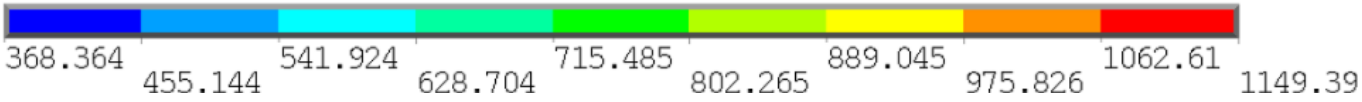
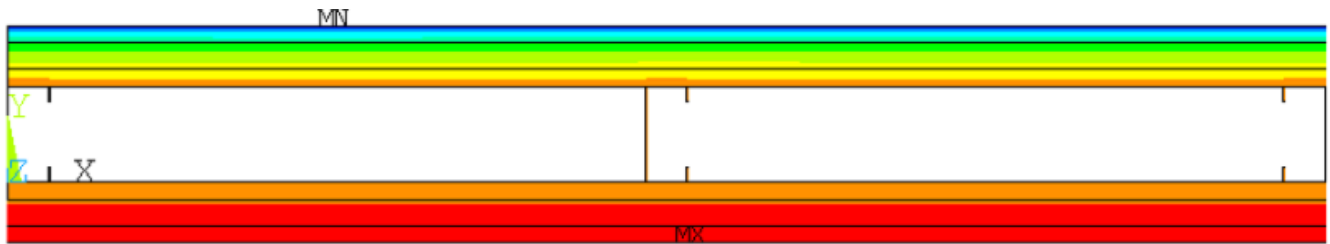


Average temperature results



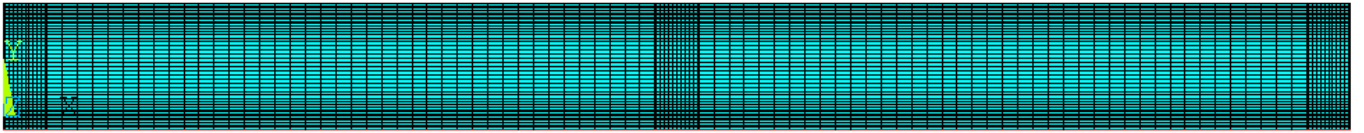
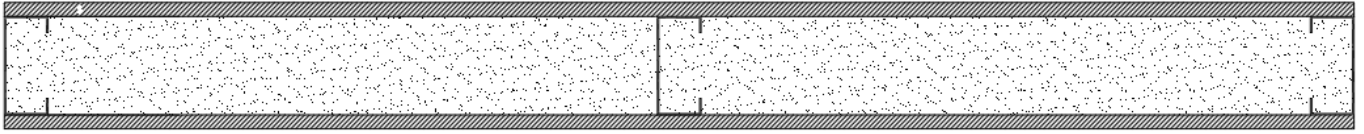
Unexposed curves

Ansys Fire Resistance(min)

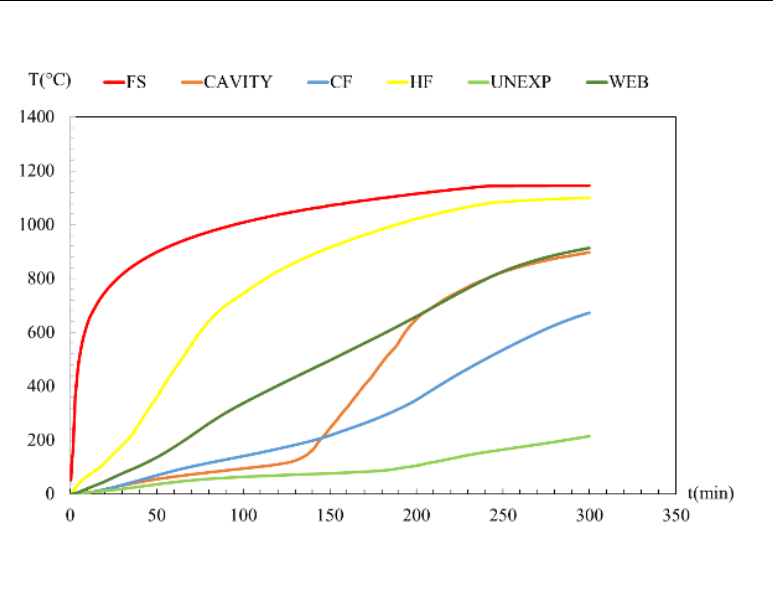


Ansys result in t= 240 min

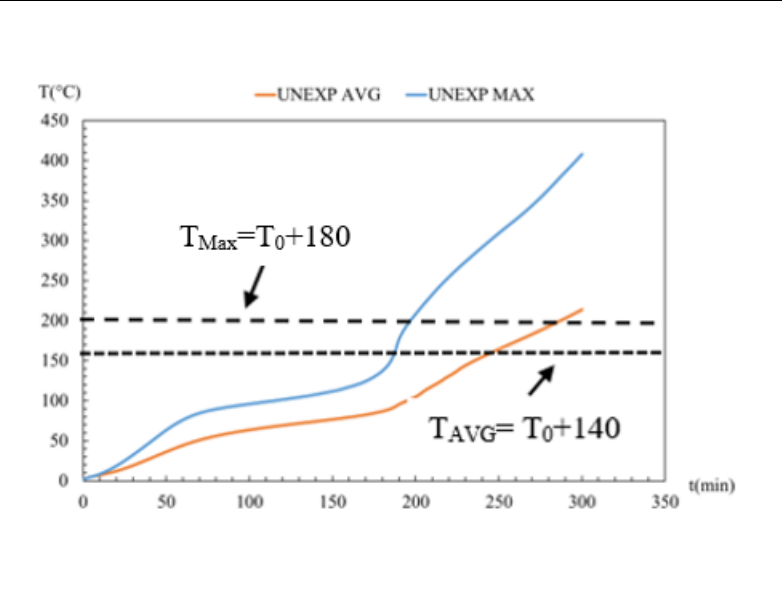
Specimen n°	Steel Section	Spacing between the studs (mm)	N° Layers gyps	Cavity insulation
7	C90x40x15x1.15	600	1Gypsum12.5	Rockwool



Mesh from Ansys



Average temperature results

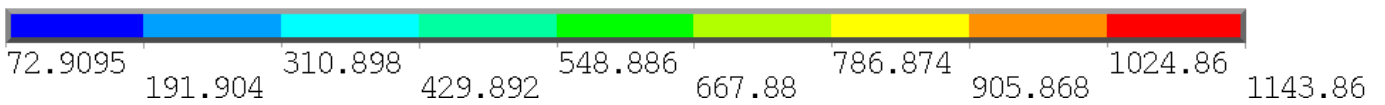
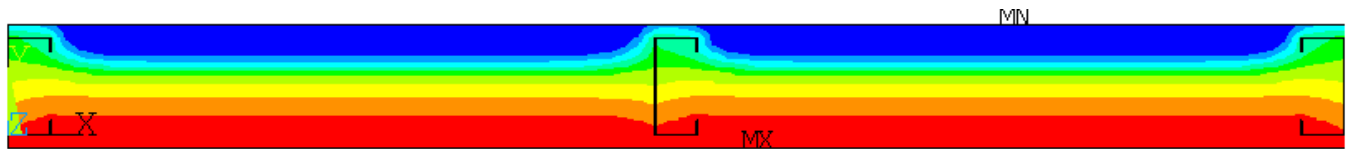


Unexposed curves

Ansys Fire Resistance(min)

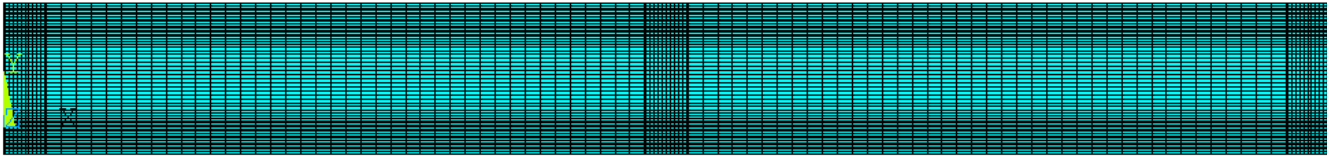
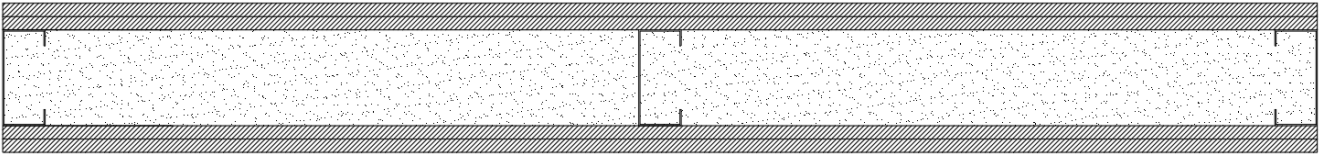
Avg : 243

Max : 199

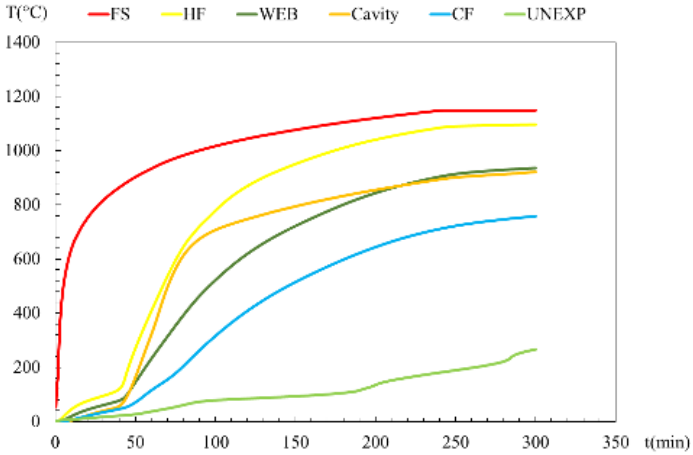


Ansys result in t= 240

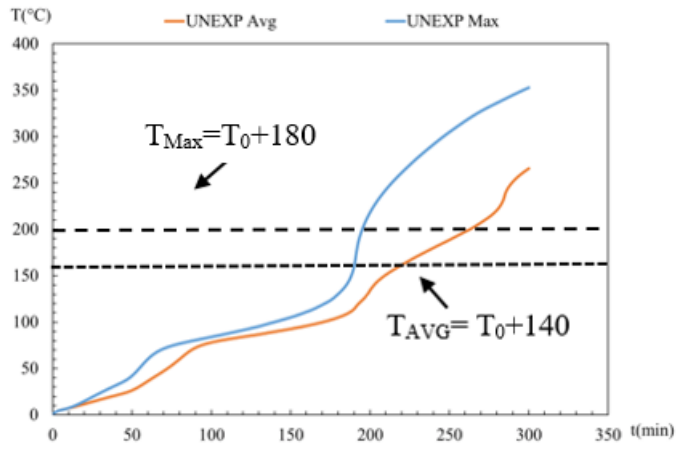
Specimen n°	Steel Section	Spacing between the studs (mm)	N° Layers gyps	Cavity insulation
8	C90x40x15x1.15	600	2Gypsum12.5	Rockwool



Mesh from Ansys



Average temperature results

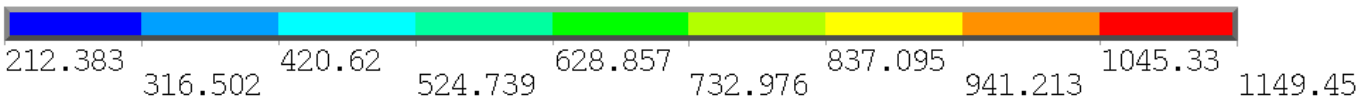
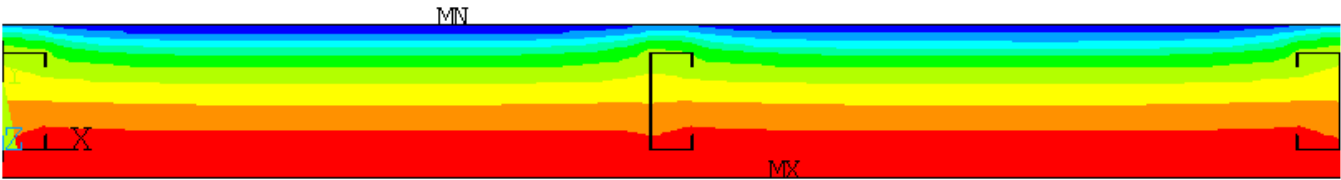


Unexposed curves

Ansys Fire Resistance(min)

Avg :218

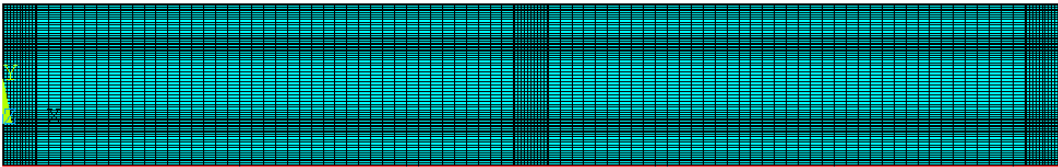
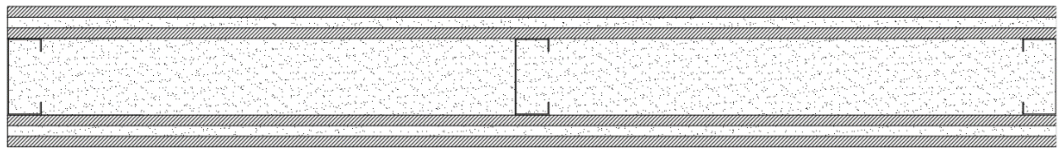
Max :195



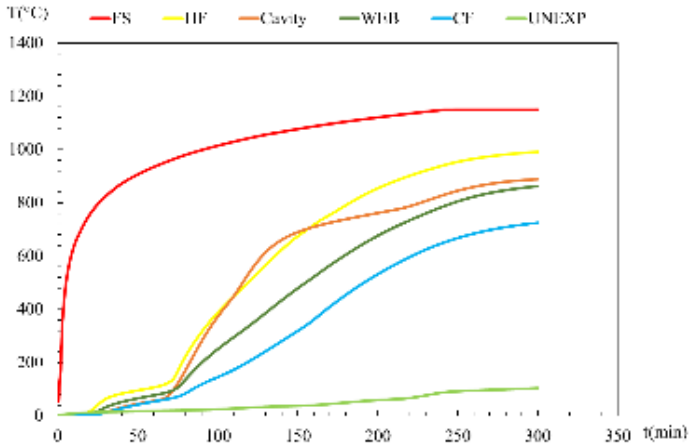
Ansys result in t= 300 min



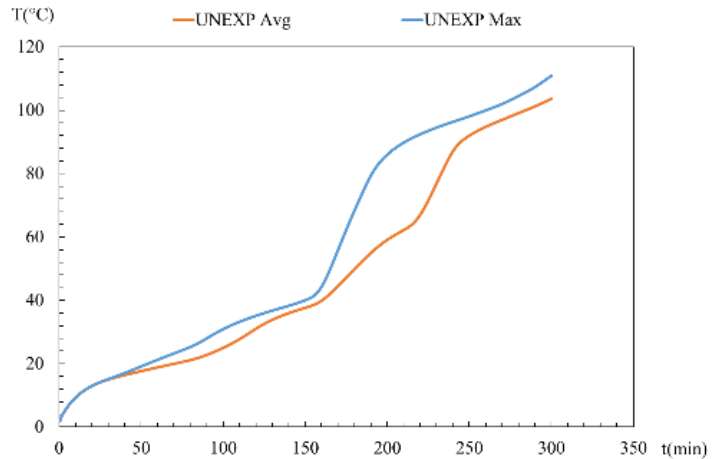
Specimen n°	Steel Section	Spacing between the studs (mm)	N° Layers gyps	Cavity insulation
9	C90x40x15x1.15	600	1Gypsum12.5 1Rockwool25 1Gypsum12.5	Rockwool



Mesh from Ansys

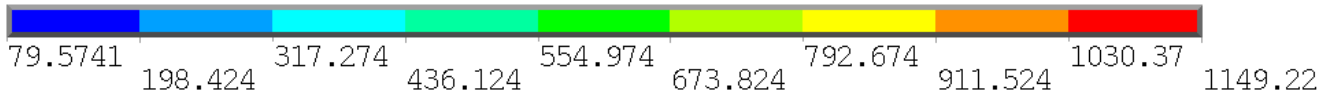
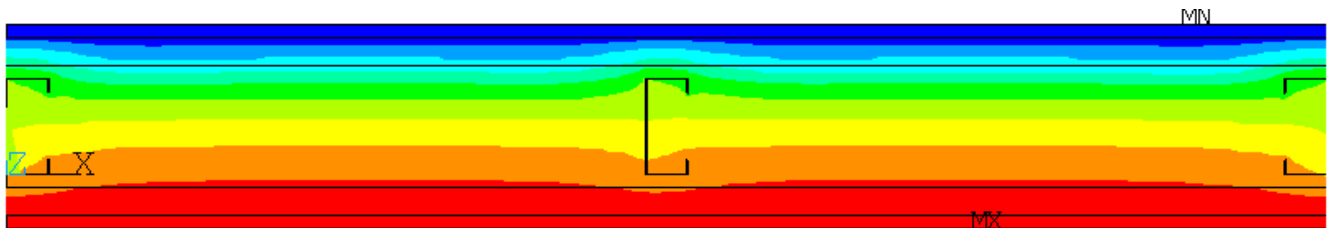


Average temperature results



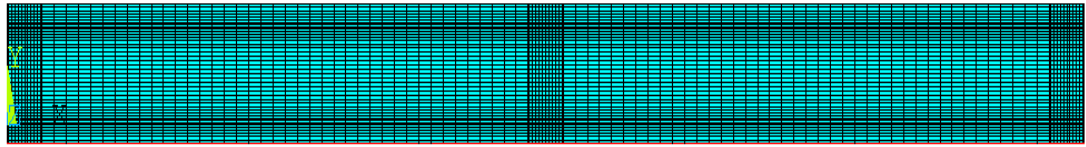
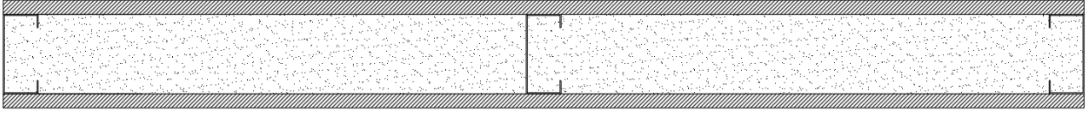
Unexposed curves

Ansys Fire Resistance(min)

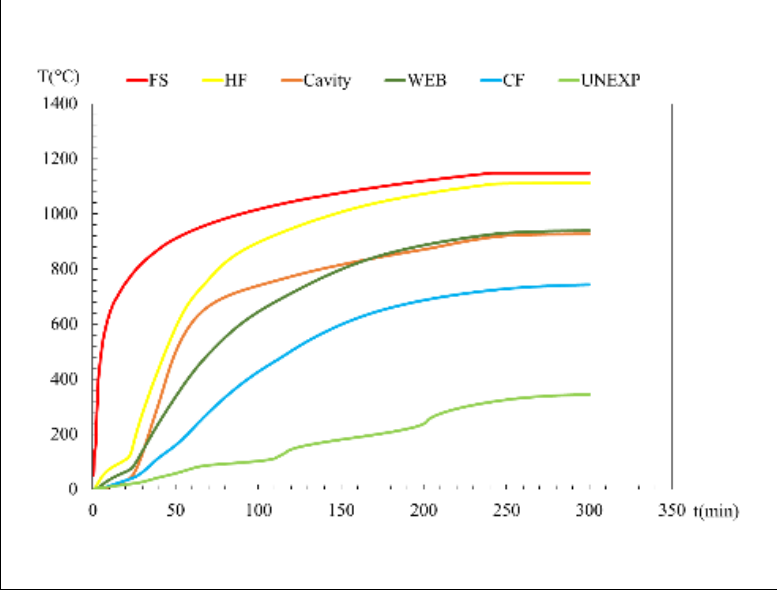


Ansys result in t= 240 min

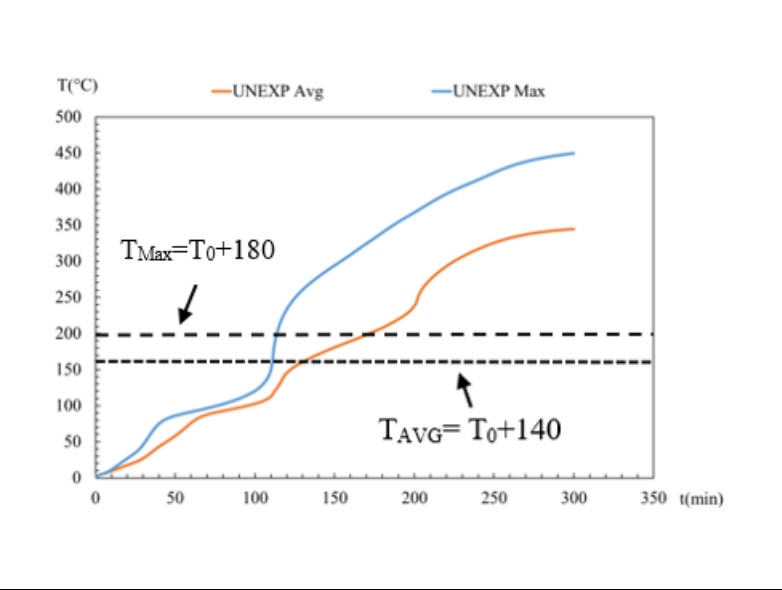
Specimen n°	Steel Section	Spacing between the studs (mm)	N° Layers gyps	Cavity insulation
10	C90x40x15x1.15	600	1Gypsum16	Rockwool



Mesh from Ansys

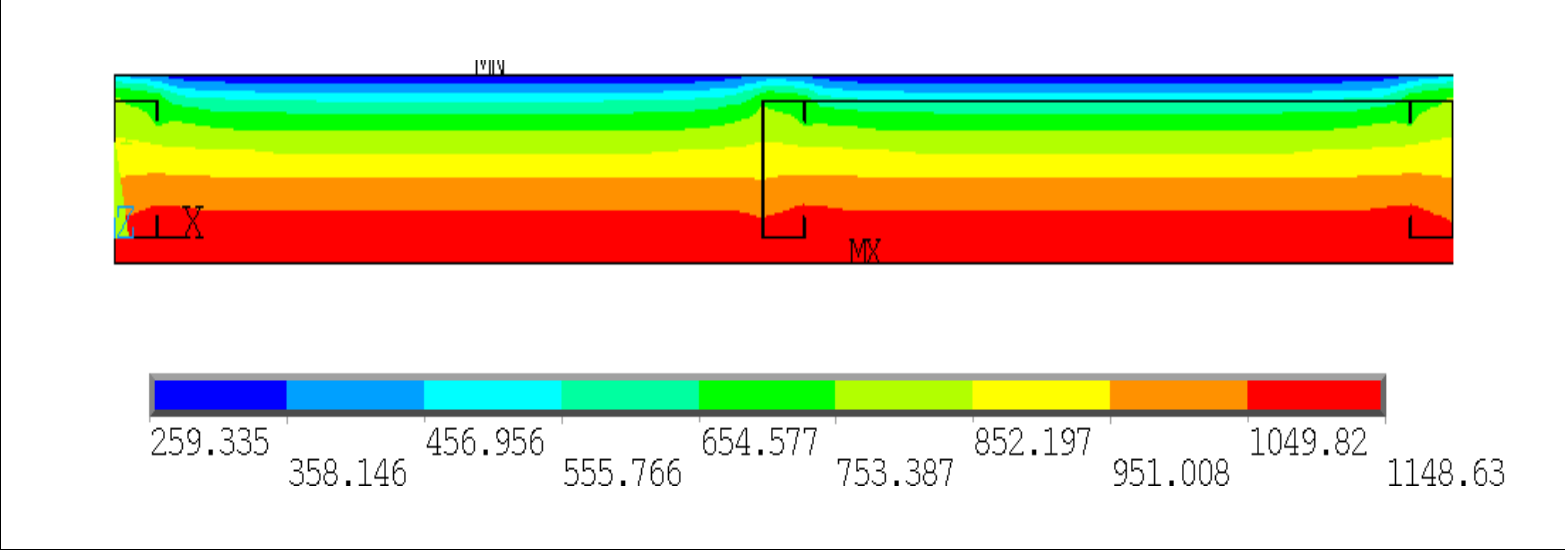


Average temperature results



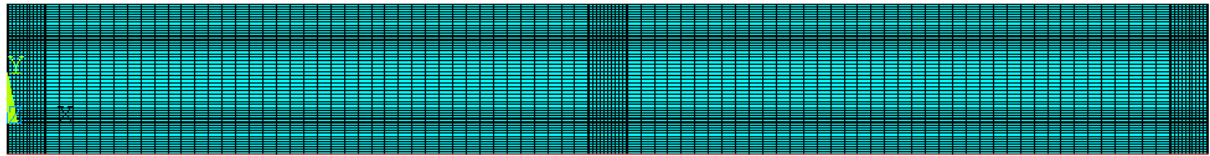
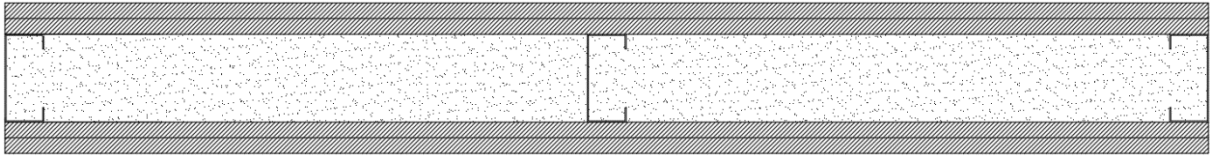
Unexposed curves

Ansys Fire Resistance(min)	Avg : 130	Max : 112
----------------------------	-----------	-----------

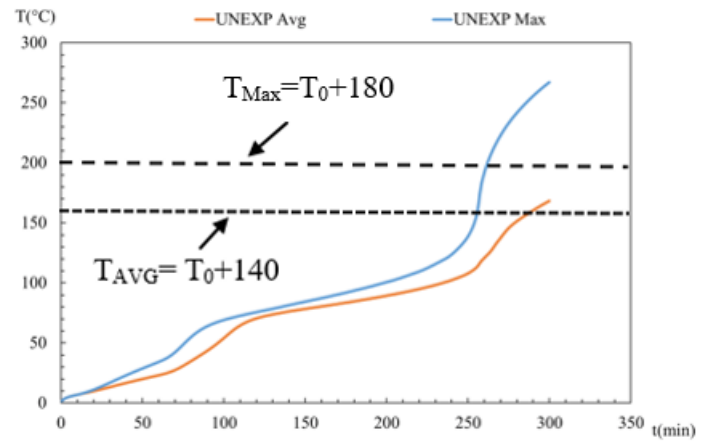
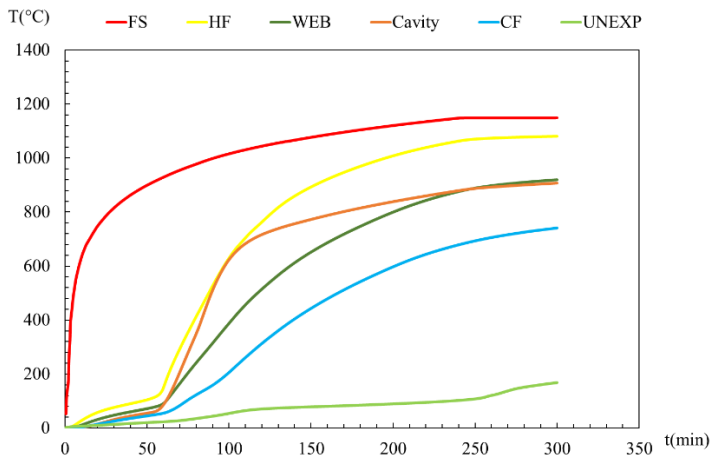


Ansys result in t= 240 min

Specimen n°	Steel Section	Spacing between the studs (mm)	N° Layers gyps	Cavity insulation
11	C90x40x15x1.15	600	2Gypsum16	Rockwool



Mesh from Ansys



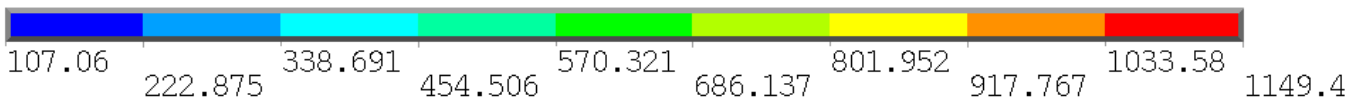
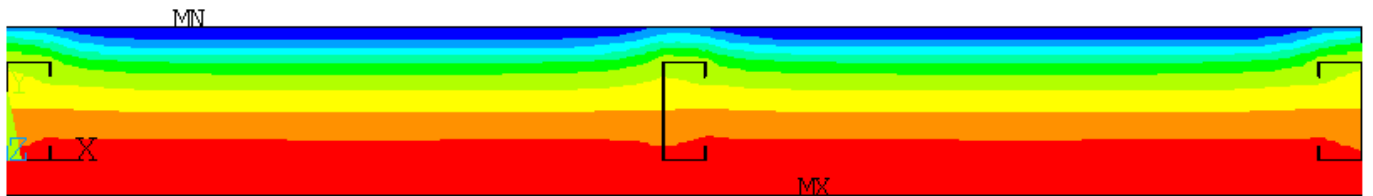
Average temperature results

Unexposed curves

Ansys Fire Resistance(min)

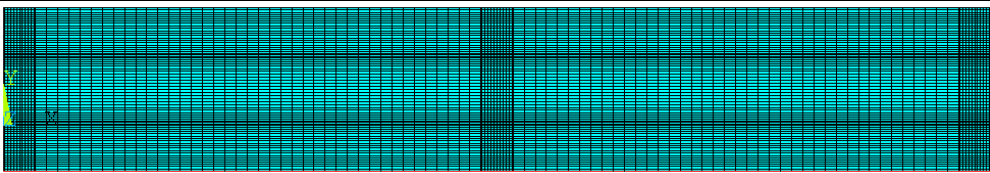
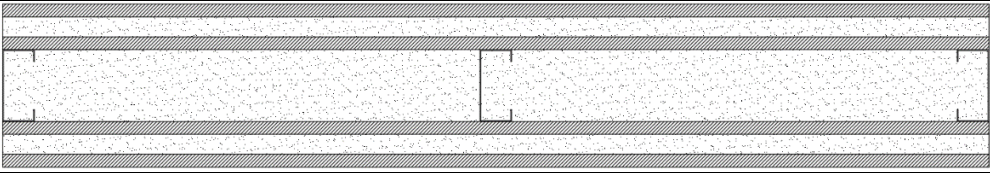
Avg : 288

Max : 261

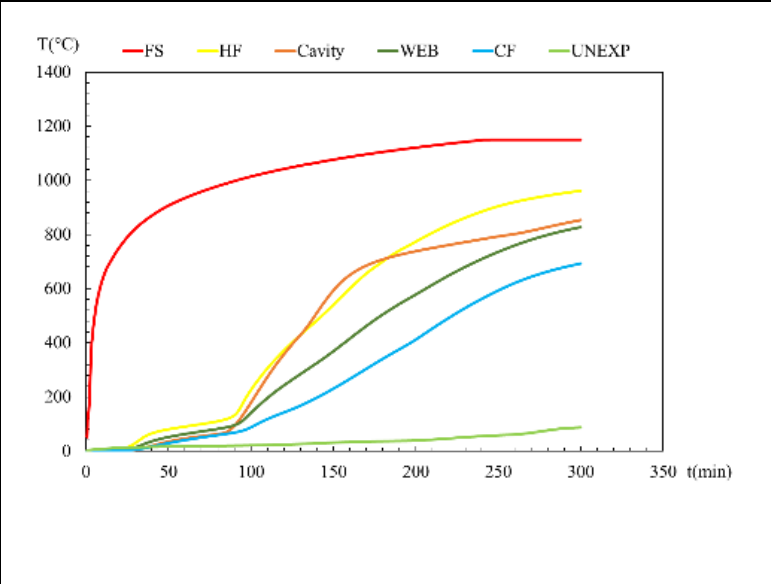


Ansys result in t= 300 min

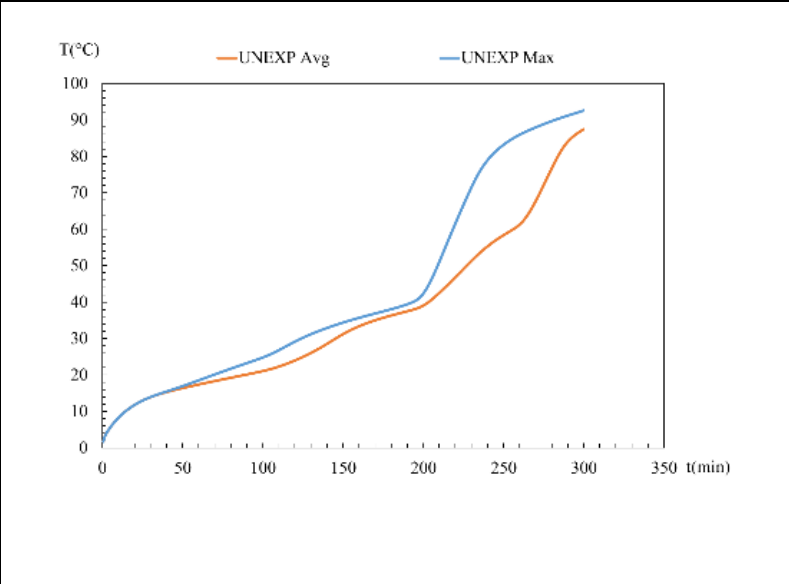
Specimen n°	Steel Section	Spacing between the studs (mm)	N° Layers gyps	Cavity insulation
12	C90x40x15x1.15	600	1Gypsum16 1Rockwool25 1Gypsum16	Rockwool



Mesh from Ansys

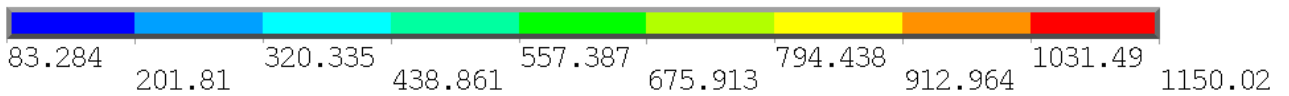
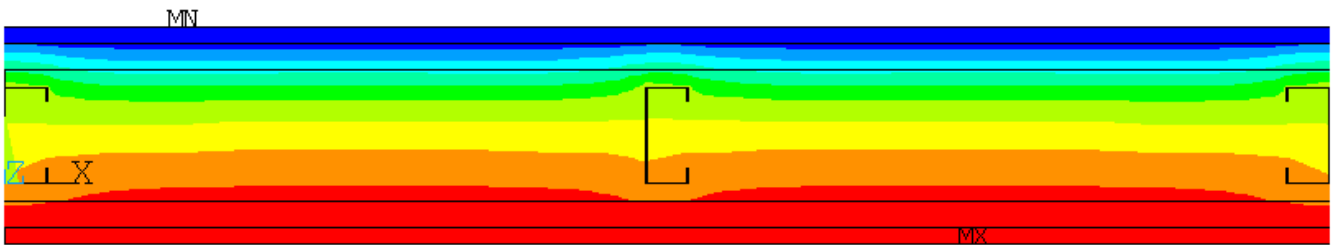


Average temperature results



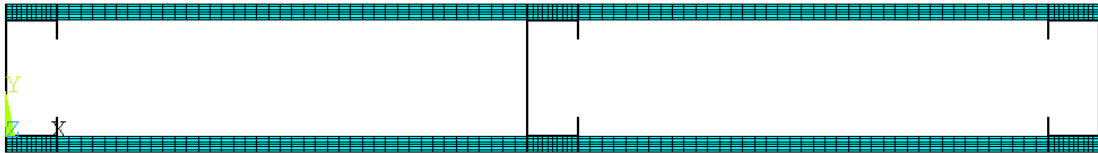
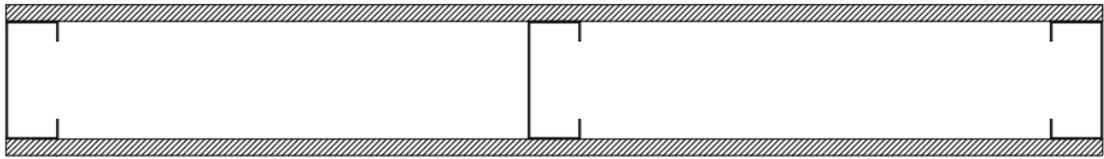
Unexposed curves

Anslys Fire Resistance(min)		
-----------------------------	--	--

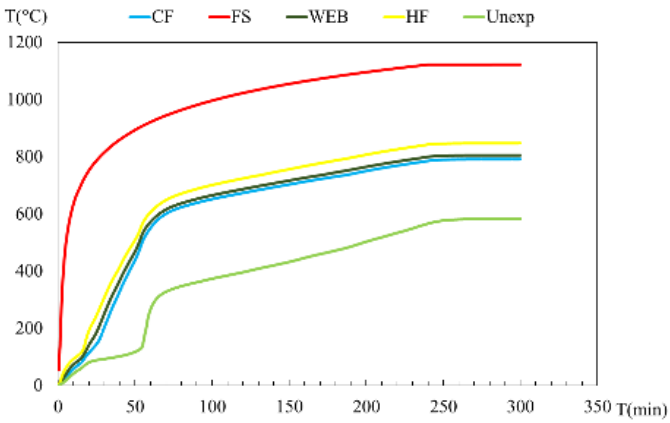


Anslys result in t= 300 min

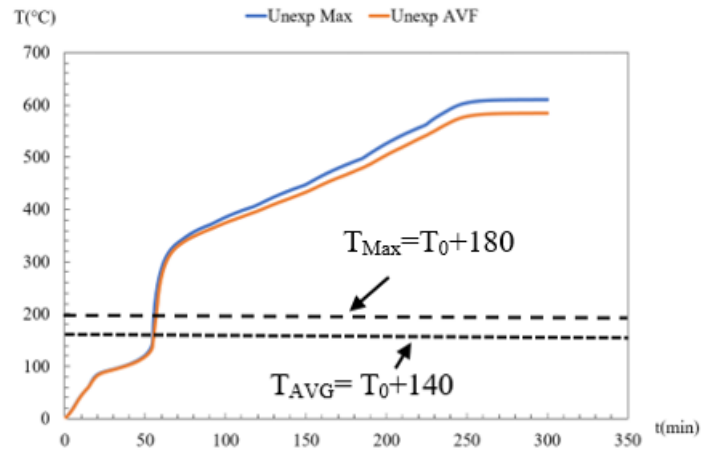
Specimen n°	Steel Section	Spacing between the studs (mm)	N° Layers gyps	Cavity insulation
13	C90x40x15x1.15	400	1Gypsum12.5	/



Mesh from Ansys



Average temperature results

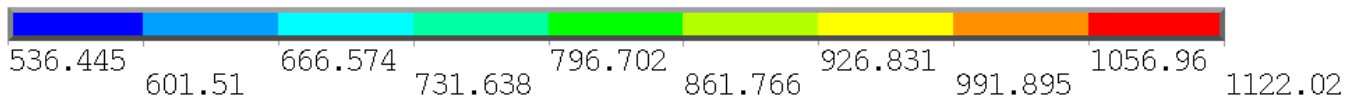
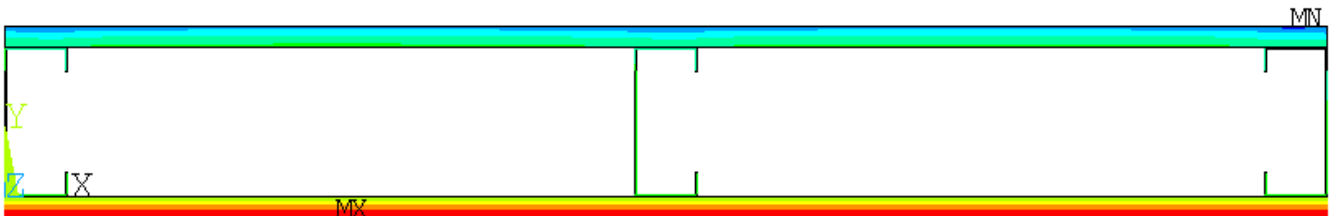


Unexposed curves

Ansys Fire Resistance(min)

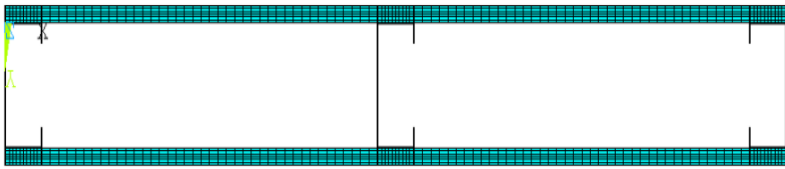
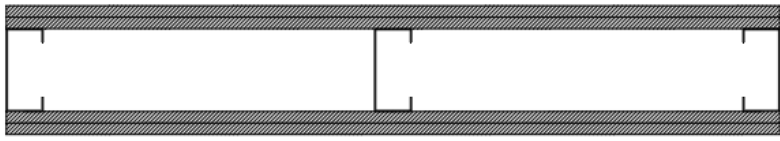
Avg : 55

Max : 56

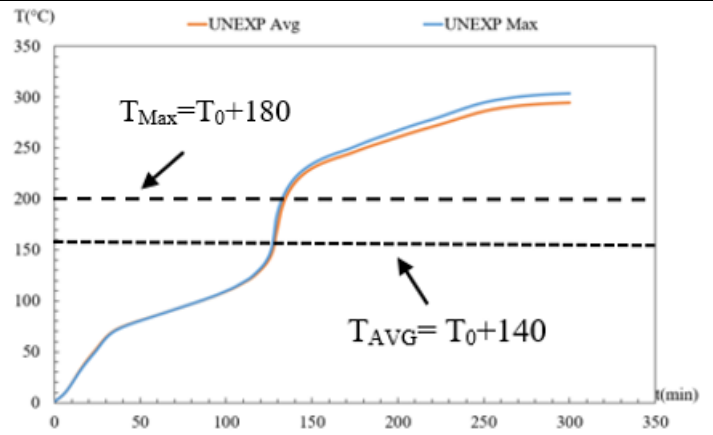
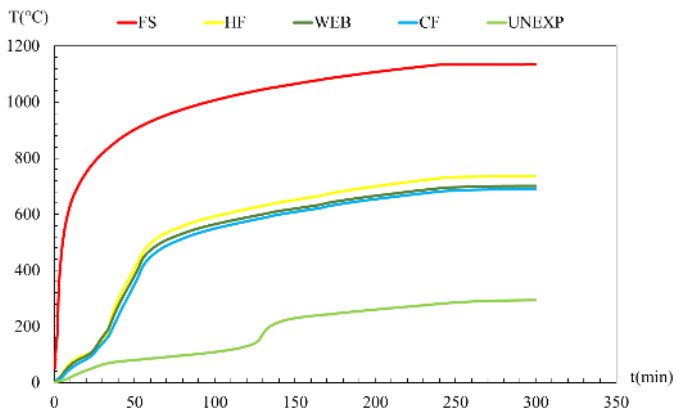


Ansys result in  $t = 240$  min

Specimen n°	Steel Section	Spacing between the studs (mm)	N° Layers gyps	Cavity insulation
14	C90x40x15x1.15	400	2Gypsum12.5	/



Mesh from Ansys



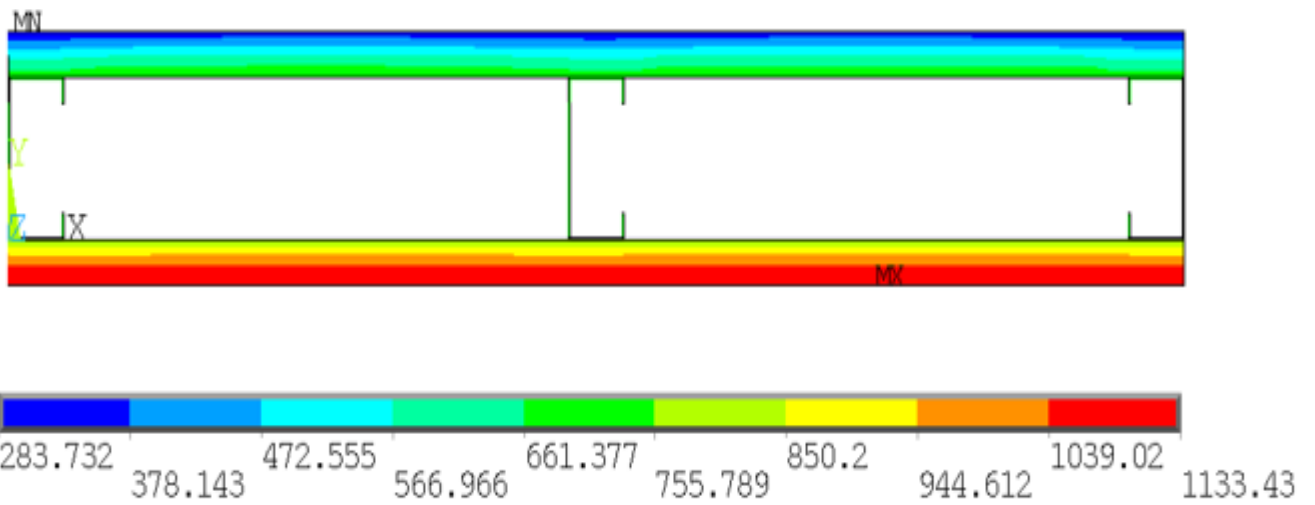
Average temperature results

Unexposed curves

Ansys Fire Resistance(min)

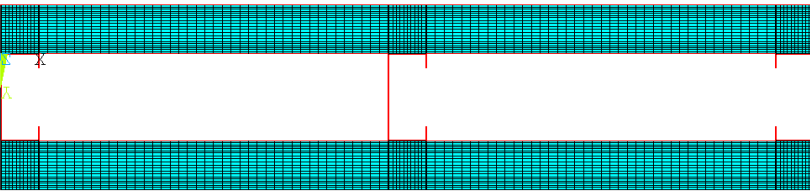
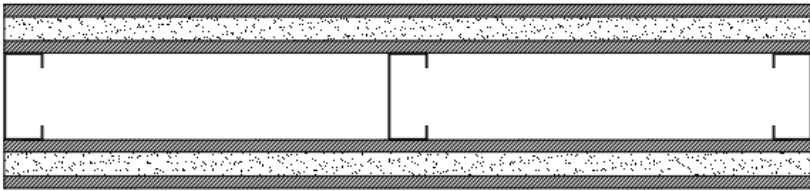
Avg : 129

Max : 133

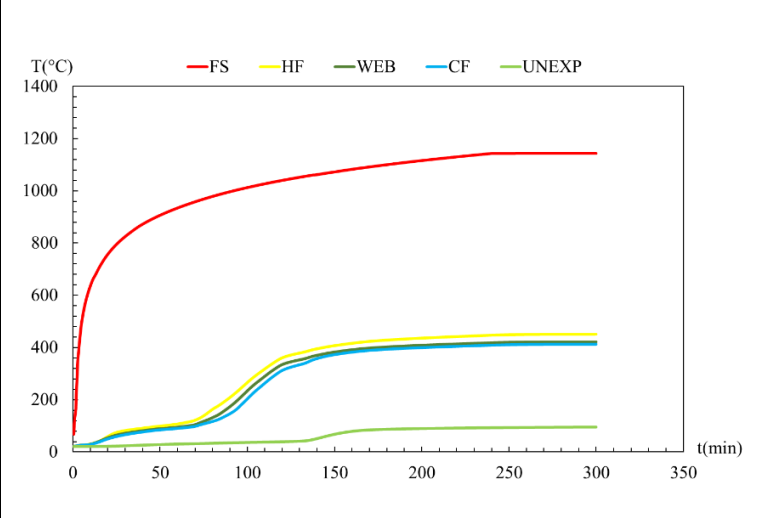


Ansys result in t= 300 min

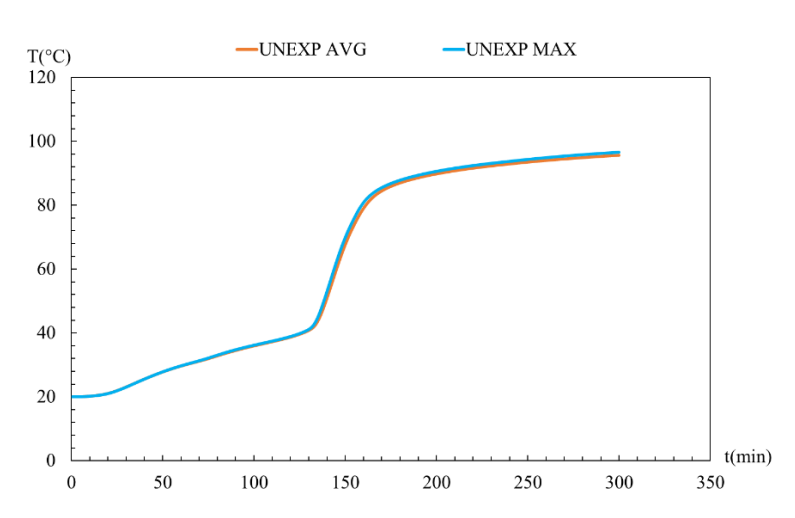
Specimen n°	Steel Section	Spacing between the studs (mm)	N° Layers gyps	Cavity insulation
15	C90x40x15x1.15	400	1Gypsum12.5 1Rockwool25 1Gypsum12.5	/



Mesh from Ansys

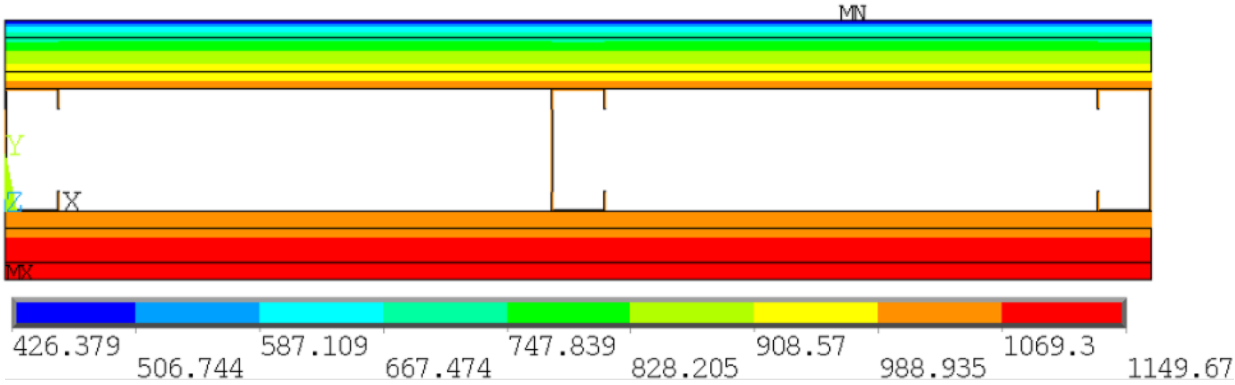


Average temperature results



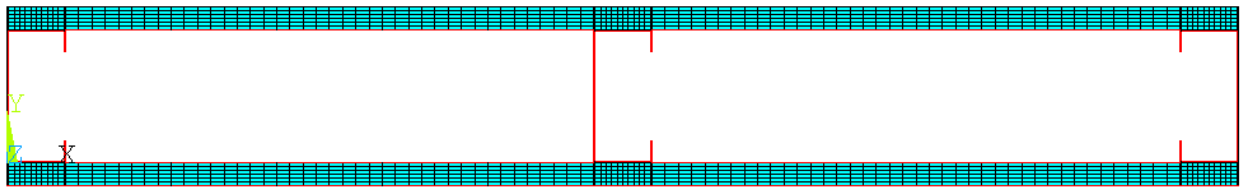
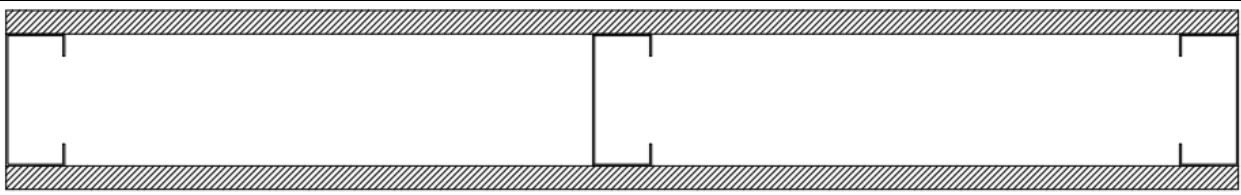
Unexposed curves

Ansys Fire Resistance(min)	
----------------------------	--

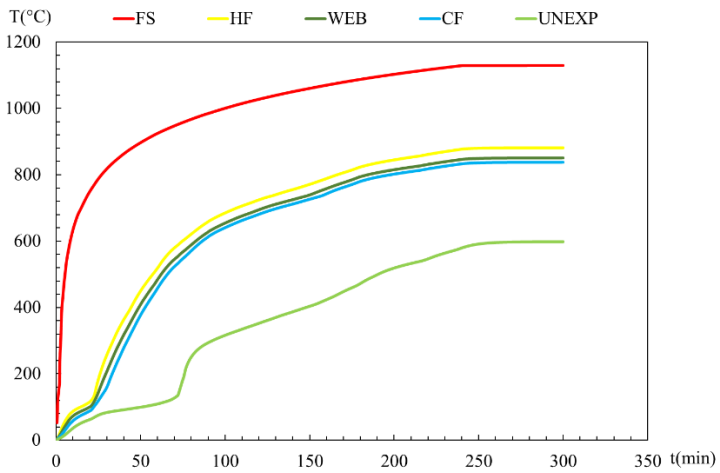


Ansys result in t= 300 min

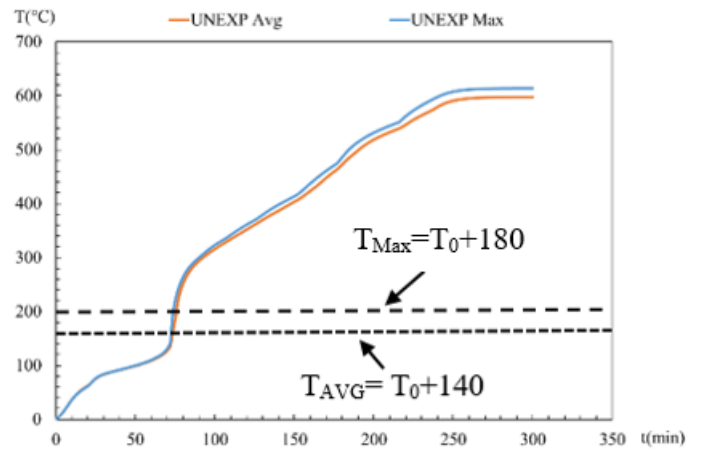
Specimen n°	Steel Section	Spacing between the studs (mm)	N° Layers gyps	Cavity insulation
16	C90x40x15x1.15	400	1Gypsum16	/



Mesh from Ansys



Average temperature results

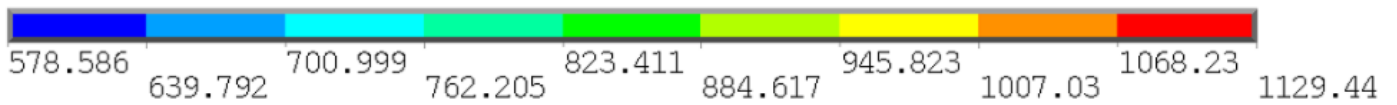
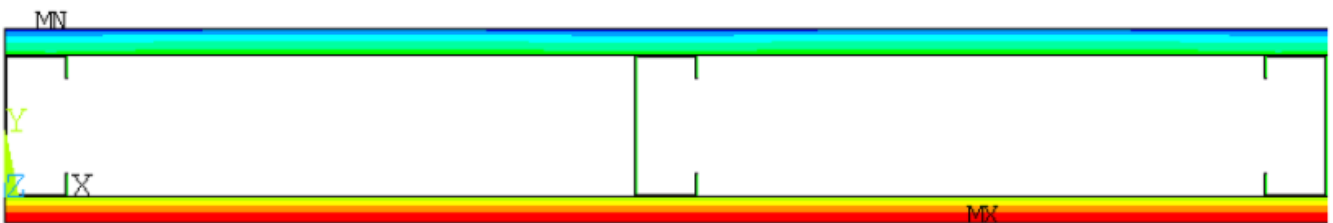


Unexposed curves

Ansys Fire Resistance(min)

Avg : 74

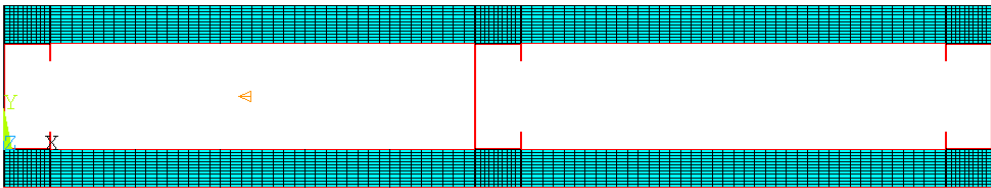
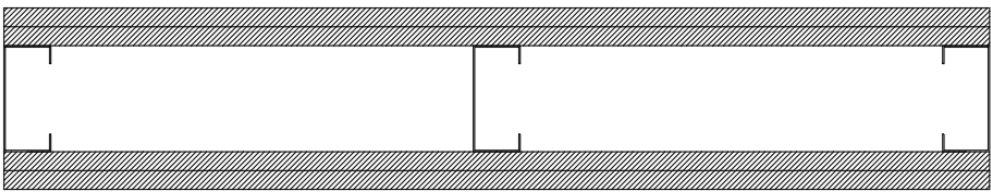
Max : 74



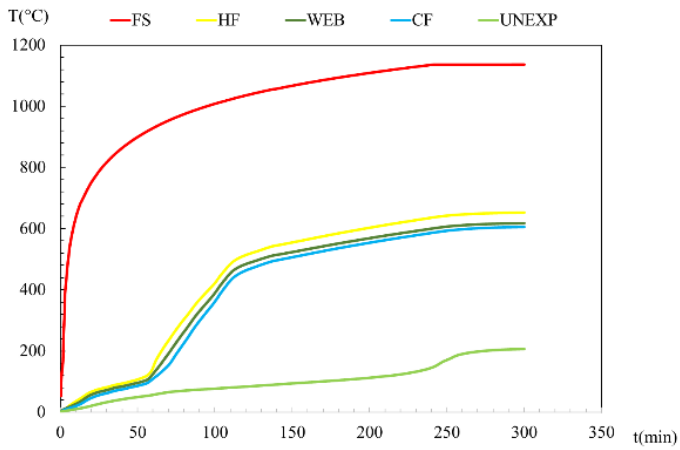
Ansys result in t= 300 min



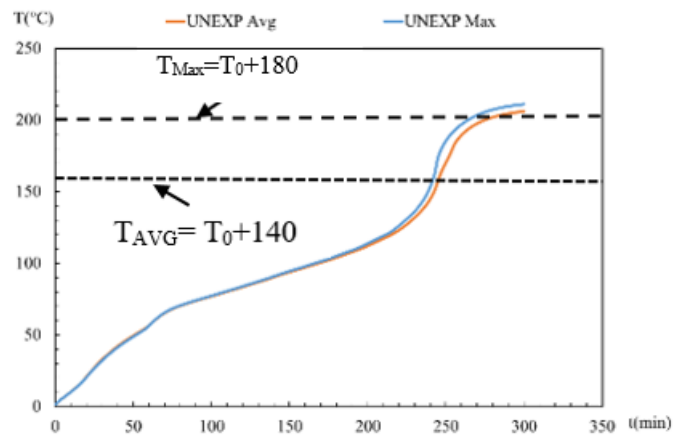
Specimen n°	Steel Section	Spacing between the studs (mm)	N° Layers gyps	Cavity insulation
17	C90x40x15x1.15	400	2Gypsum16	/



Mesh from Ansys



Average temperature results

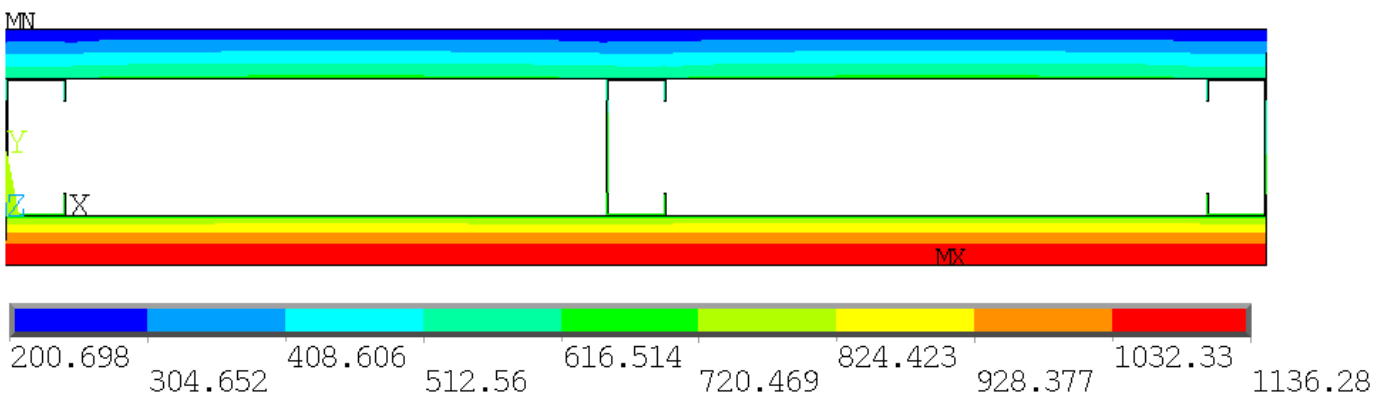


Unexposed curves

Ansys Fire Resistance(min)

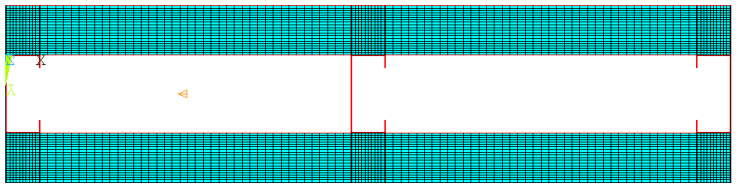
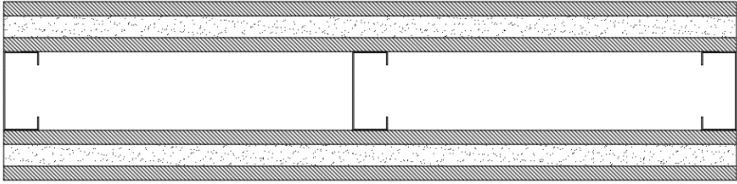
Avg : 264

Max : 243

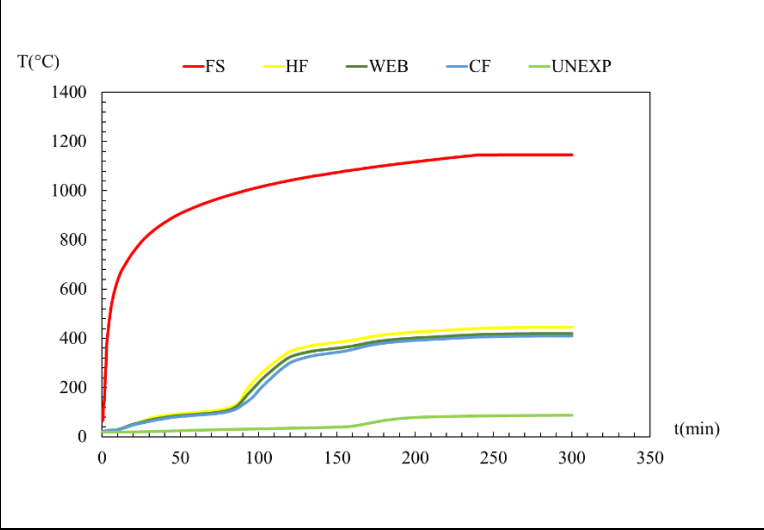


Ansys result in t= 300 min

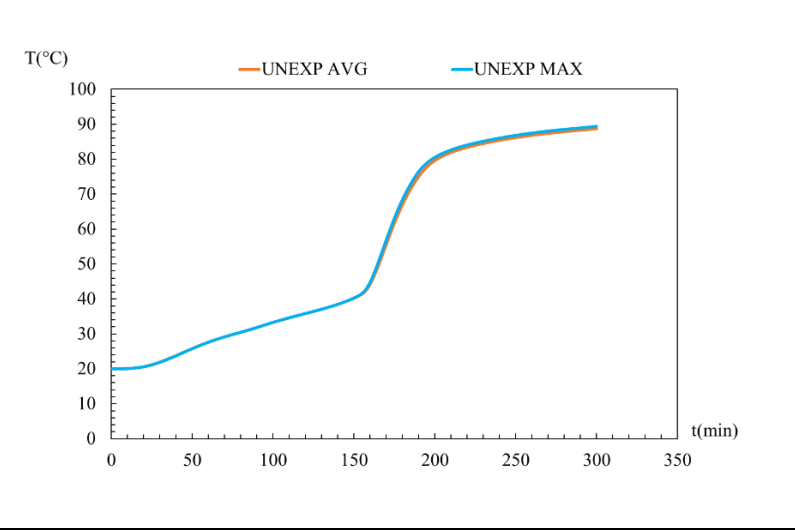
Specimen n°	Steel Section	Spacing between the studs (mm)	N° Layers gyps	Cavity insulation
18	C90x40x15x1.15	400	1Gypsum16 1Rockwool25 1Gypsum16	/



Mesh from Ansys

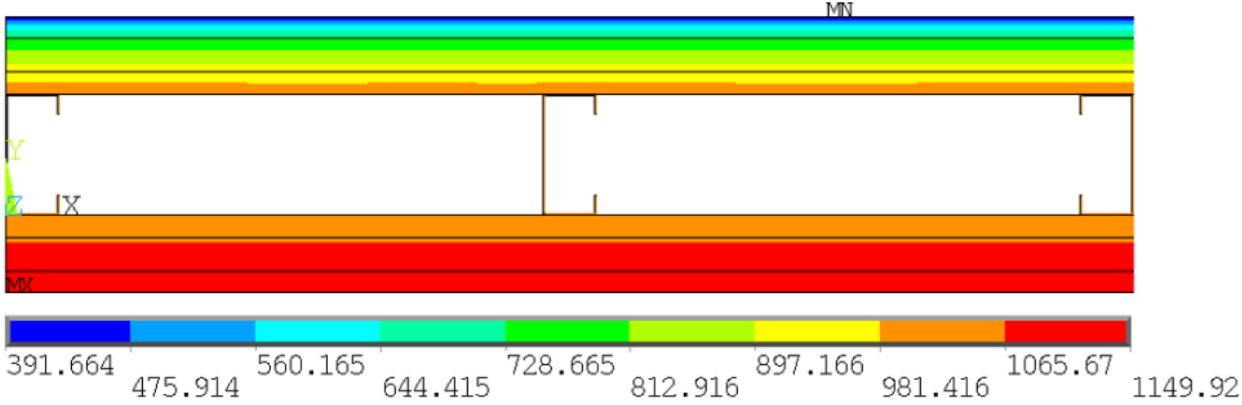


Average temperature results



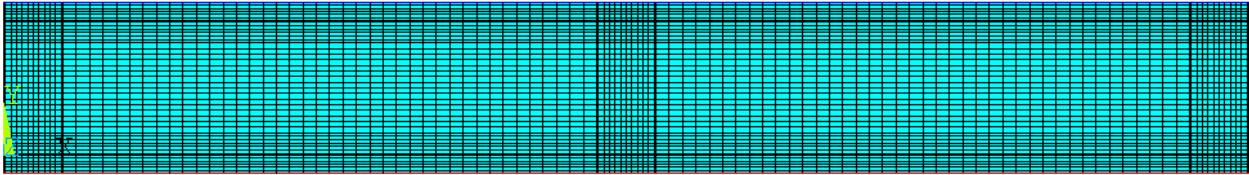
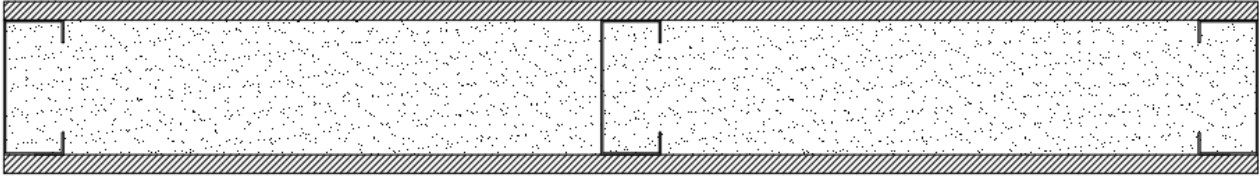
Unexposed curves

Ansys Fire Resistance(min)	
----------------------------	--

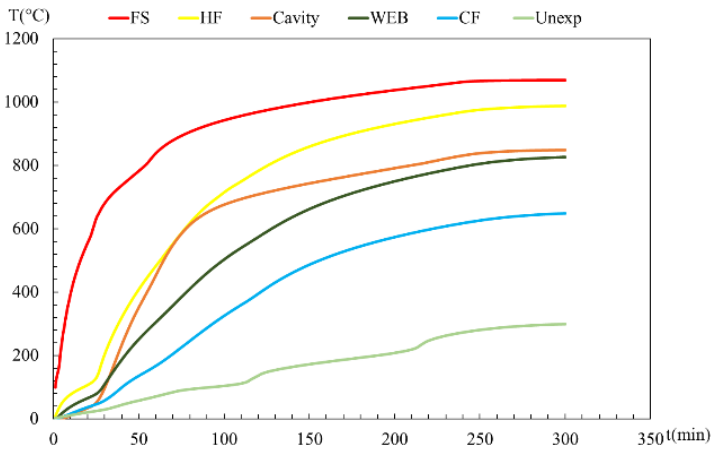


Ansys result in t= 300 min

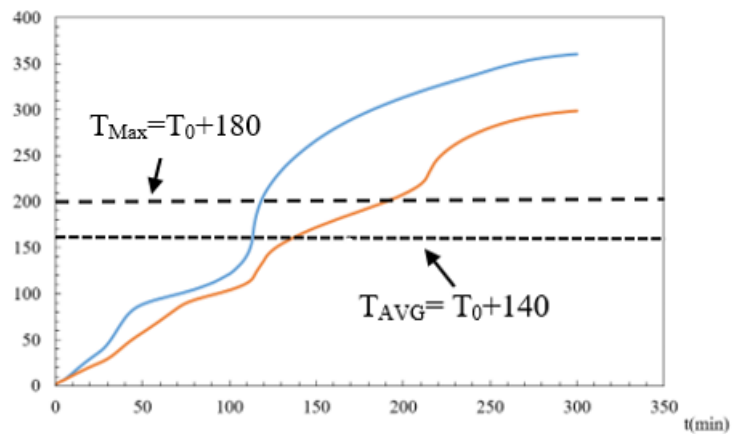
Specimen n°	Steel Section	Spacing between the studs (mm)	N° Layers gyps	Cavity insulation
19	C90x40x15x1.15	400	1Gypsum12.5	Rockwool



Mesh from Ansys



Average temperature results

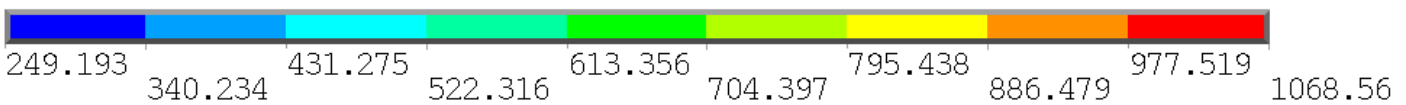
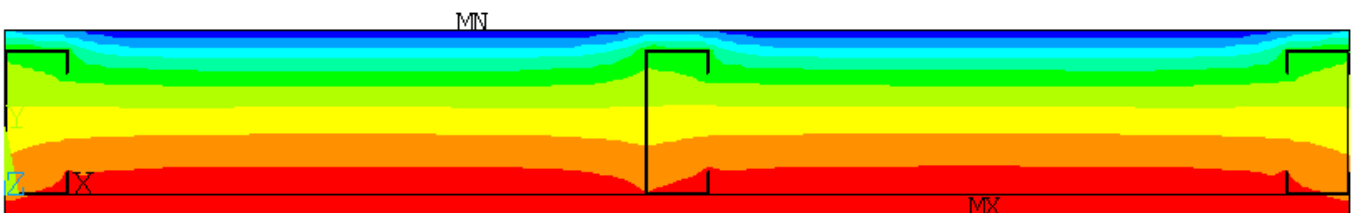


Unexposed curves

Ansys Fire Resistance(min)

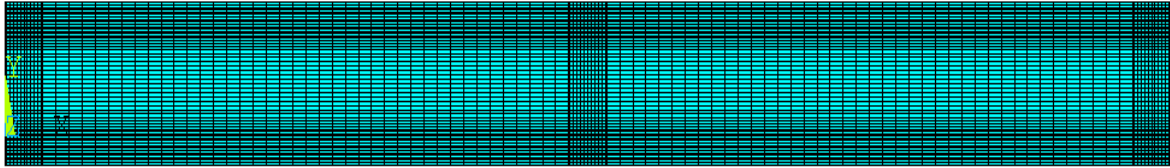
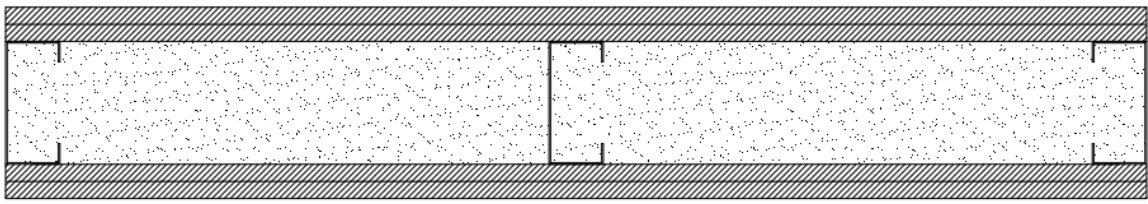
Avg : 136

Max : 118

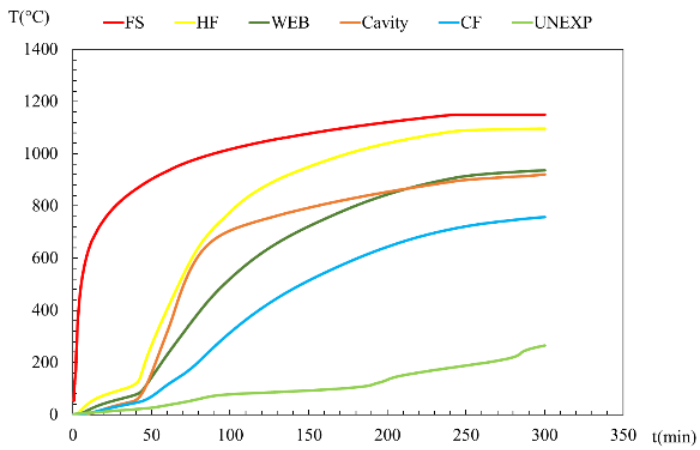


Ansys result in t= 300 min

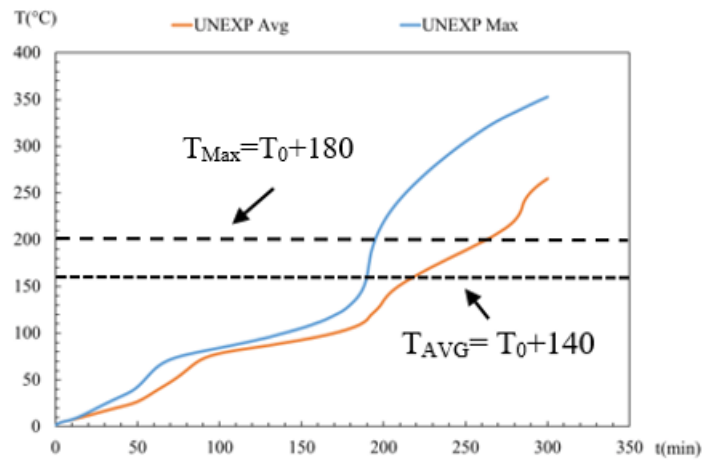
Specimen n°	Steel Section	Spacing between the studs (mm)	N° Layers gyps	Cavity insulation
20	C90x40x15x1.15	400	2Gypsum12.5	Rockwool



Mesh from Ansys



Average temperature results

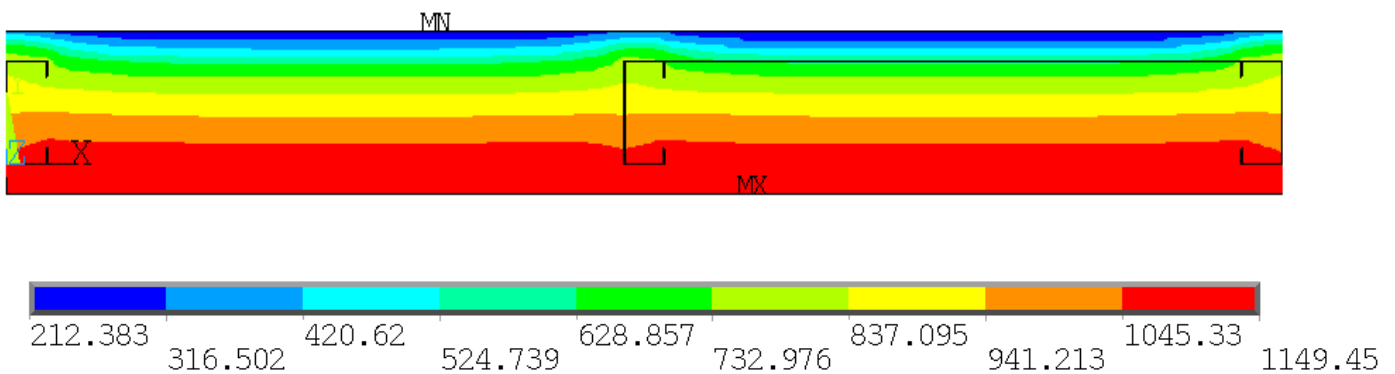


Unexposed curves

Ansys Fire Resistance(min)

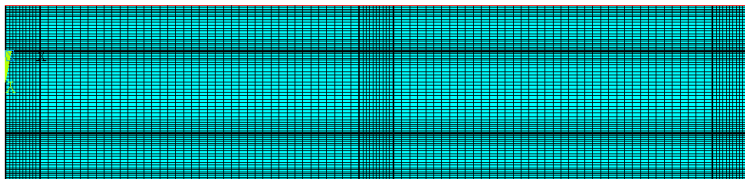
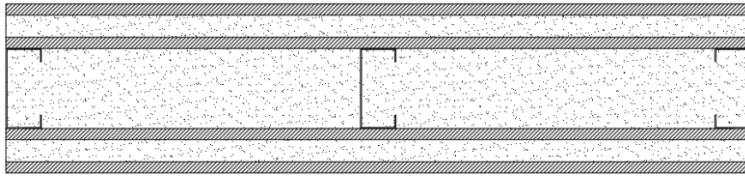
Avg : 218

Max : 195

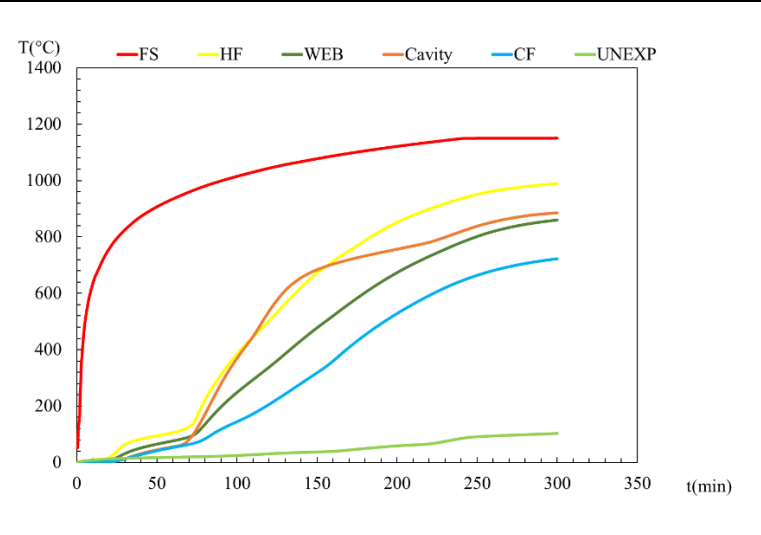


Ansys result in t= 300 min

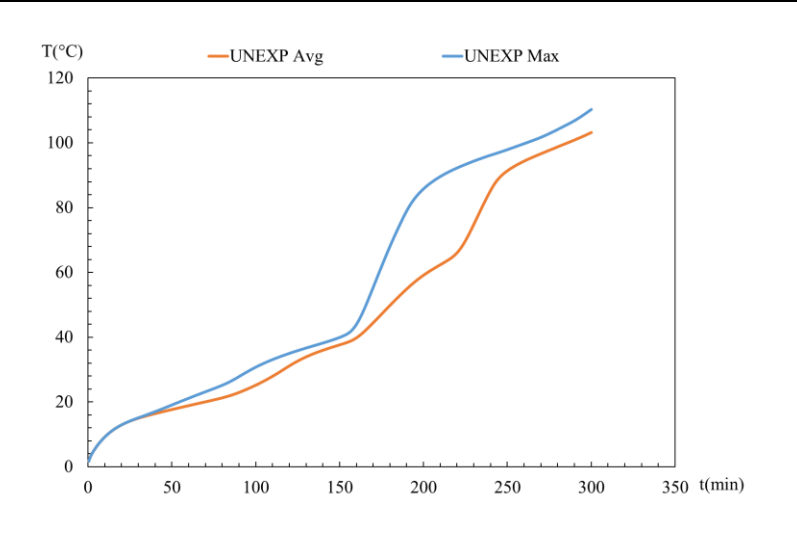
Specimen n°	Steel Section	Spacing between the studs (mm)	N° Layers gyps	Cavity insulation
21	C90x40x15x1.15	400	1Gypsum12.5 1Rockwool25 1Gypsum12.5	Rockwool



Mesh from Ansys

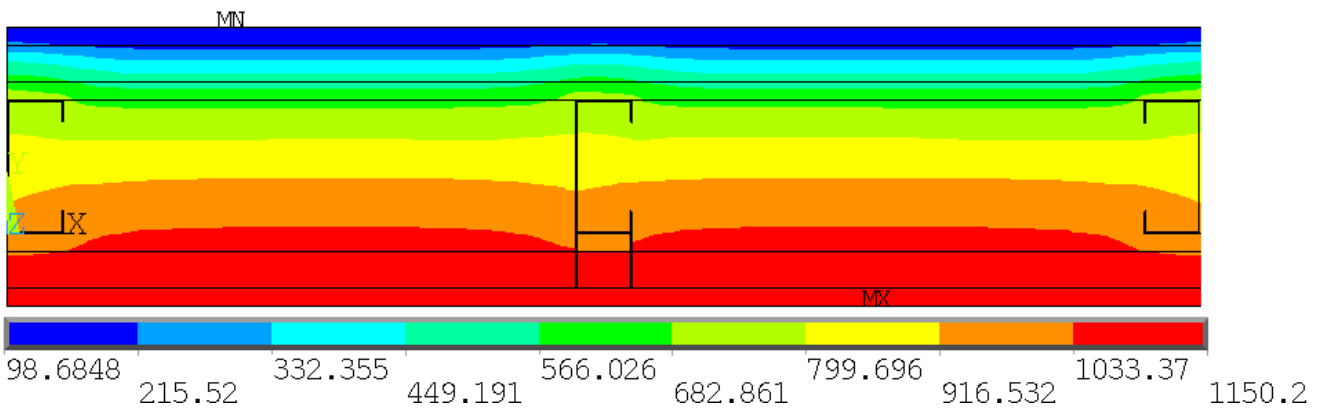


Average temperature results



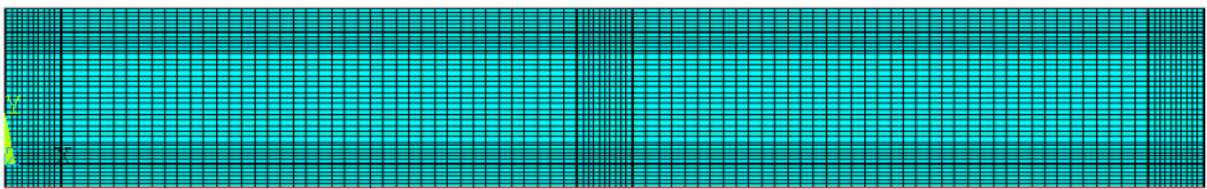
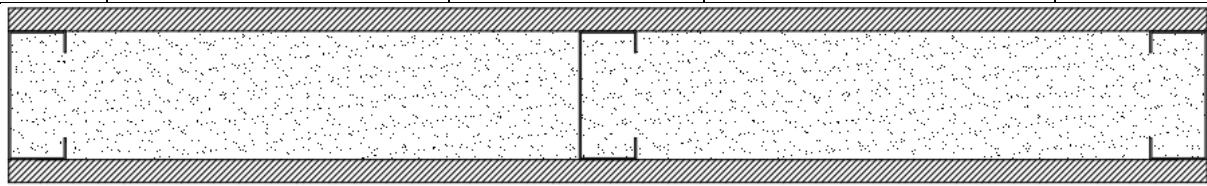
Unexposed curves

Ansys Fire Resistance(min)

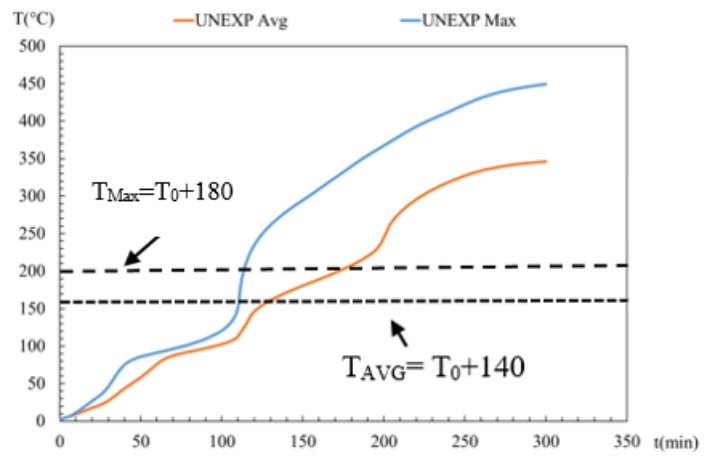
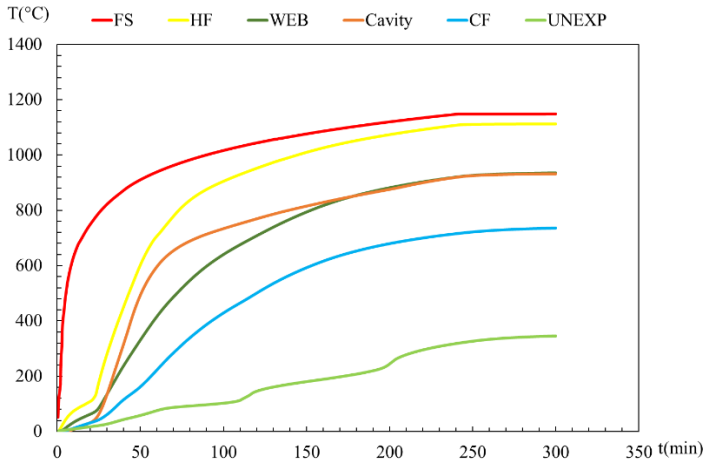


Ansys result in t= 300 min

Specimen n°	Steel Section	Spacing between the studs (mm)	N° Layers gyps	Cavity insulation
22	C90x40x15x1.15	400	1Gypsum16	Rockwool



Mesh from Ansys



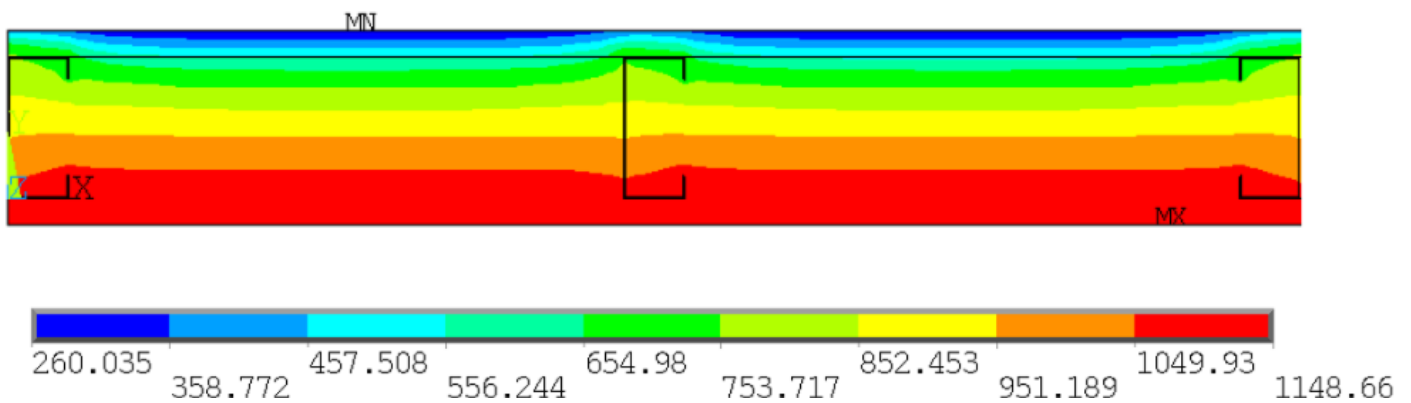
Average temperature results

Unexposed curves

Ansys Fire Resistance(min)

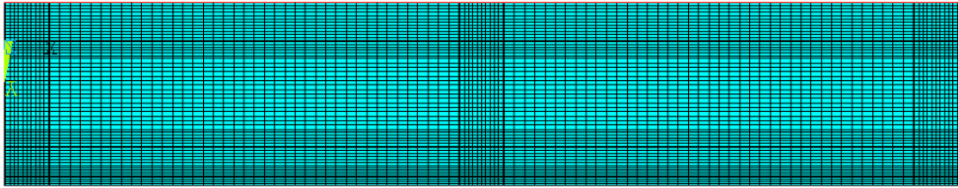
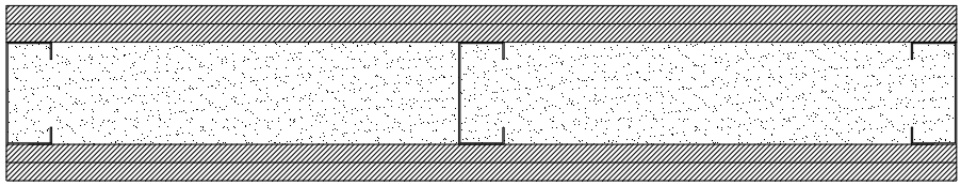
Avg : 129

Max : 112

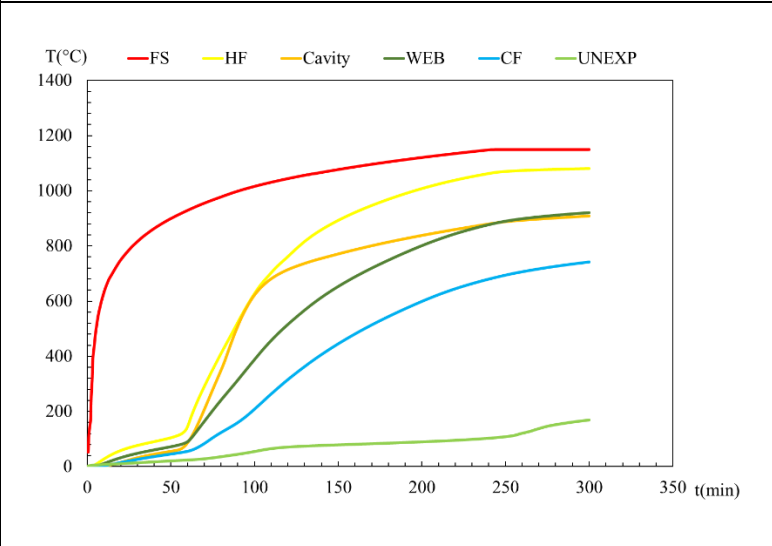


Ansys result in t= 240 min

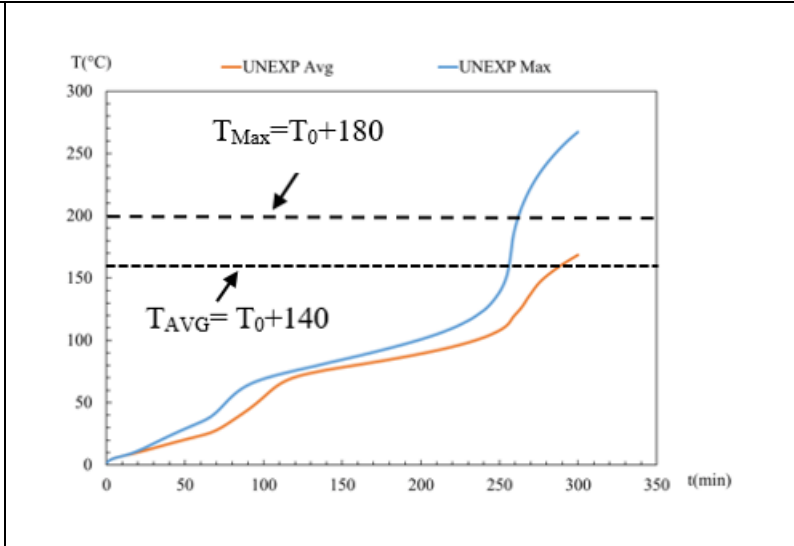
Specimen n°	Steel Section	Spacing between the studs (mm)	N° Layers gyps	Cavity insulation
23	C90x40x15x1.15	400	2Gypsum16	Rockwool



Mesh from Ansys

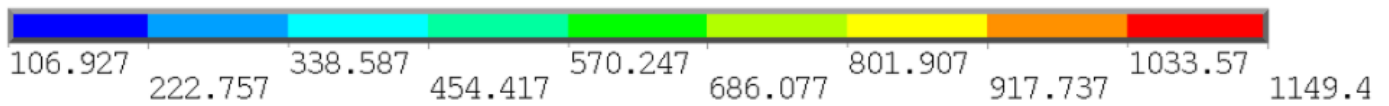
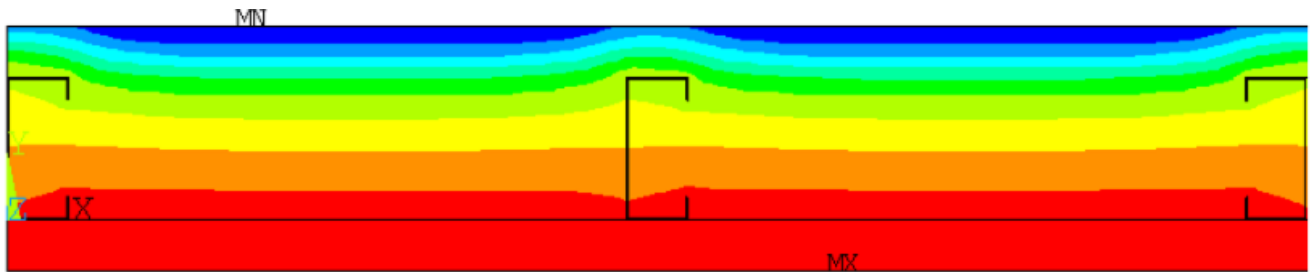


Average temperature results



Unexposed curves

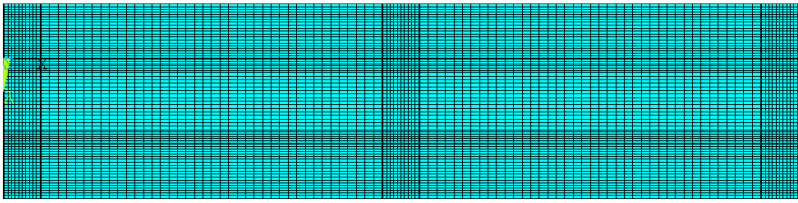
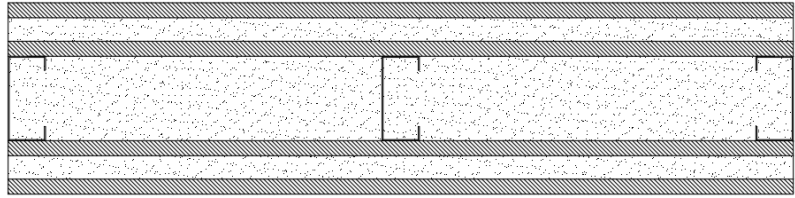
Anslys Fire Resistance(min)	Avg : 289	Max : 262
-----------------------------	-----------	-----------



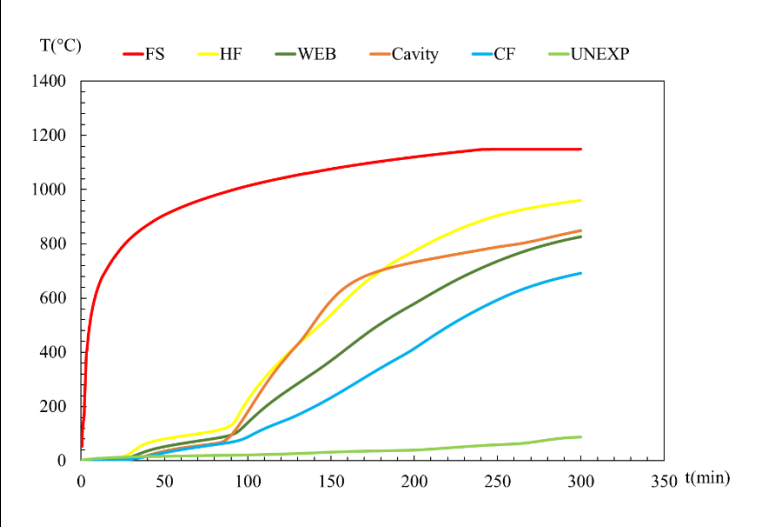
Anslys result in t= 300 min



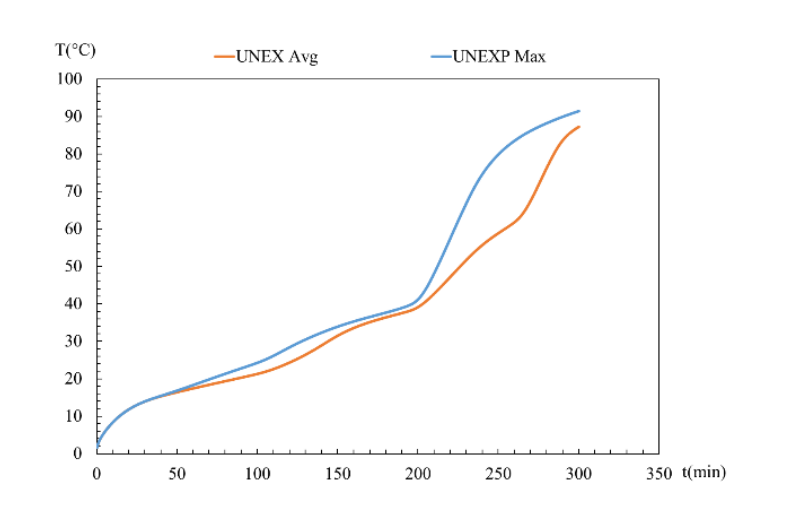
Specimen n°	Steel Section	Spacing between the studs (mm)	N° Layers gyps	Cavity insulation
24	C90x40x15x1.15	400	1Gypsum16 1Rockwool25 1Gypsum16	Rockwool



Mesh from Ansys

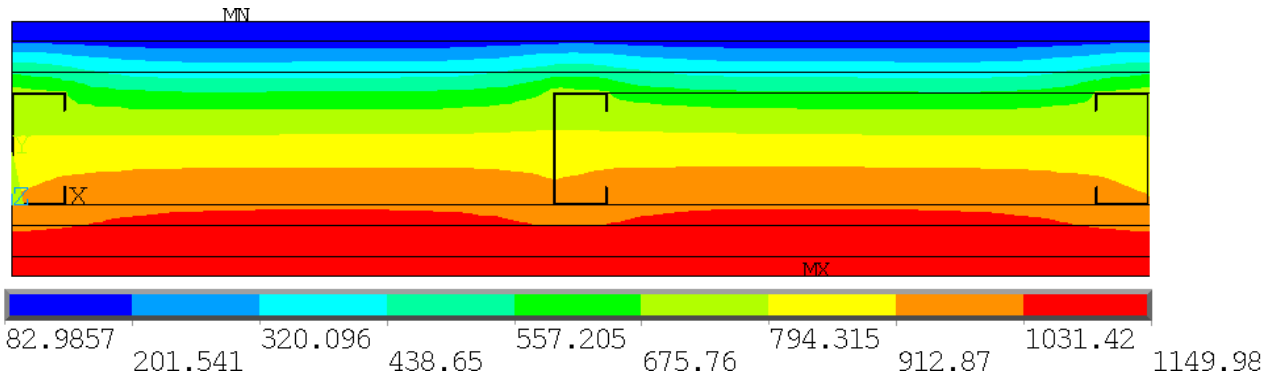


Average temperature results



Unexposed curves

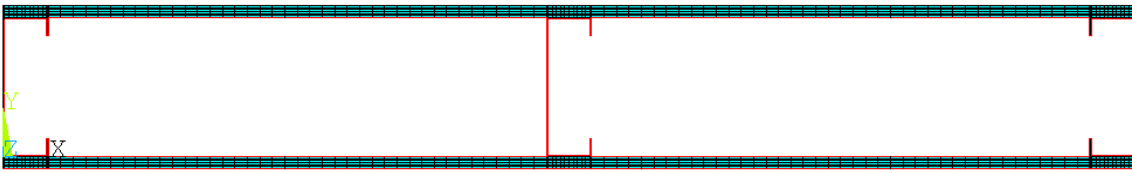
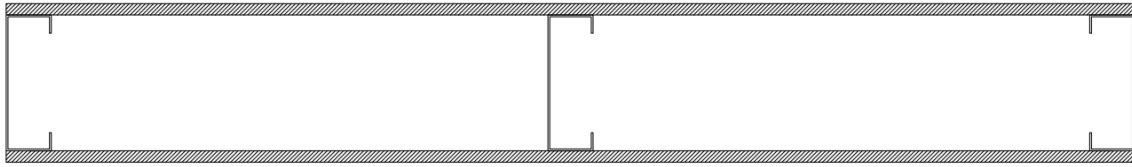
Ansys Fire Resistance(min)	
----------------------------	--



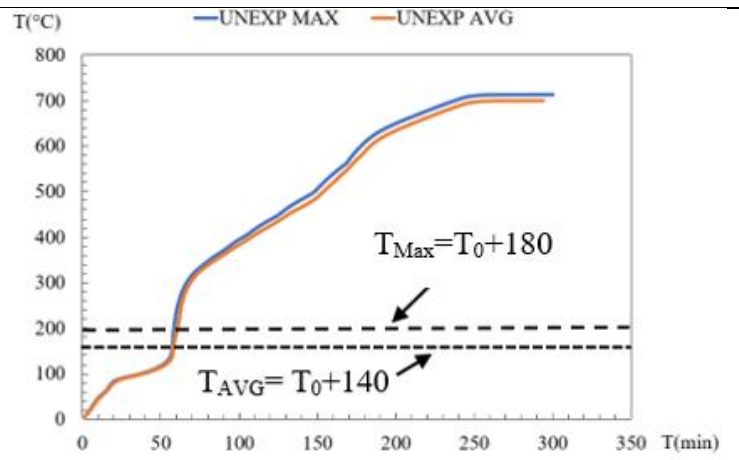
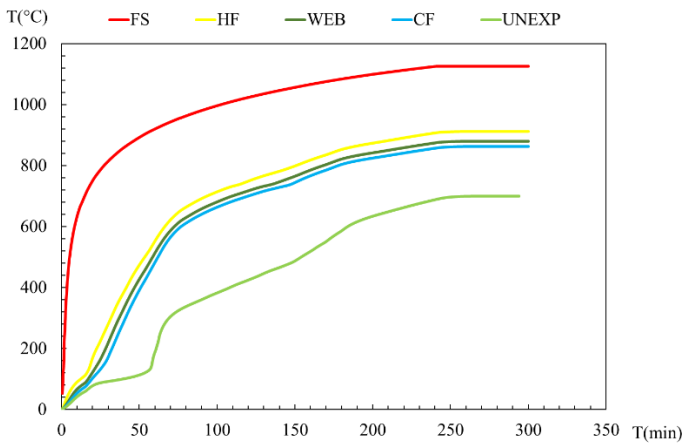
Ansys result in t= 300 min



Specimen n°	Steel Section	Spacing between the studs (mm)	N° Layers gyps	Cavity insulation
25	C150x50x20x2.0	600	1Gypsum12.5	/



Mesh from Ansys



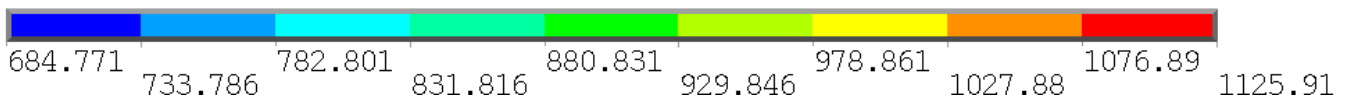
Average temperature results

Unexposed curves

Ansys Fire Resistance(min)

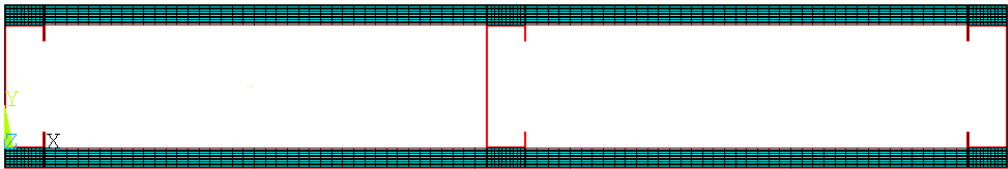
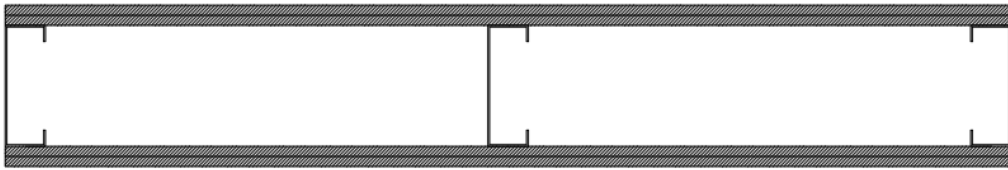
Avg : 49

Max : 48

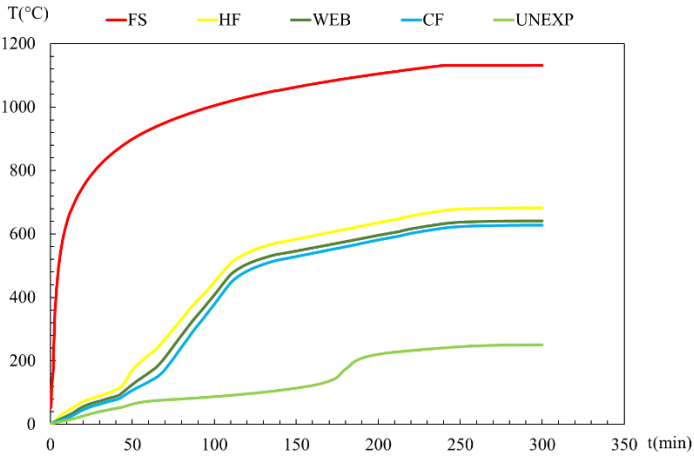


Ansys result in t= 300 min

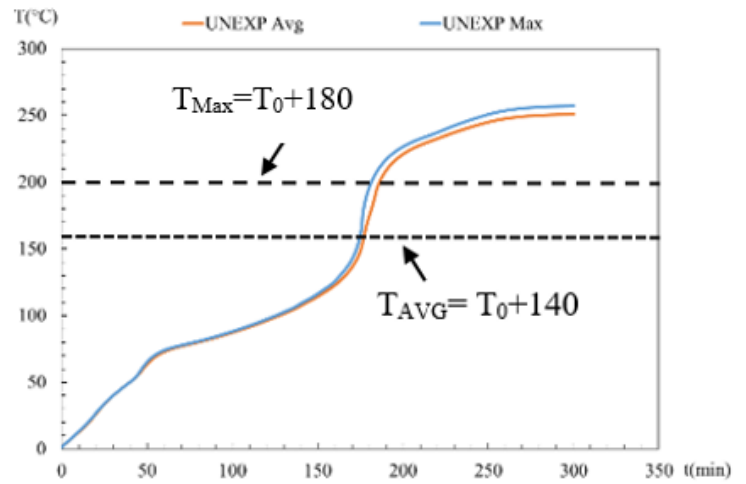
Specimen n°	Steel Section	Spacing between the studs (mm)	N° Layers gyps	Cavity insulation
26	C150x50x20x2.0	600	2Gypsum12.5	/



Mesh from Ansys



Average temperature results

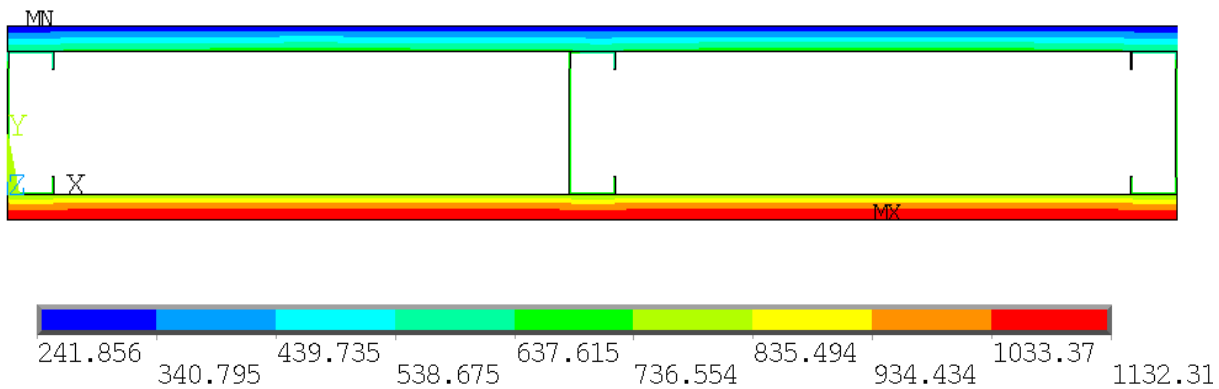


Unexposed curves

Ansys Fire Resistance(min)

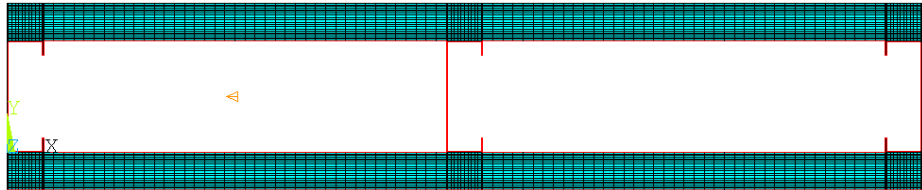
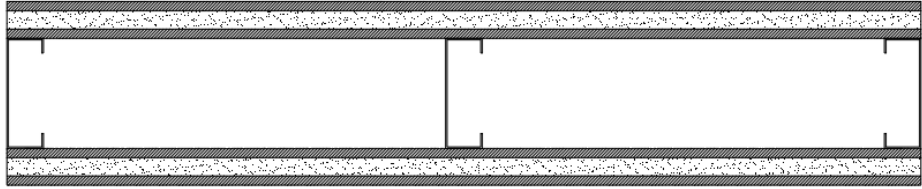
Avg : 178

Max : 186

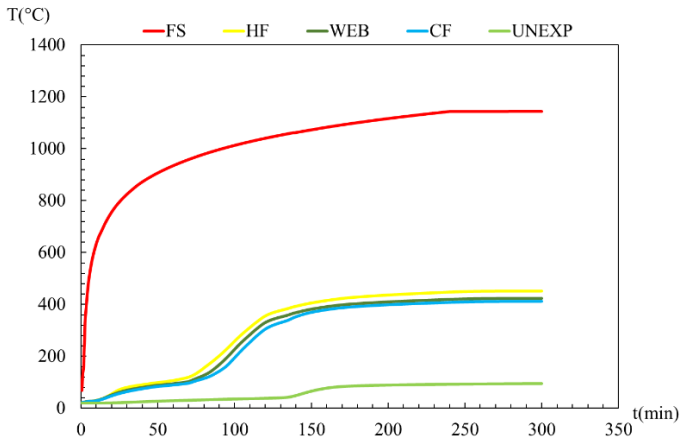


Ansys result in t= 240 min

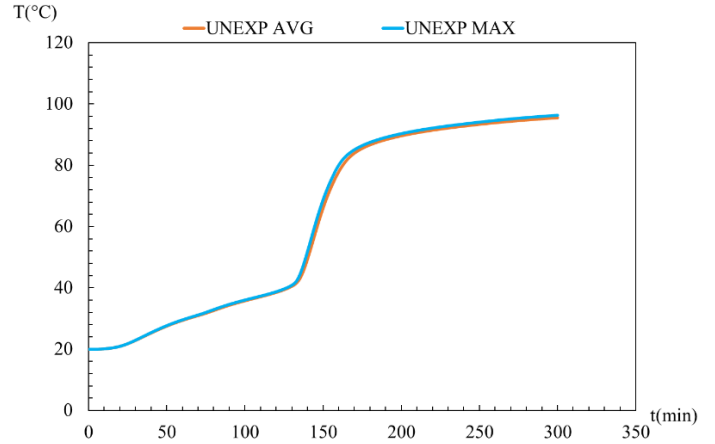
Specimen n°	Steel Section	Spacing between the studs (mm)	N° Layers gyps	Cavity insulation
27	C150x50x20x2.0	600	1Gypsum12.5 1Rockwool25 1Gypsum12.5	/



Mesh from Ansys

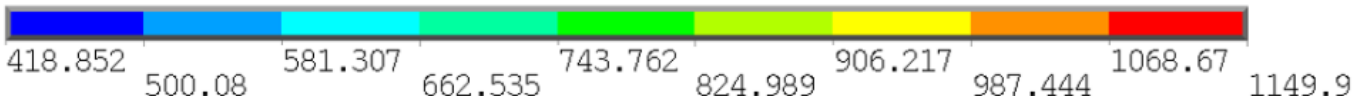
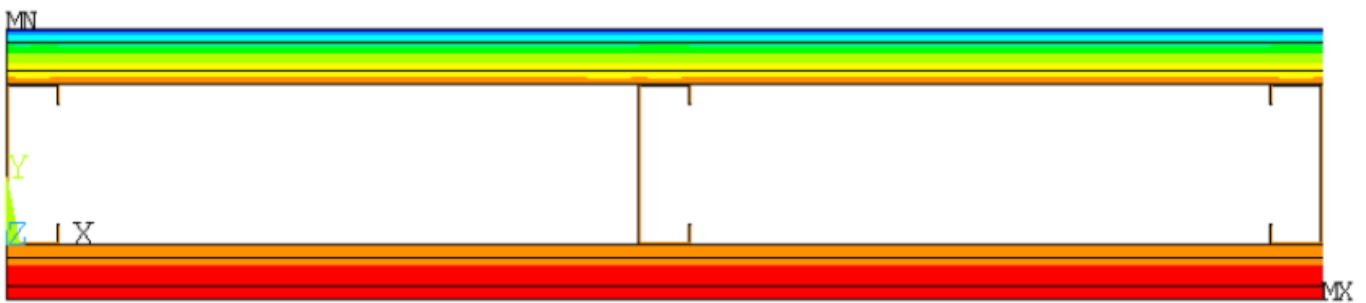


Average temperature results



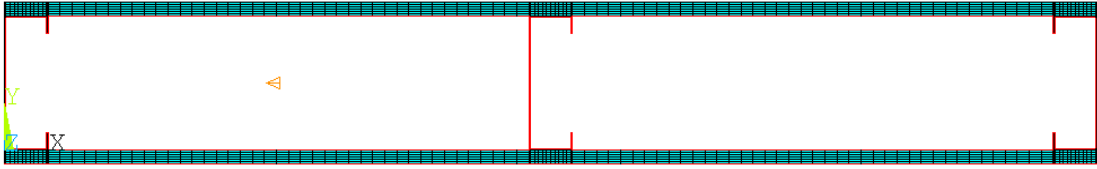
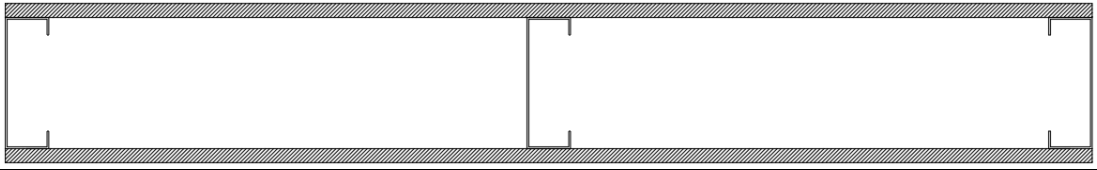
Unexposed curves

Ansys Fire Resistance(min)

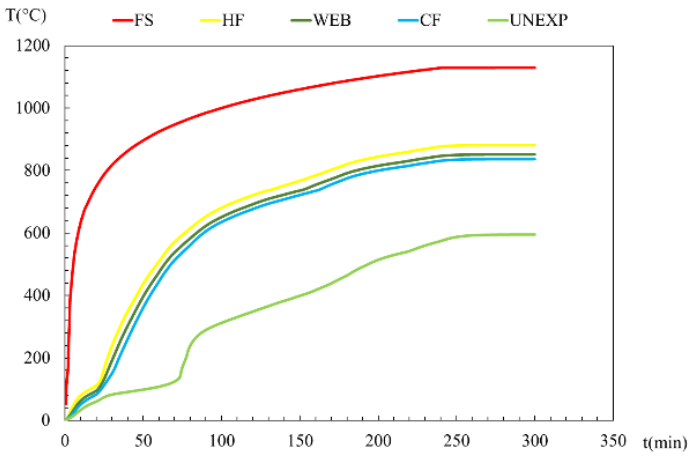


Ansys result in t= 240 min

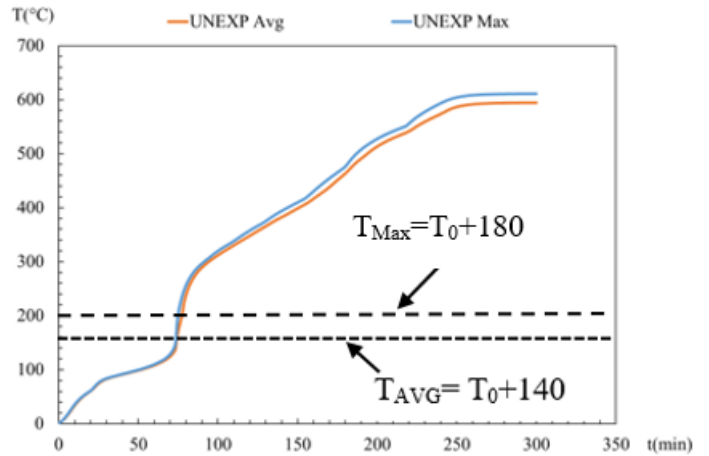
Specimen n°	Steel Section	Spacing between the studs (mm)	N° Layers gyps	Cavity insulation
28	C150x50x20x2.0	600	1Gypsum16	/



Mesh from Ansys



Average temperature results

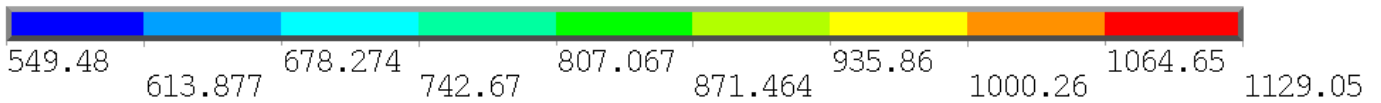
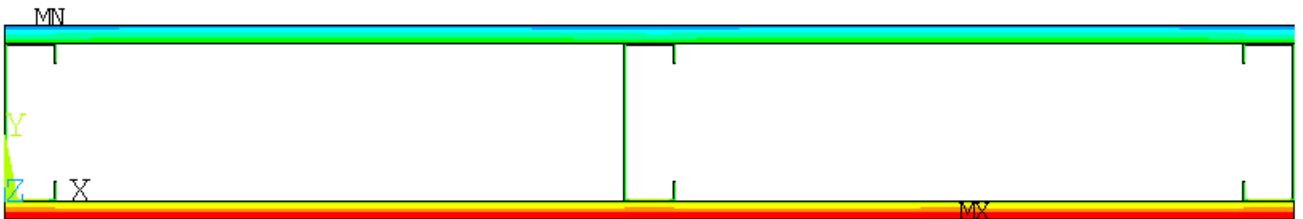


Unexposed curves

Ansys Fire Resistance(min)

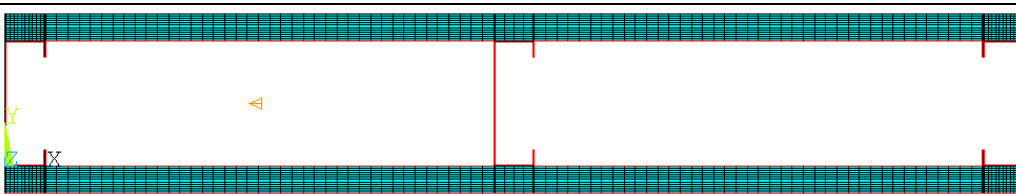
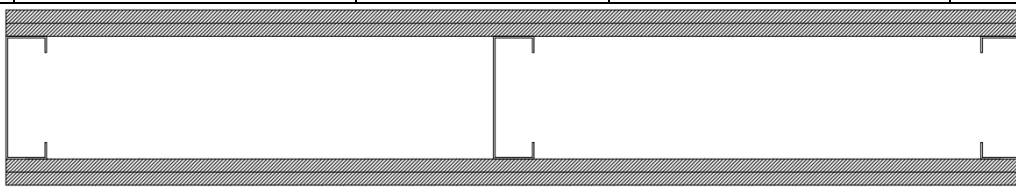
Avg :

Max :

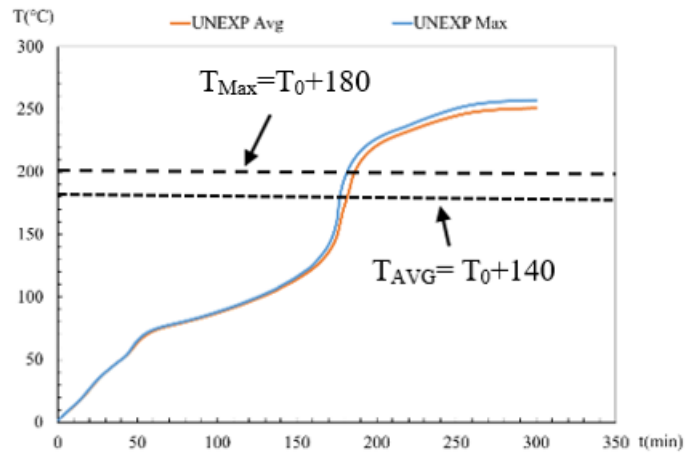
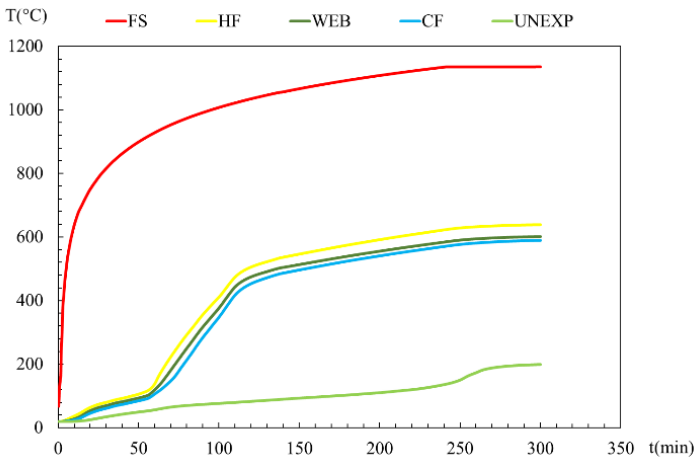


Ansys result in t= 240 MIN

Specimen n°	Steel Section	Spacing between the studs (mm)	N° Layers gyps	Cavity insulation
29	C150x50x20x2.0	600	2Gypsum16	/



Mesh from Ansys



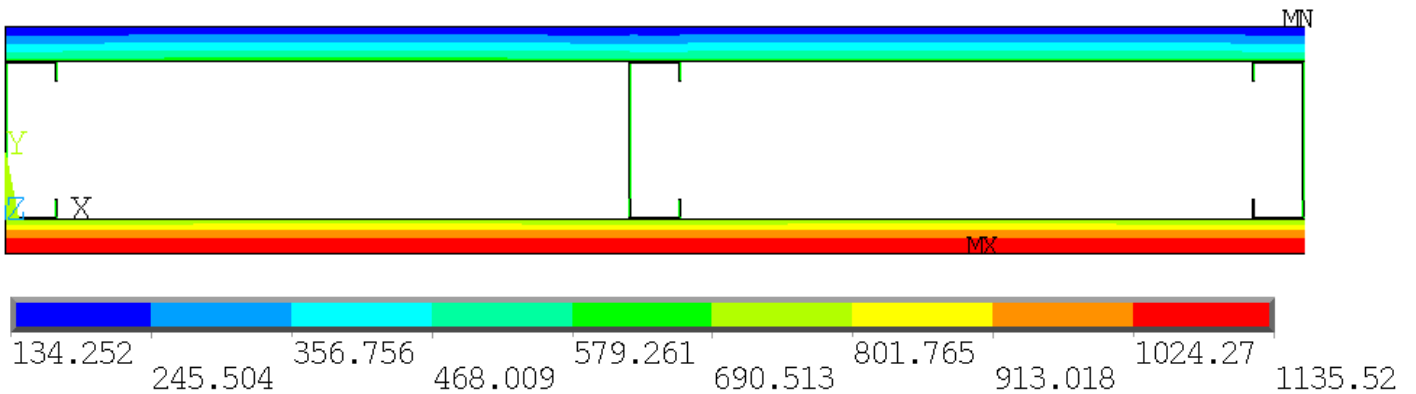
Average temperature results

Unexposed curves

Ansys Fire Resistance(min)

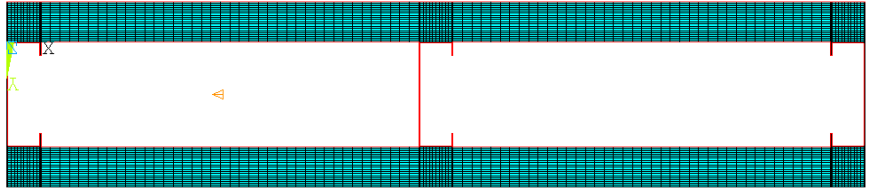
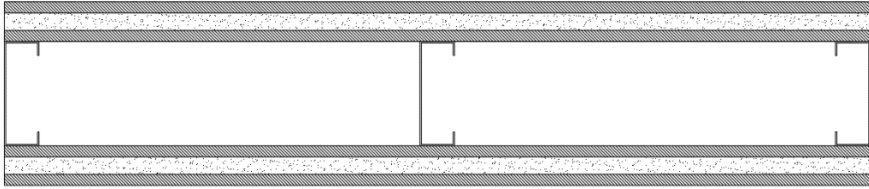
Avg : 192

Max : 192

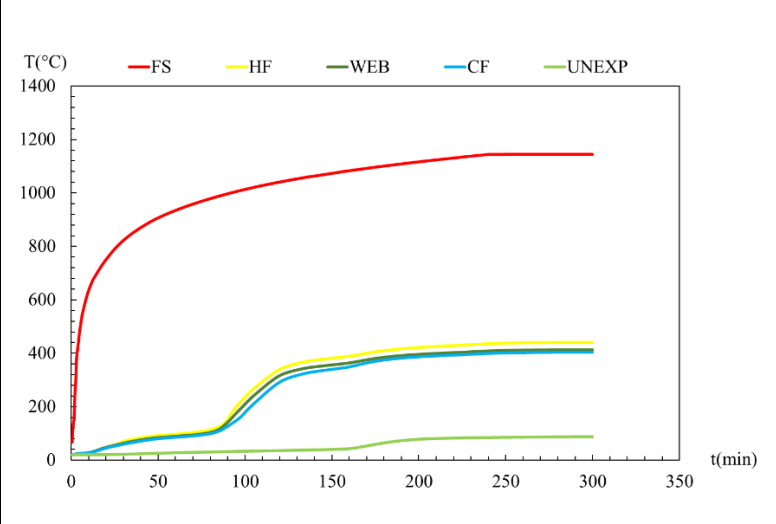


Ansys result in t= 240 min

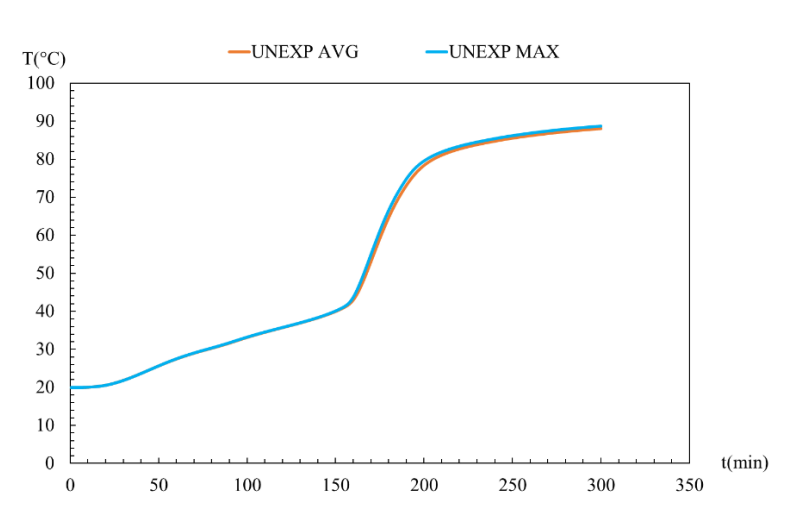
Specimen n°	Steel Section	Spacing between the studs (mm)	N° Layers gyps	Cavity insulation
30	C150x50x20x2.0	600	1Gypsum16 1Rockwool25 1Gypsum16	/



Mesh from Ansys

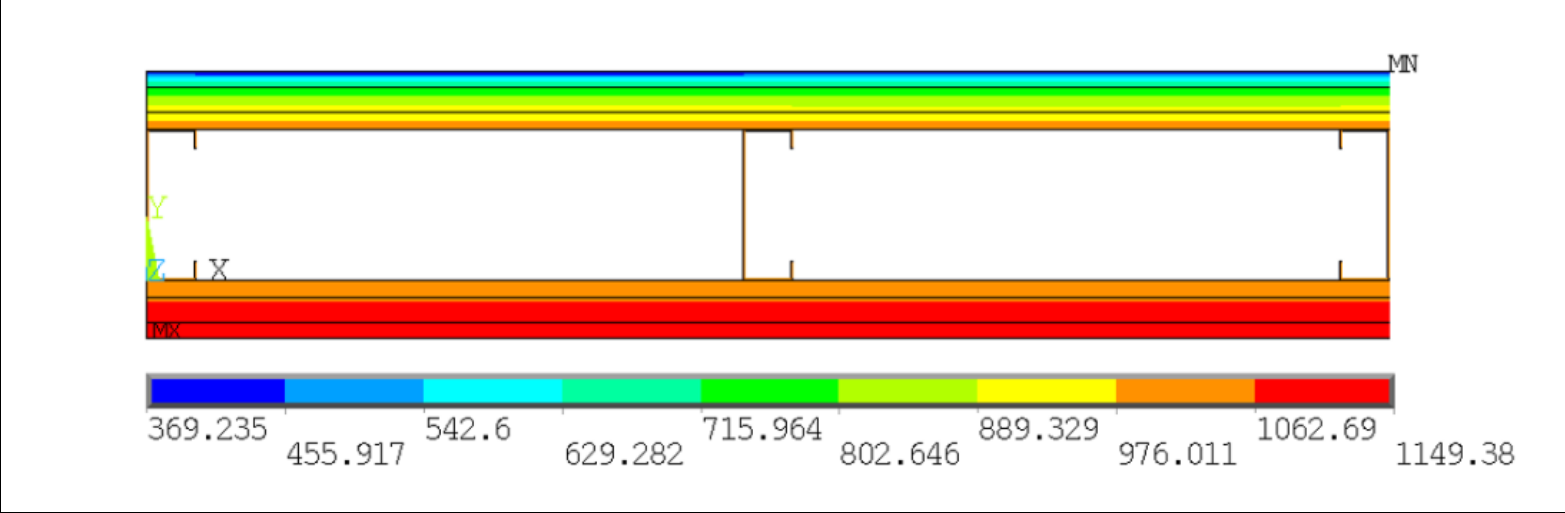


Average temperature results



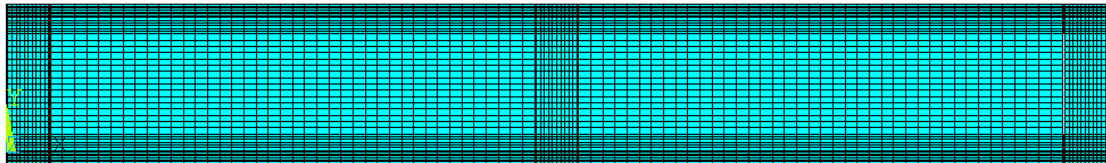
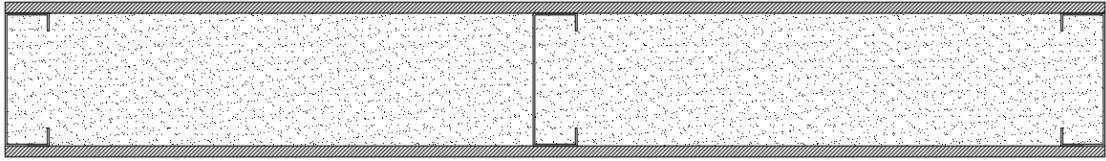
Unexposed curves

Ansys Fire Resistance(min)

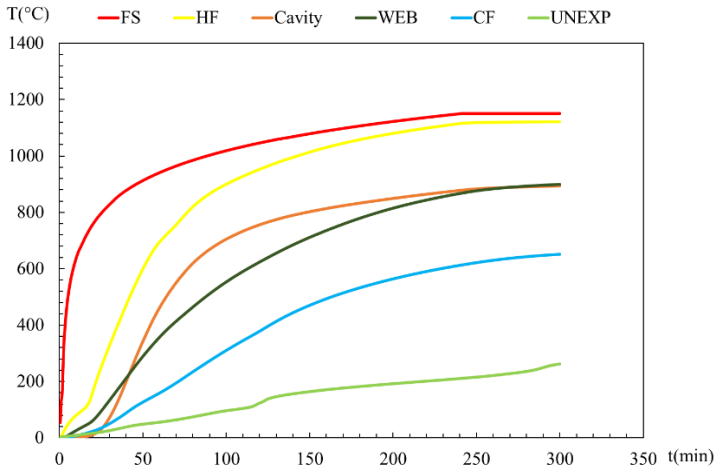


Ansys result in t= 240 min

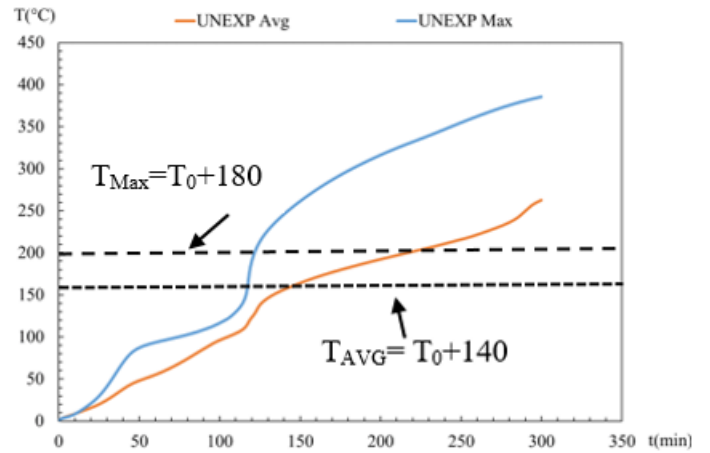
Specimen n°	Steel Section	Spacing between the studs (mm)	N° Layers gyps	Cavity insulation
31	C150x50x20x2.0	600	1Gypsum12.5	Rockwool



Mesh from Ansys



Average temperature results

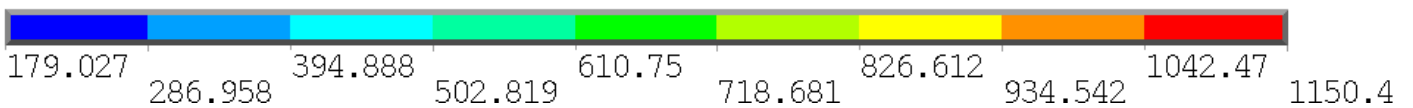
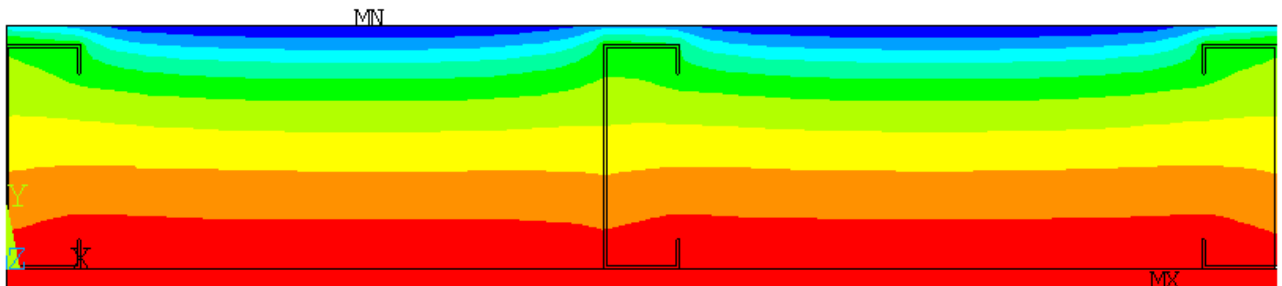


Unexposed curves

Ansys Fire Resistance(min)

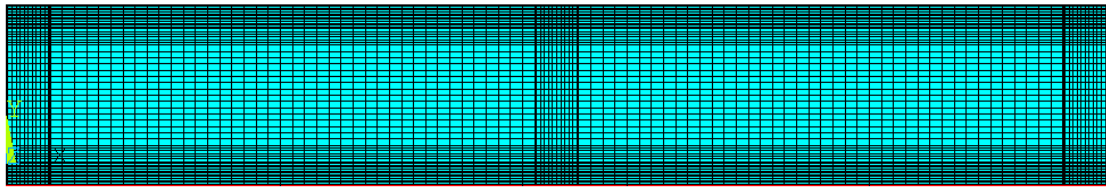
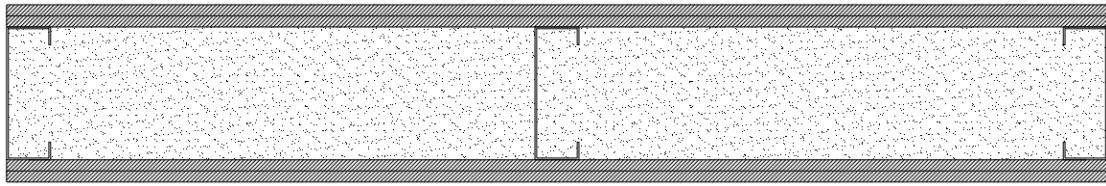
Avg : 145

Max : 122

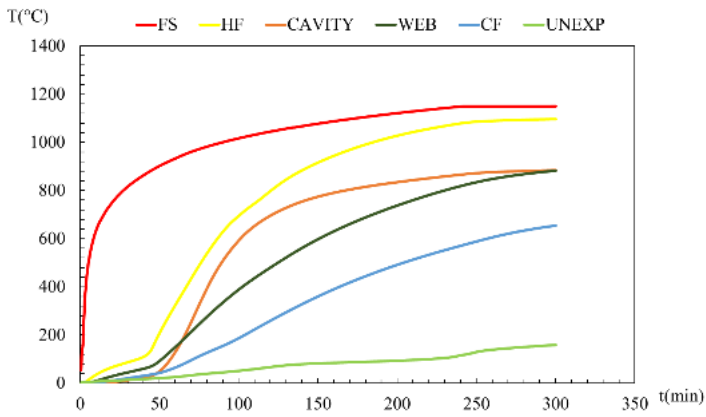


Ansys result in t= 300 min

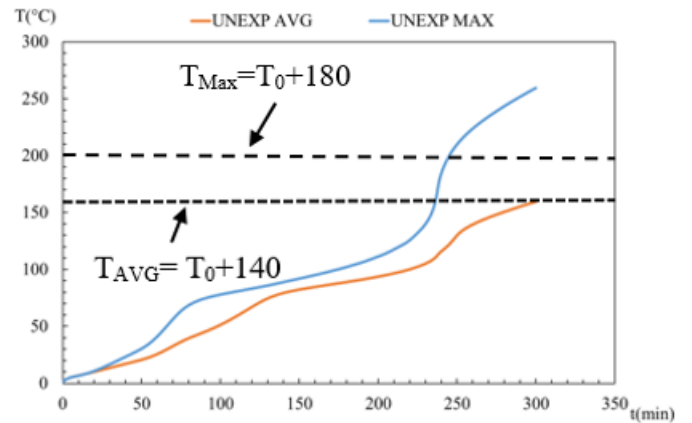
Specimen n°	Steel Section	Spacing between the studs (mm)	N° Layers gyps	Cavity insulation
32	C150x50x20x2.0	600	2Gypsum12.5	Rockwool



Mesh from Ansys



Average temperature results

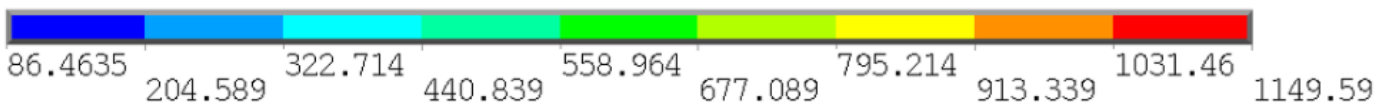
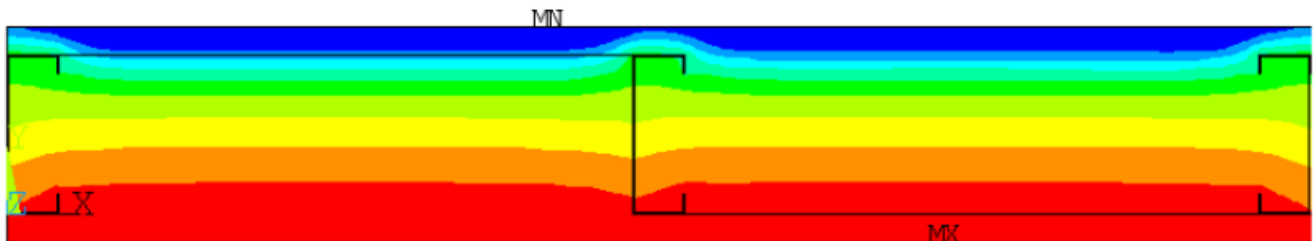


Unexposed curves

Ansys Fire Resistance(min)

Avg : 300

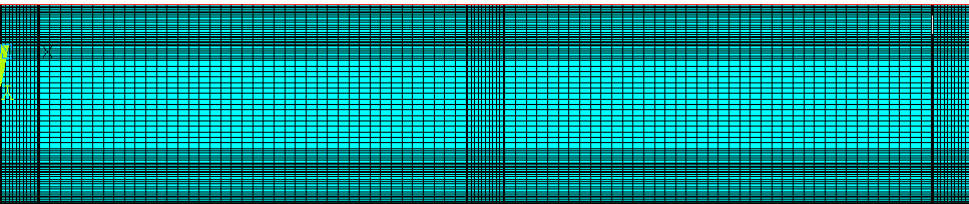
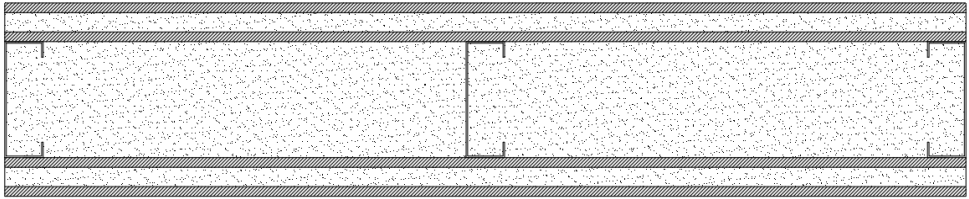
Max : 244



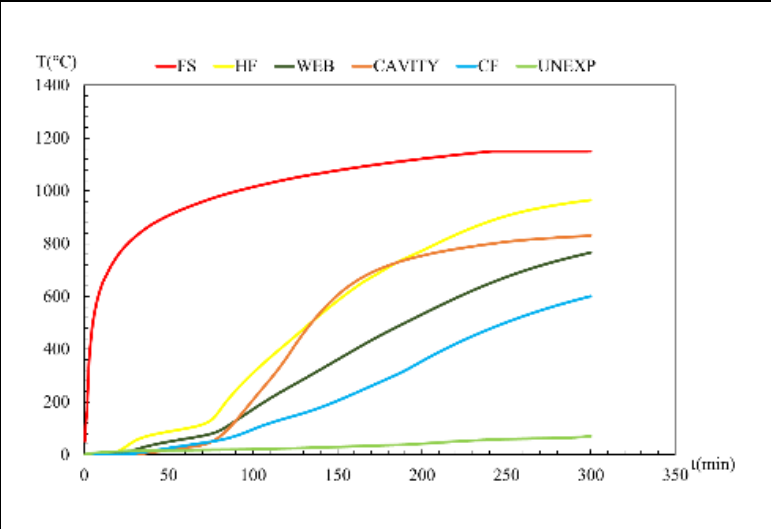
Ansys result in t= 240 min



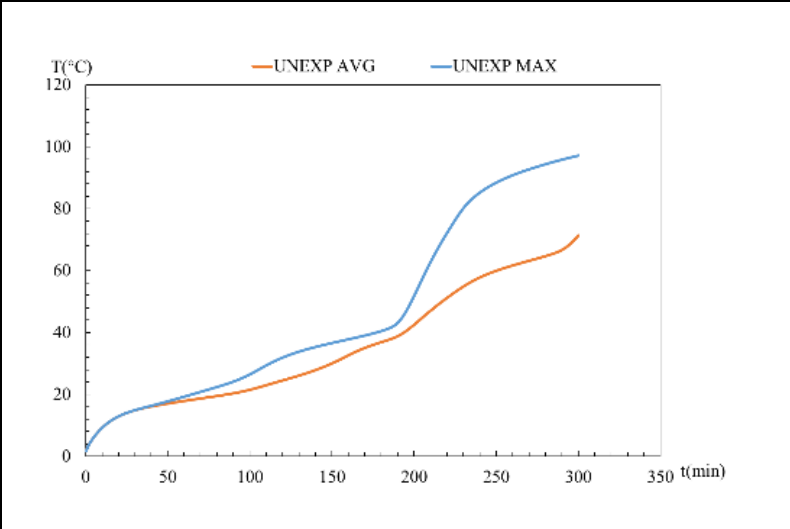
Specimen n°	Steel Section	Spacing between the studs (mm)	N° Layers gyps	Cavity insulation
33	C150x50x20x2.0	600	1Gypsum12.5 1Rockwool25 1Gypsum12.5	Rockwool



Mesh from Ansys

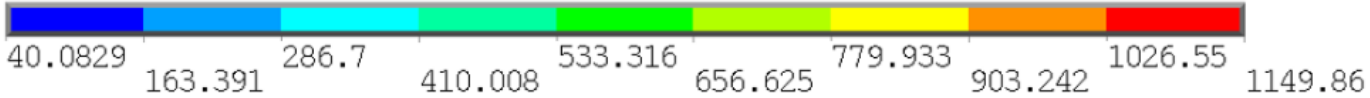
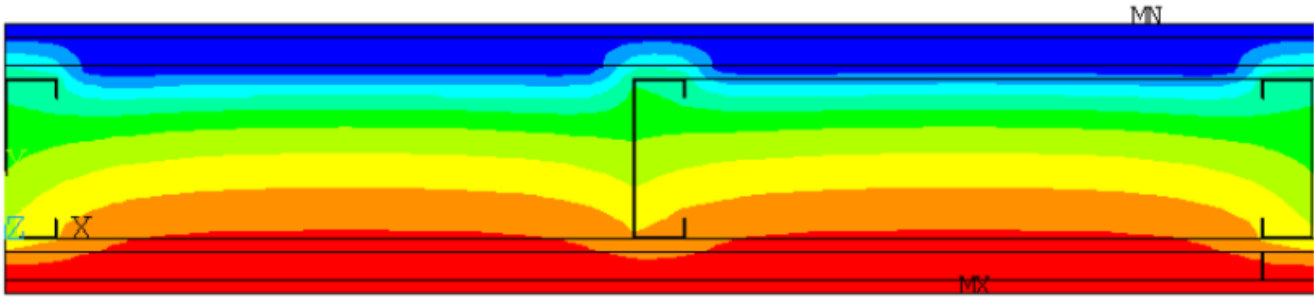


Average temperature results



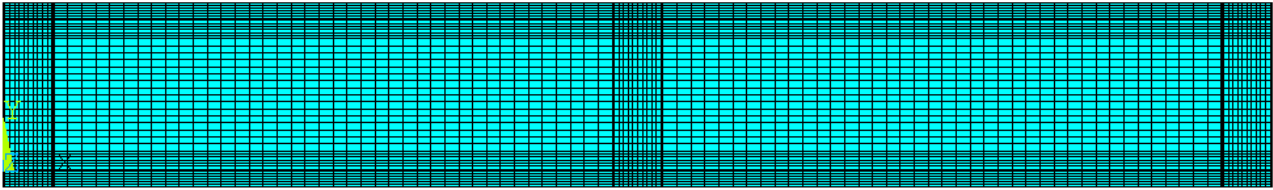
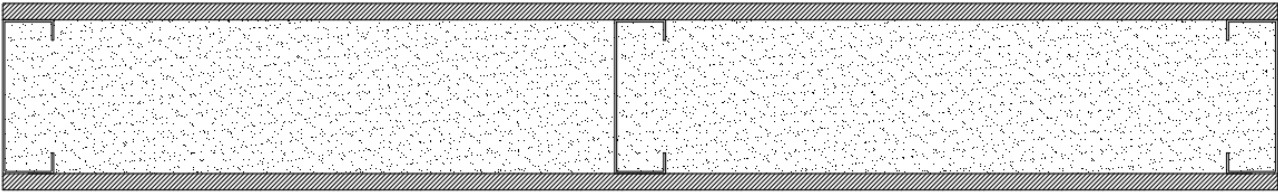
Unexposed curves

Ansys Fire Resistance(min)		
----------------------------	--	--

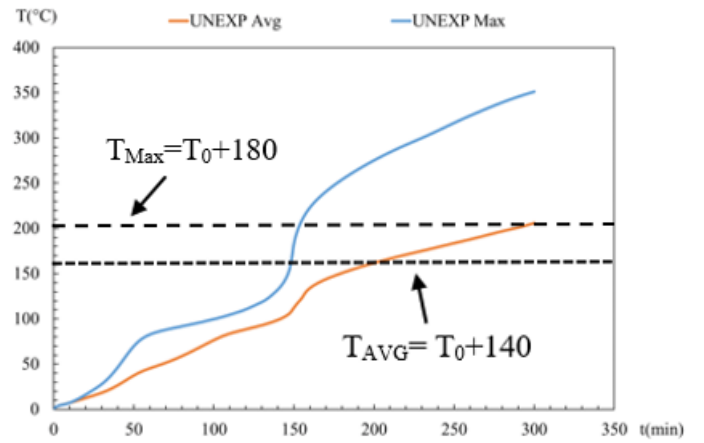
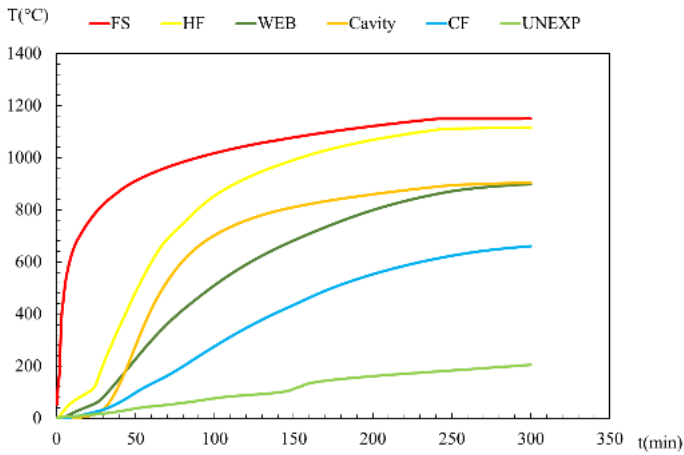


Ansys result in t= 240 min

Specimen n°	Steel Section	Spacing between the studs (mm)	N° Layers gyps	Cavity insulation
34	C150x50x20x2.0	600	1Gypsum16	Rockwool



Mesh from Ansys



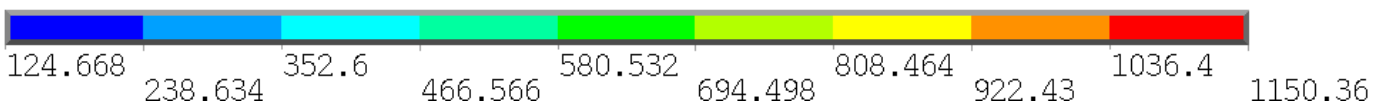
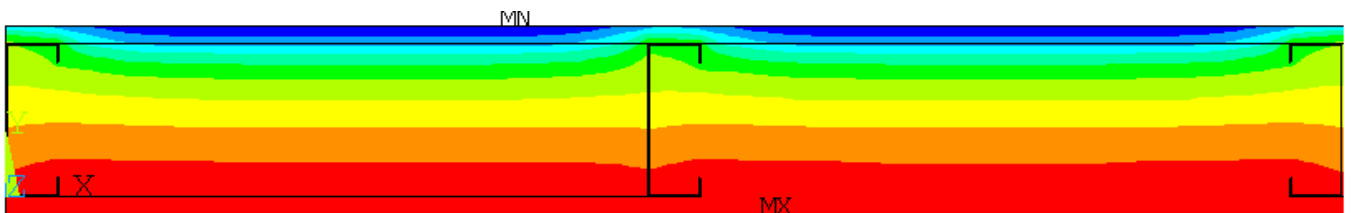
Average temperature results

Unexposed curves

Ansys Fire Resistance(min)

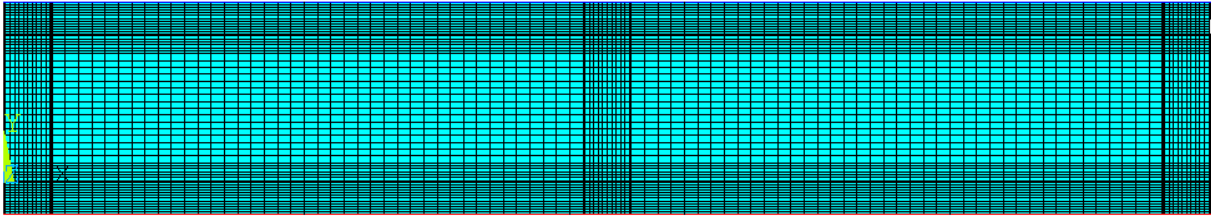
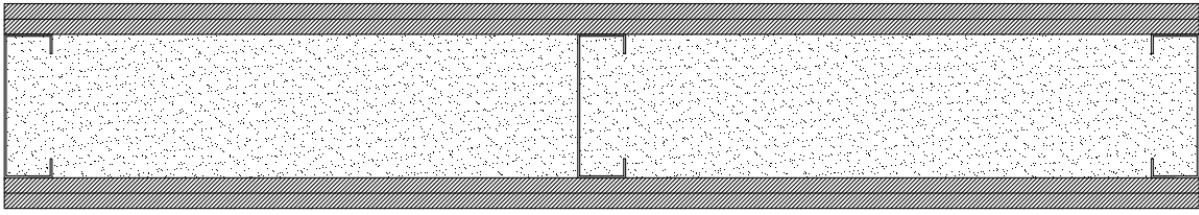
Avg : 197

Max : 153

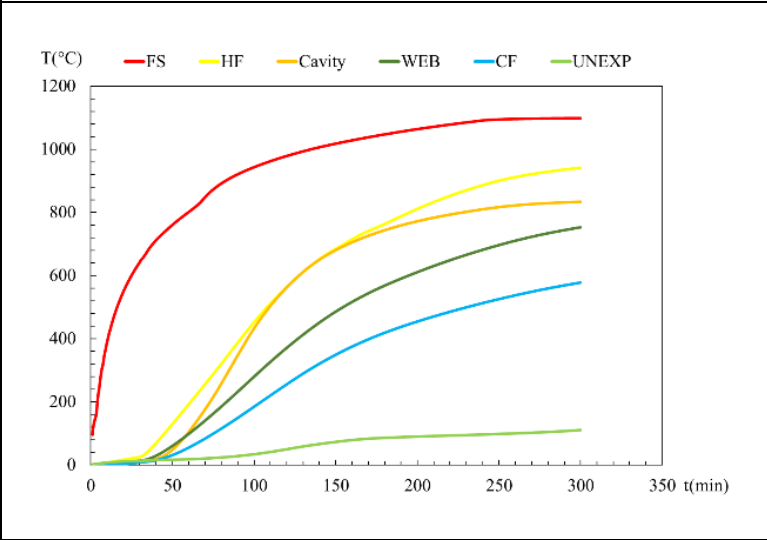


Ansys result in t= 300 min

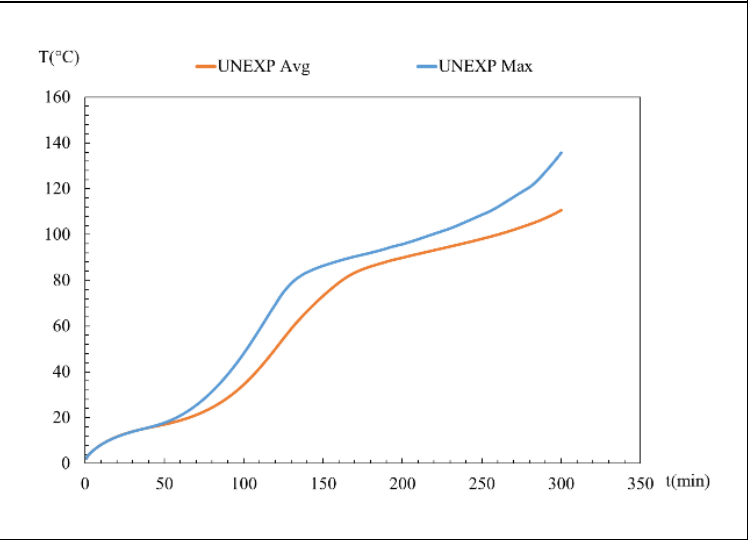
Specimen n°	Steel Section	Spacing between the studs (mm)	N° Layers gyps	Cavity insulation
35	C150x50x20x2.0	600	2Gypsum16	Rockwool



Mesh from Ansys

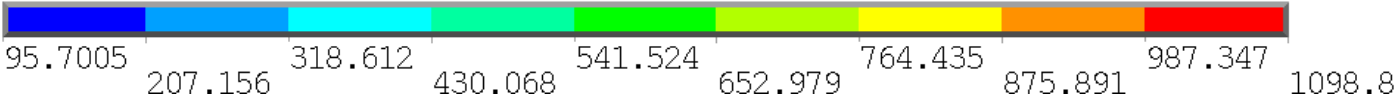
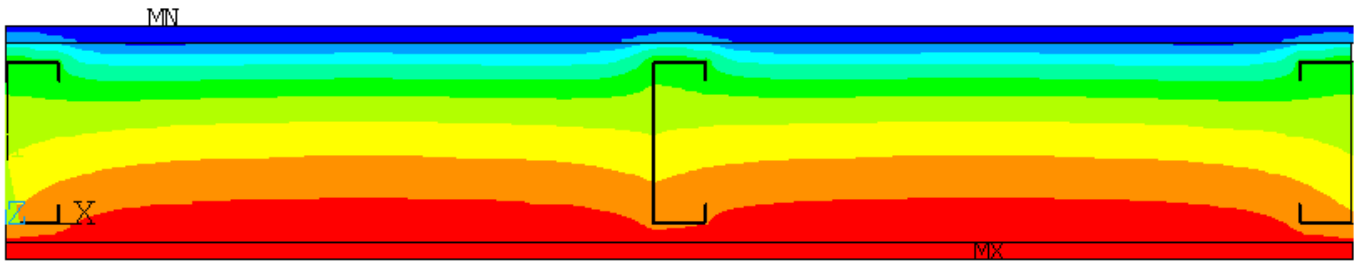


Average temperature results



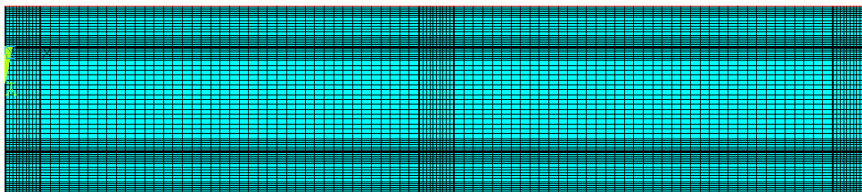
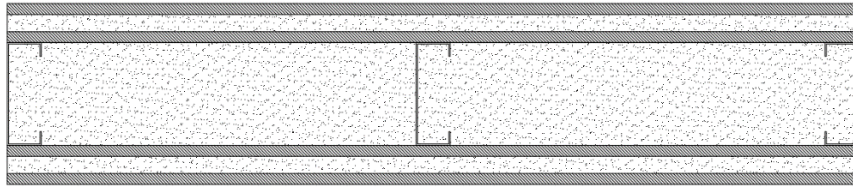
Unexposed curves

Ansys Fire Resistance(min)		
----------------------------	--	--

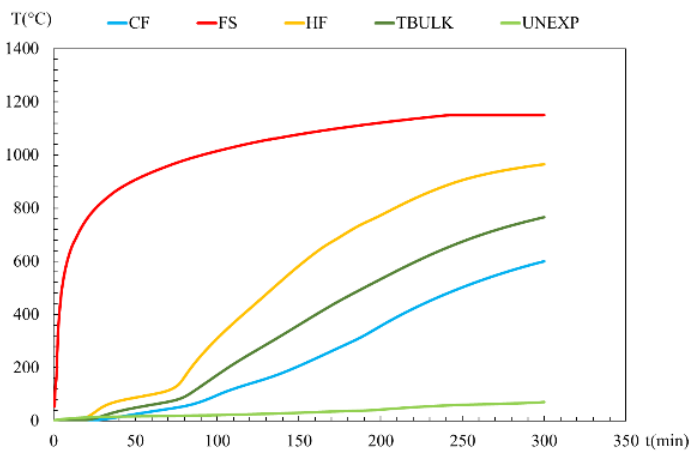


Ansys result in t= 300 min

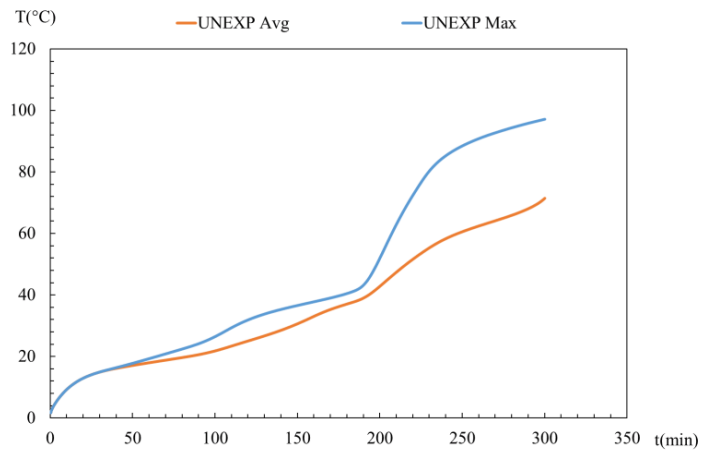
Specimen n°	Steel Section	Spacing between the studs (mm)	N° Layers gyps	Cavity insulation
36	C150x50x20x2.0	600	1Gypsum16 1Rockwool25 1Gypsum16	Rockwool



Mesh from Ansys

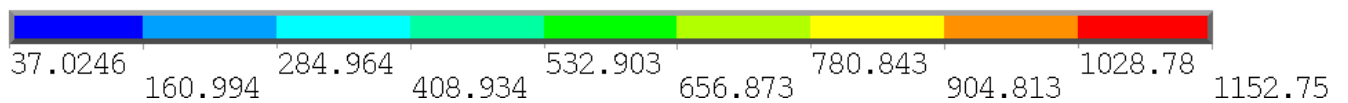
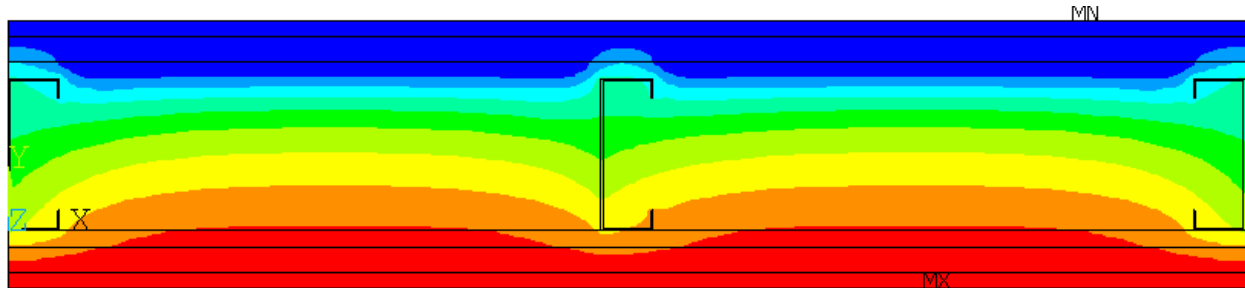


Average temperature results



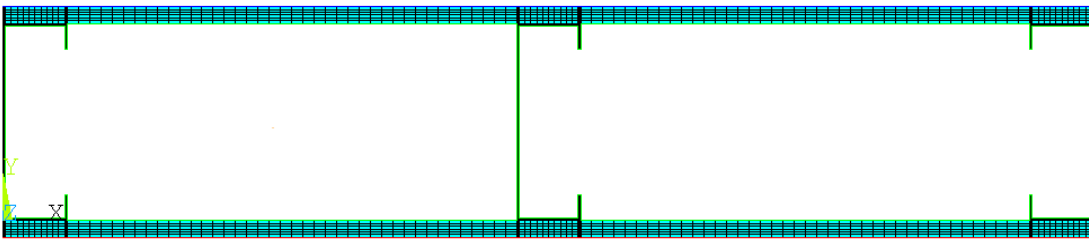
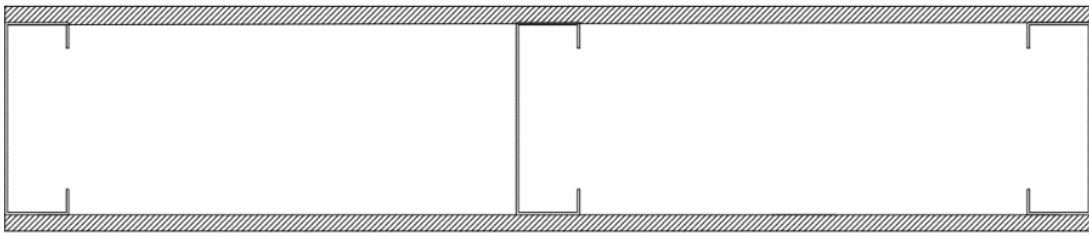
Unexposed curves

Ansys Fire Resistance(min)

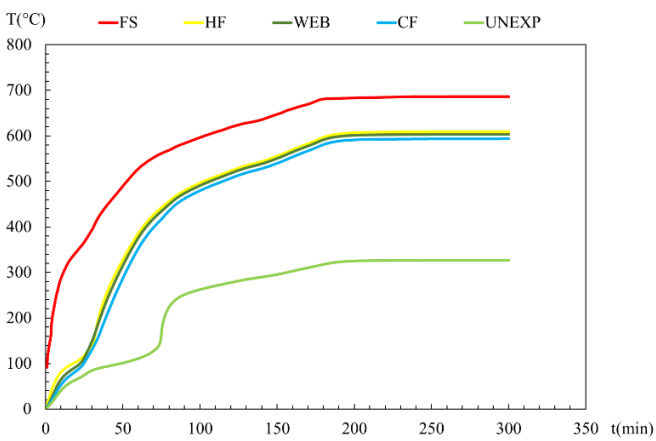


Ansys result in t= 240 min

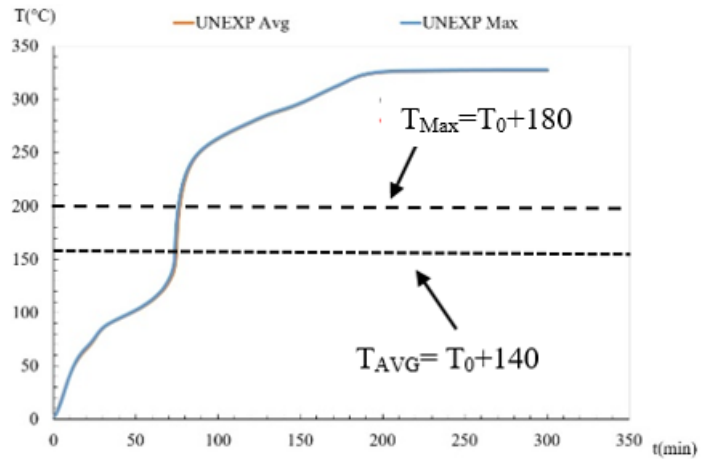
Specimen n°	Steel Section	Spacing between the studs (mm)	N° Layers gyps	Cavity insulation
37	C150x50x20x2.0	400	1Gypsum12.5	/



Mesh from Ansys



Average temperature results

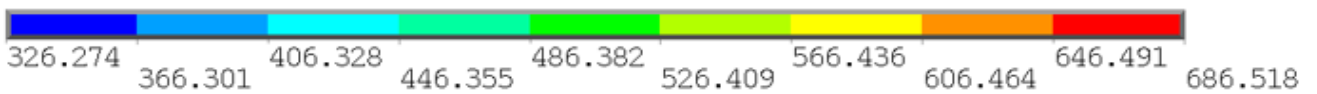
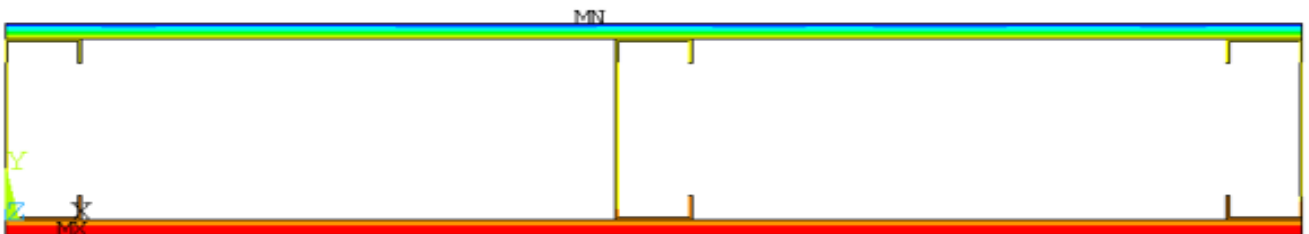


Unexposed curves

Ansys Fire Resistance(min)

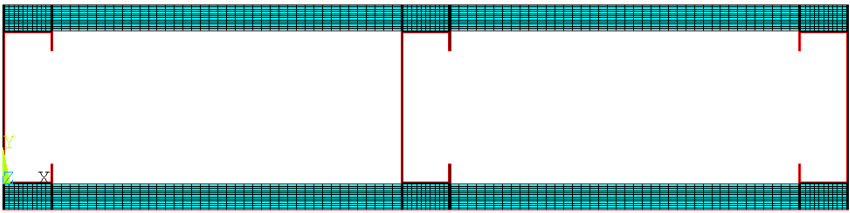
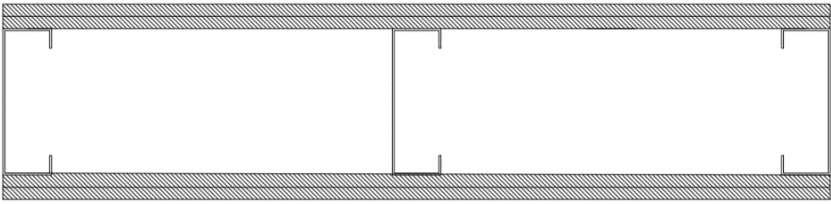
Avg : 75

Max : 76

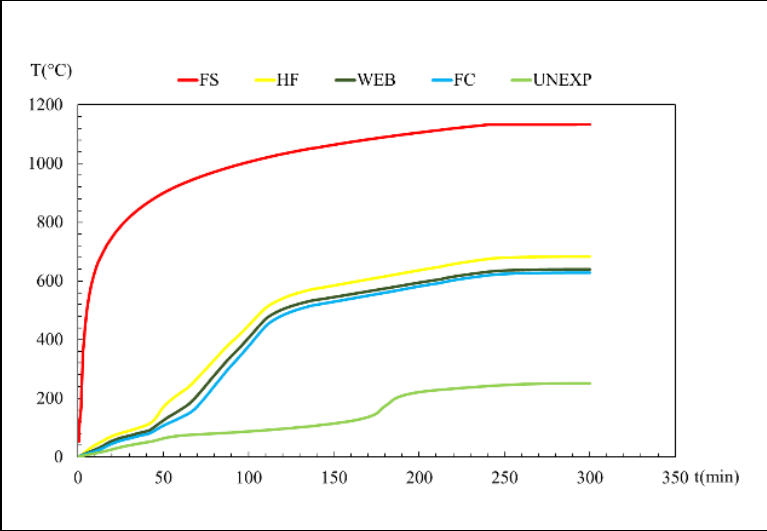


Ansys result in t= 300 min

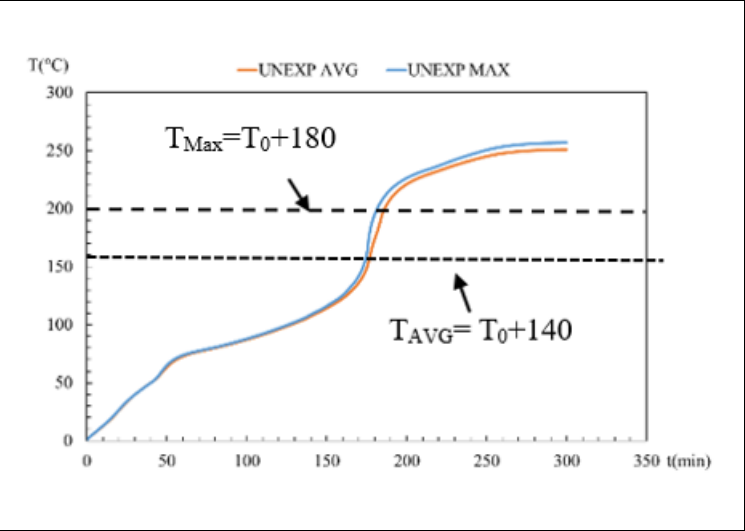
Specimen n°	Steel Section	Spacing between the studs (mm)	N° Layers gyps	Cavity insulation
38	C150x50x20x2.0	400	2Gypsum12.5	/



Mesh from Ansys

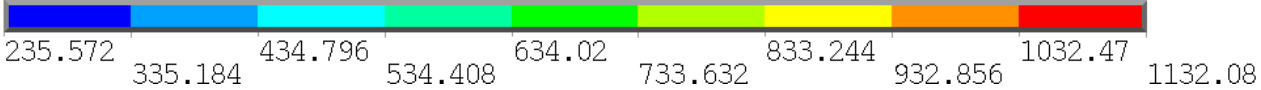
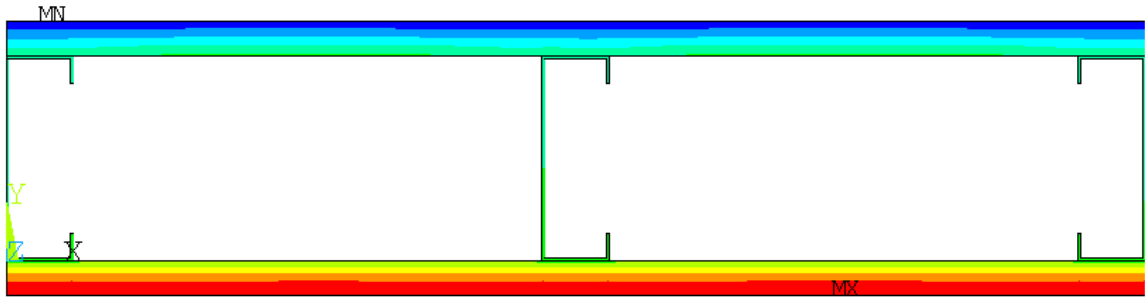


Average temperature results



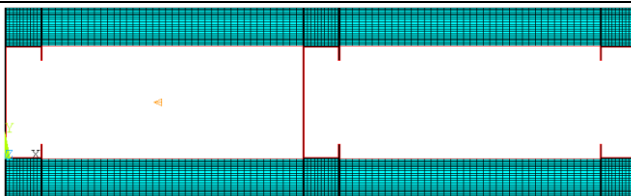
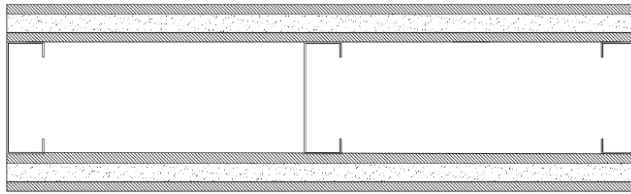
Unexposed curves

Ansys Fire Resistance(min)	Avg : 177	Max : 181
----------------------------	-----------	-----------

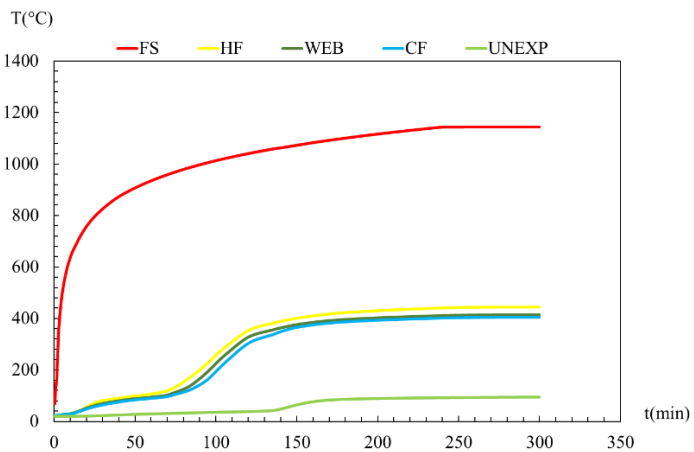


Ansys result in  $t = 240$

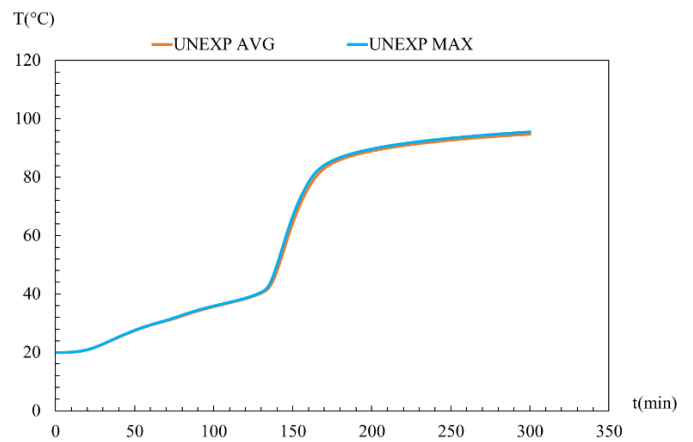
Specimen n°	Steel Section	Spacing between the studs (mm)	N° Layers gyps	Cavity insulation
39	C150x50x20x2.0	400	1Gypsum12.5 1Rockwool25 1Gypsum12.5	/



Mesh from Ansys

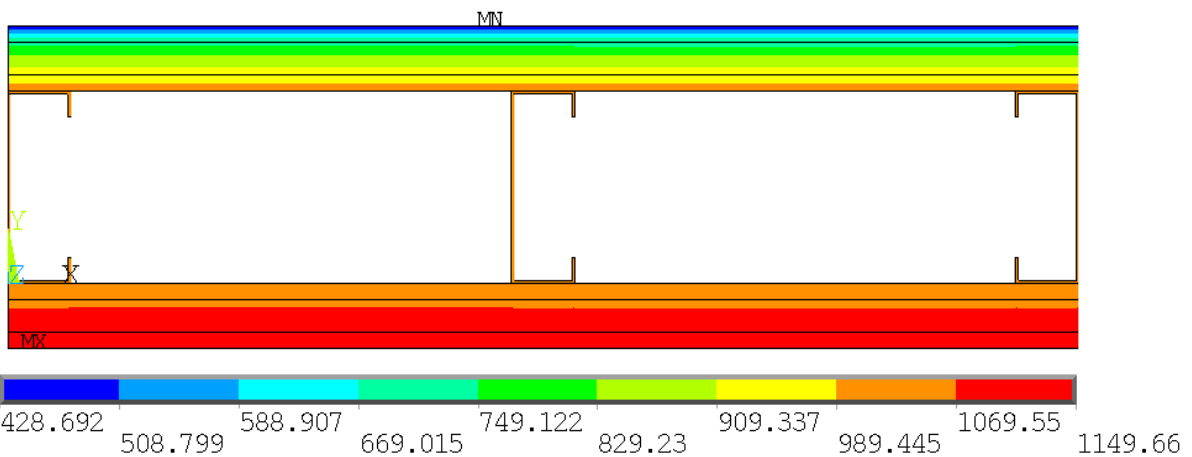


Average temperature results



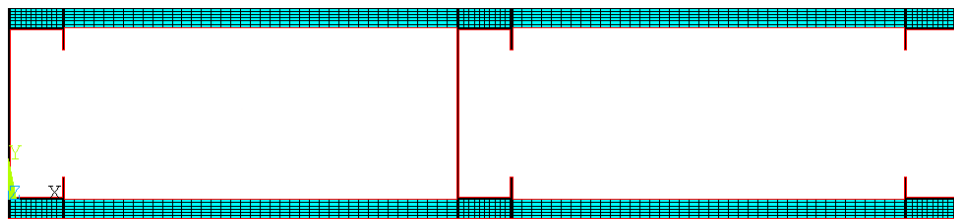
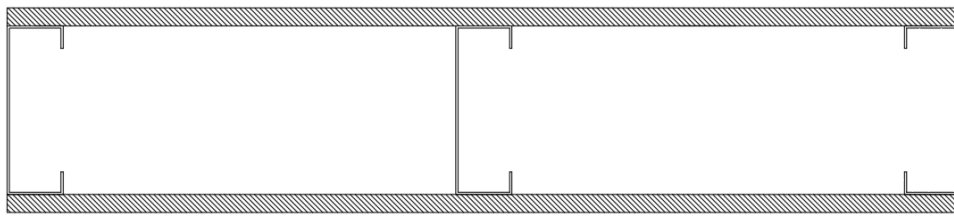
Unexposed curves

Ansys Fire Resistance(min)

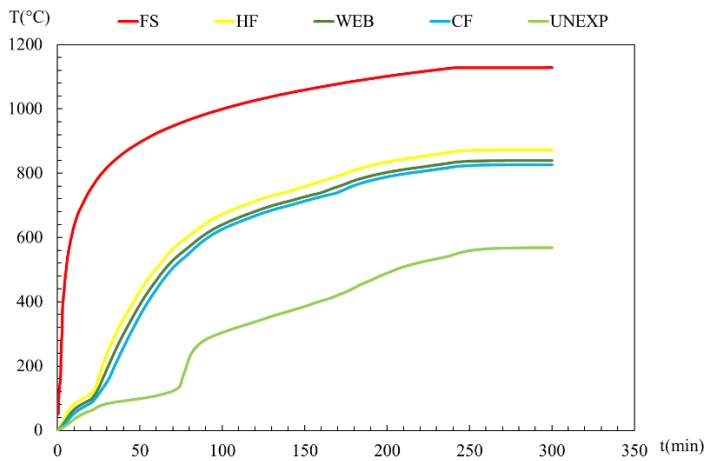


Ansys result in t= 300 min

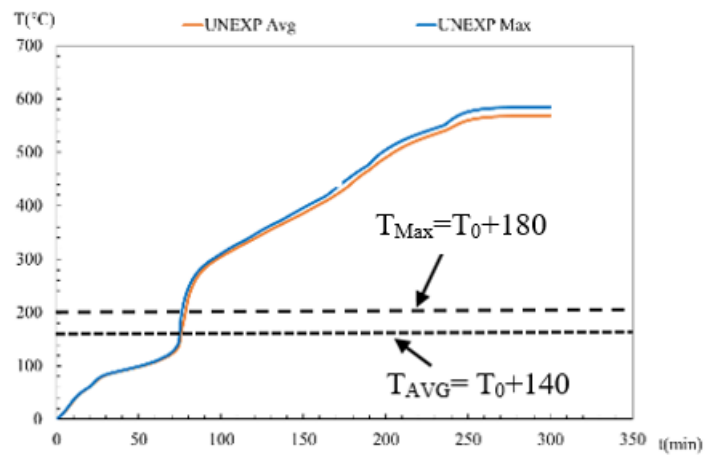
Specimen n°	Steel Section	Spacing between the studs (mm)	N° Layers gyps	Cavity insulation
40	C150x50x20x2.0	400	1Gypsum16	/



Mesh from Ansys



Average temperature results

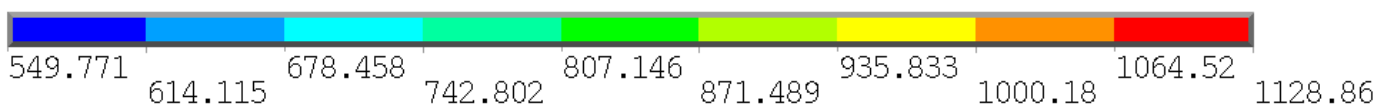
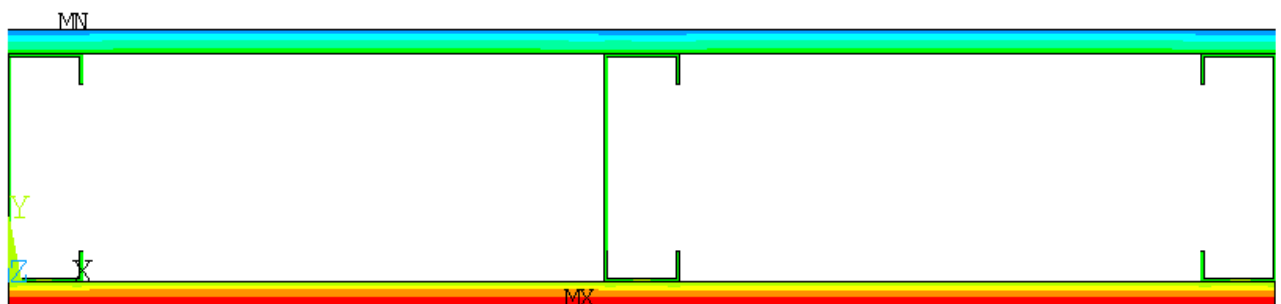


Unexposed curves

Ansys Fire Resistance(min)

Avg : 74

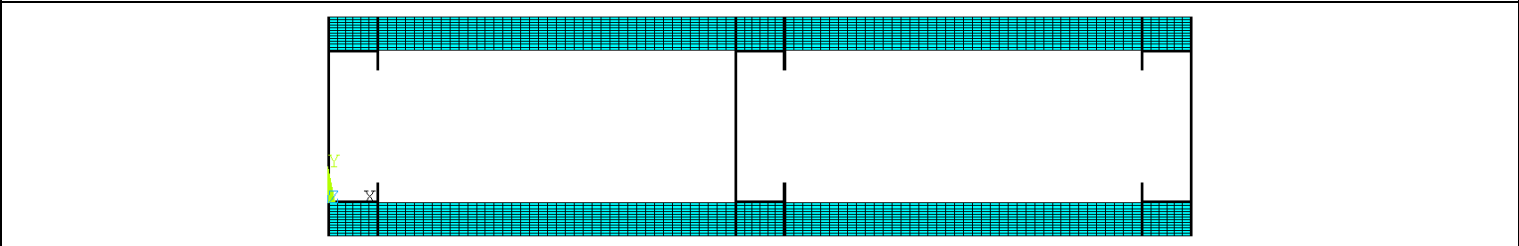
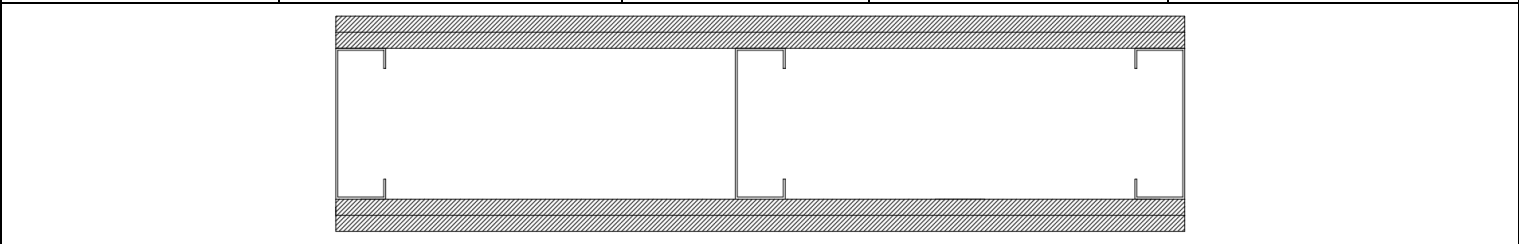
Max : 75



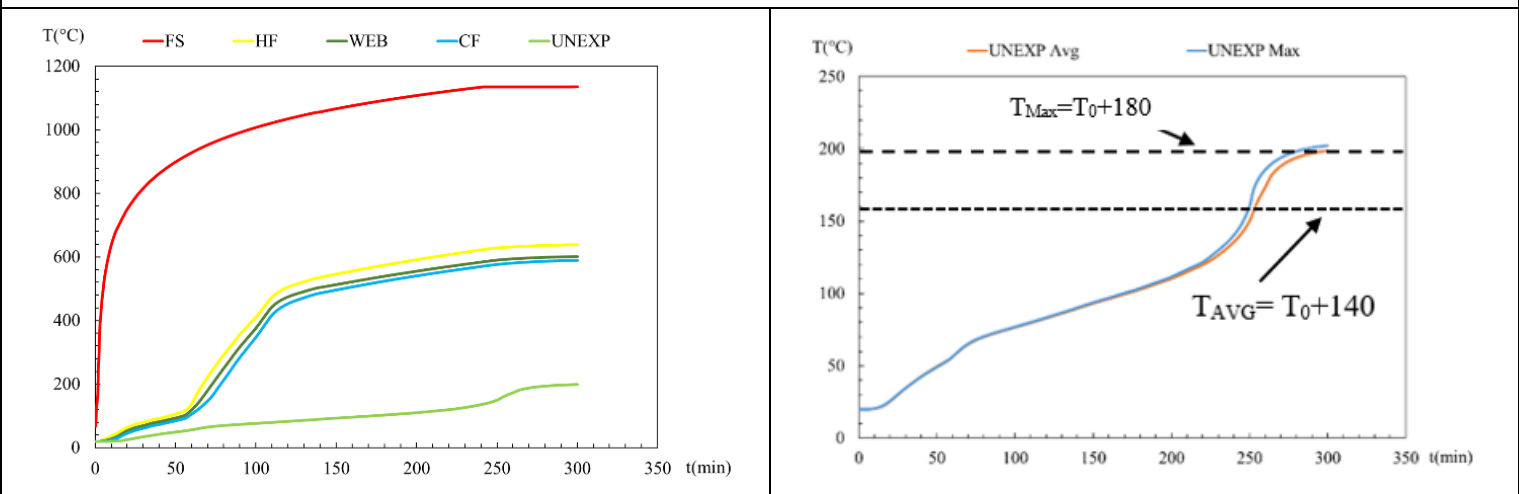
Ansys result in t= 300 min



Specimen n°	Steel Section	Spacing between the studs (mm)	N° Layers gyps	Cavity insulation
41	C150x50x20x2.0	400	2Gypsum16	/



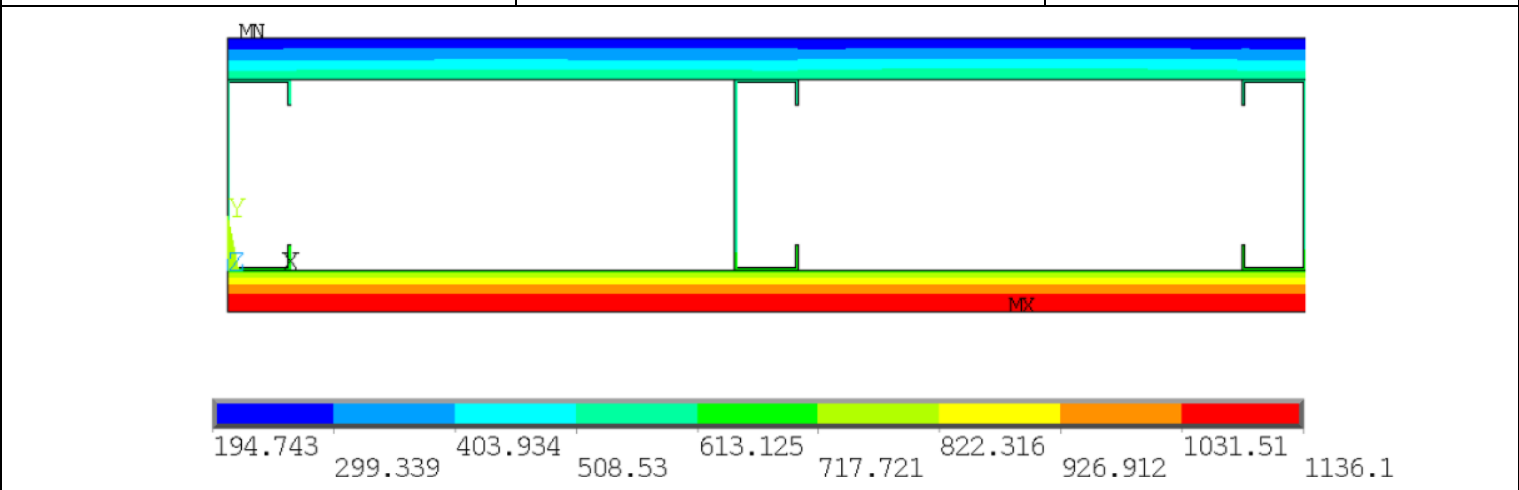
Mesh from Ansys



Average temperature results

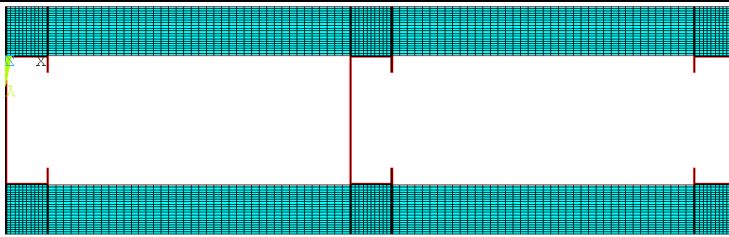
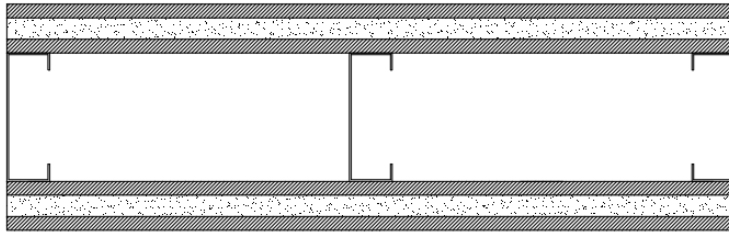
Unexposed curves

Ansys Fire Resistance(min)	Avg :254	Max :287
----------------------------	----------	----------

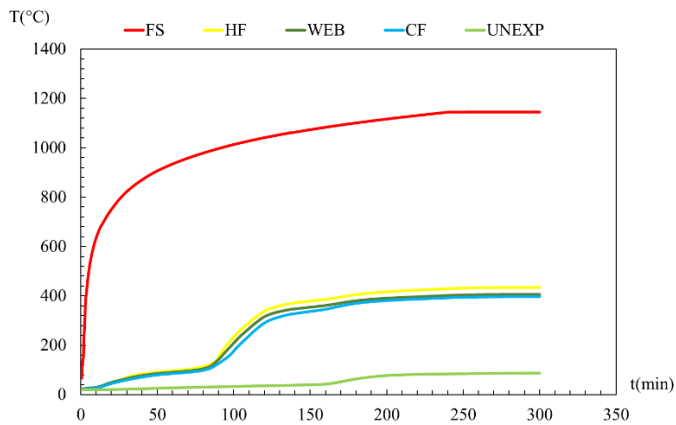


Ansys result in t= 240 min

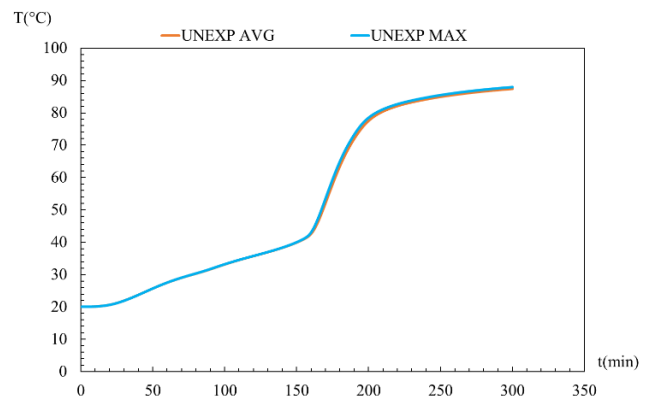
Specimen n°	Steel Section	Spacing between the studs (mm)	N° Layers gyps	Cavity insulation
42	C150x50x20x2.0	400	1Gypsum16 1Rockwool25 1Gypsum16	/



Mesh from Ansys

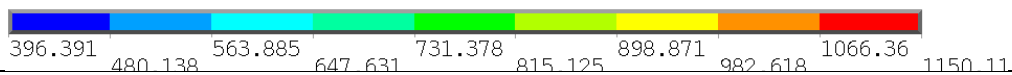
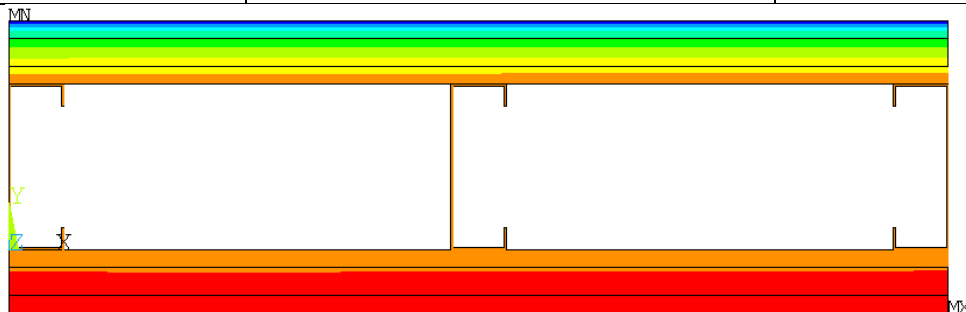


Average temperature results



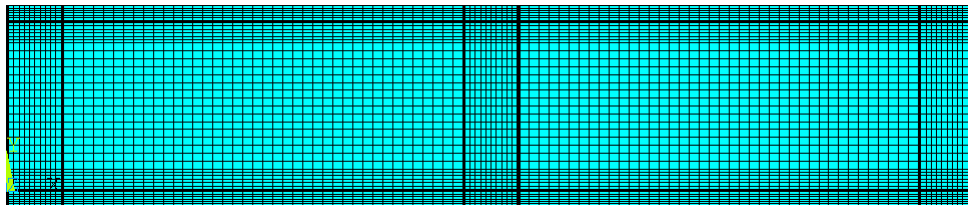
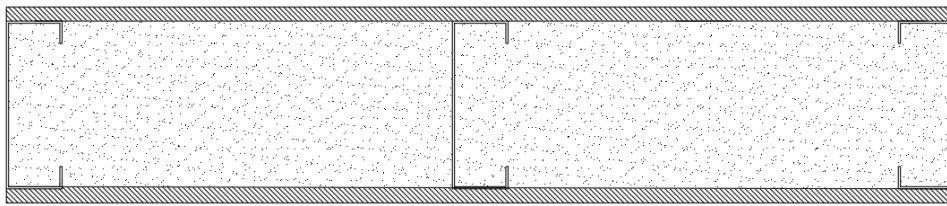
Unexposed curves

Ansys Fire Resistance(min)

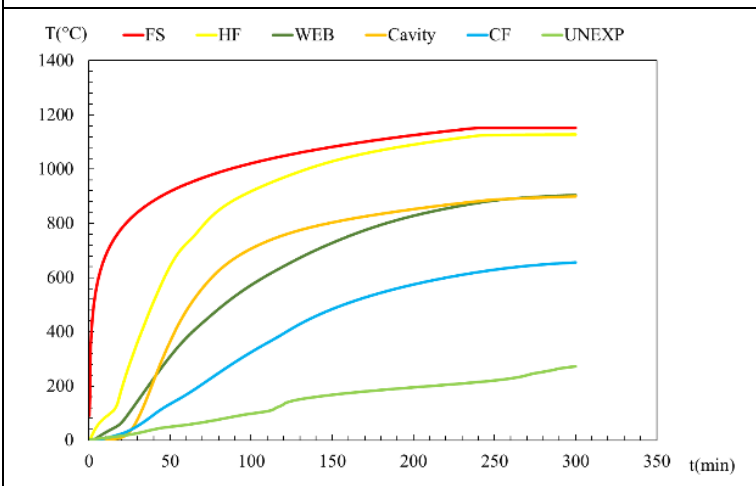


Ansys result in t= 300 min

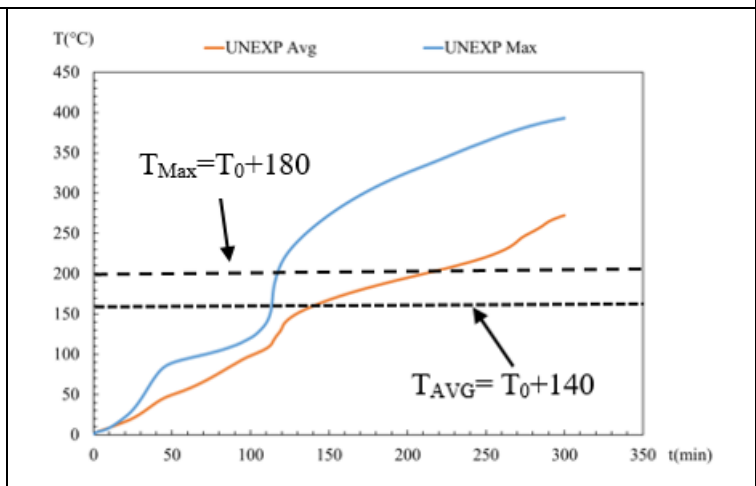
Specimen n°	Steel Section	Spacing between the studs (mm)	N° Layers gyps	Cavity insulation
43	C150x50x20x2.0	400	1Gypsum12.5	Rockwool



Mesh from Ansys

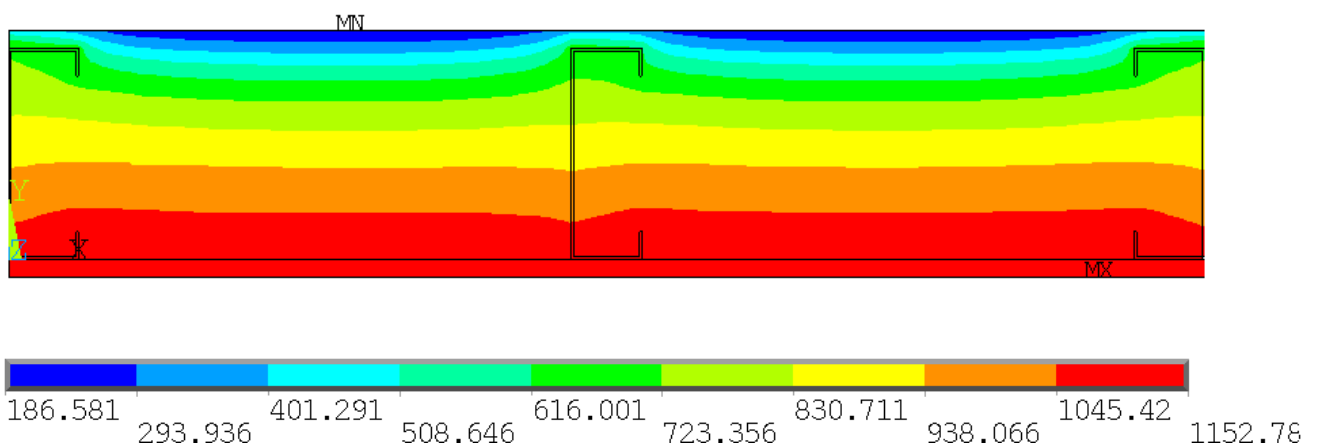


Average temperature results



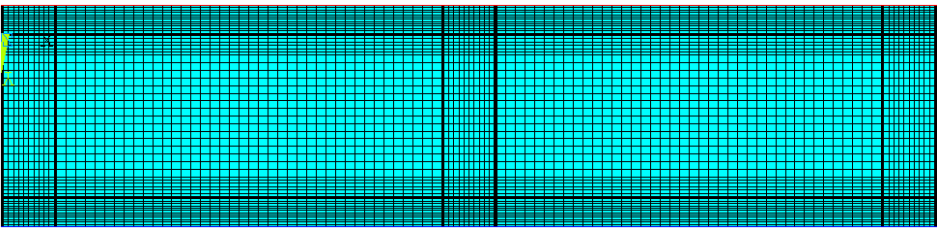
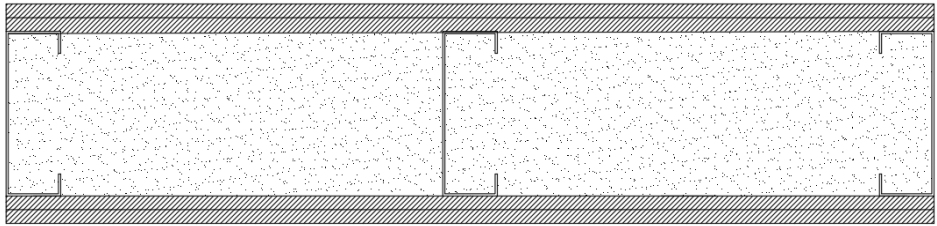
Unexposed curves

Ansys Fire Resistance(min)	Avg :139	Max :117
----------------------------	----------	----------

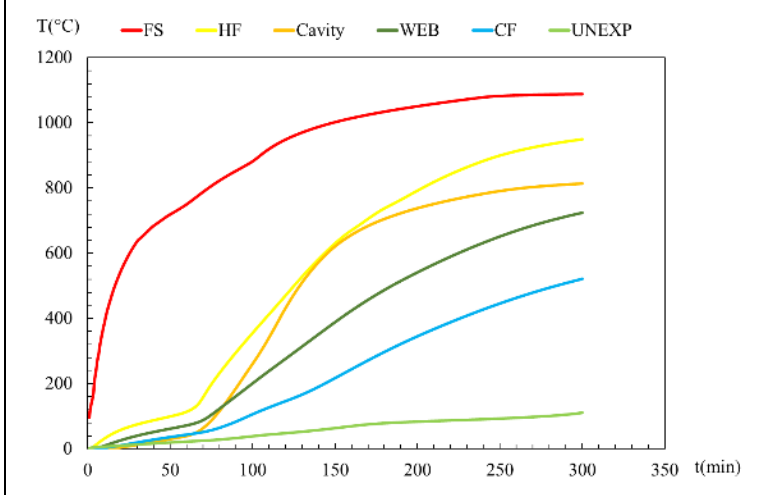


Ansys result in t= 300 min

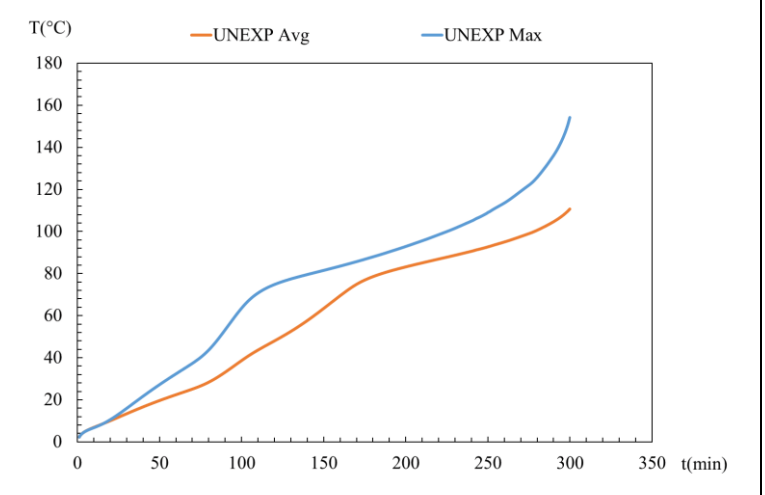
Specimen n°	Steel Section	Spacing between the studs (mm)	N° Layers gyps	Cavity insulation
44	C150x50x20x2.0	400	2Gypsum12.5	Rockwool



Mesh from Ansys

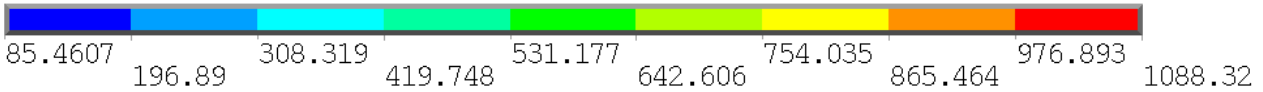
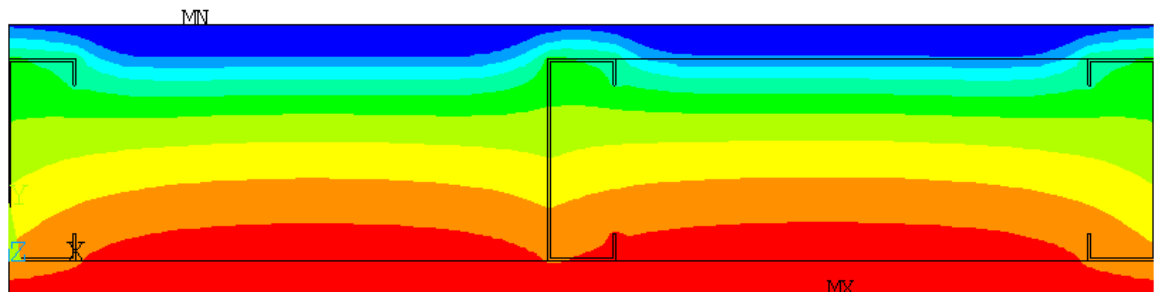


Average temperature results



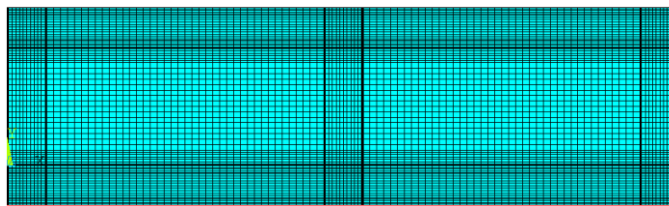
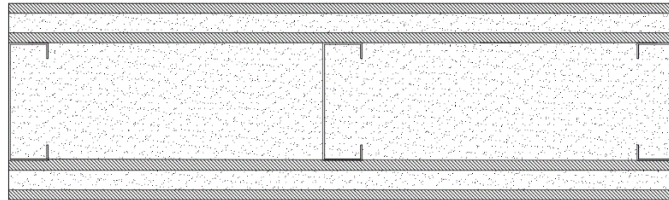
Unexposed curves

Ansys Fire Resistance(min)

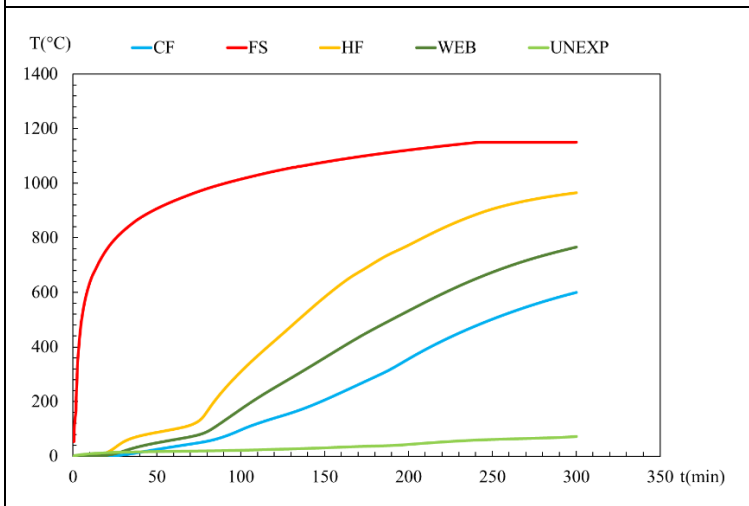


Ansys result in t= 300 min

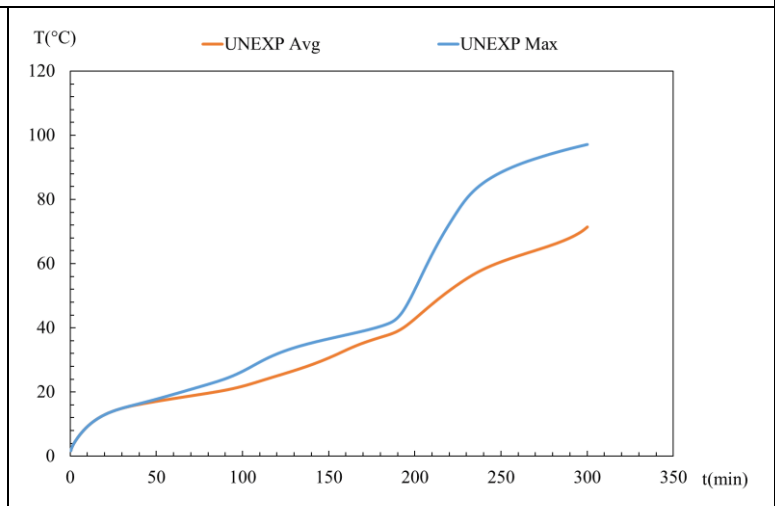
Specimen n°	Steel Section	Spacing between the studs (mm)	N° Layers gyps	Cavity insulation
45	C150x50x20x2.0	400	1Gypsum12.5 1Rockwool25 1Gypsum12.5	Rockwool



Mesh from Ansys

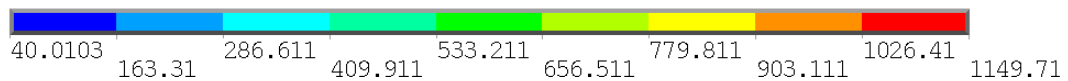
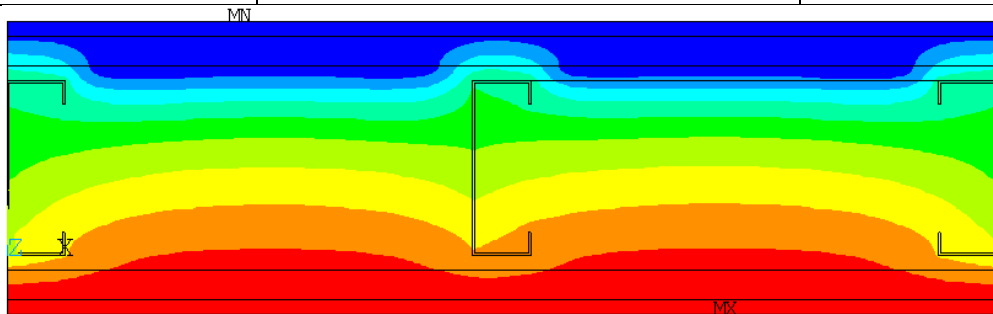


Average temperature results



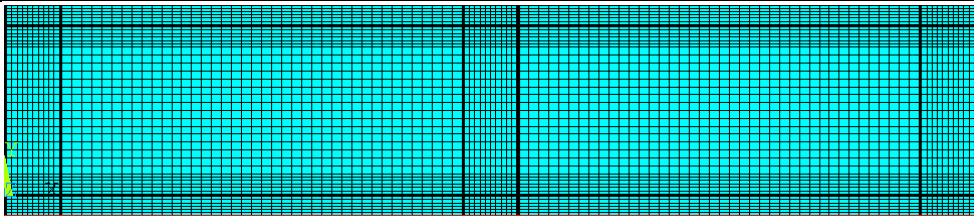
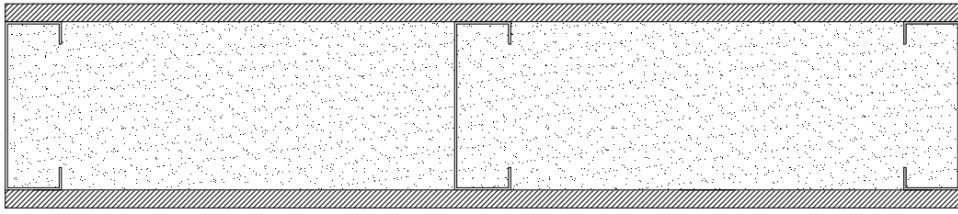
Unexposed curves

Ansys Fire Resistance(min)

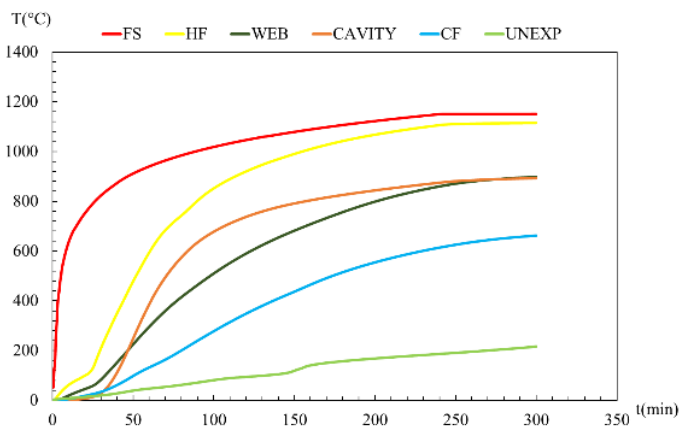


Ansys result in t= 240 min

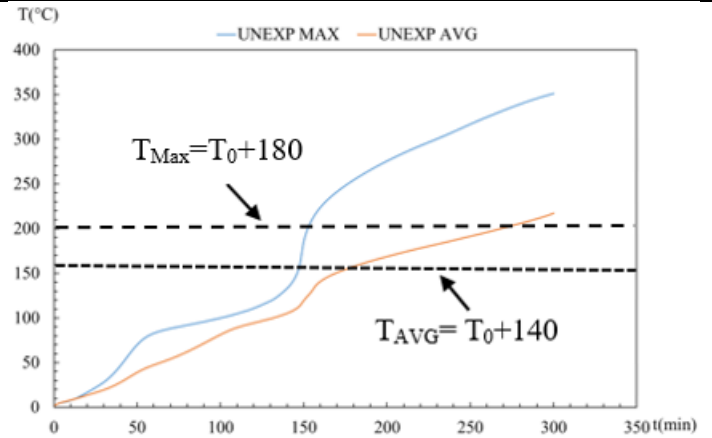
Specimen n°	Steel Section	Spacing between the studs (mm)	N° Layers gyps	Cavity insulation
46	C150x50x20x2.0	400	1Gypsum16	Rockwool



Mesh from Ansys



Average temperature results

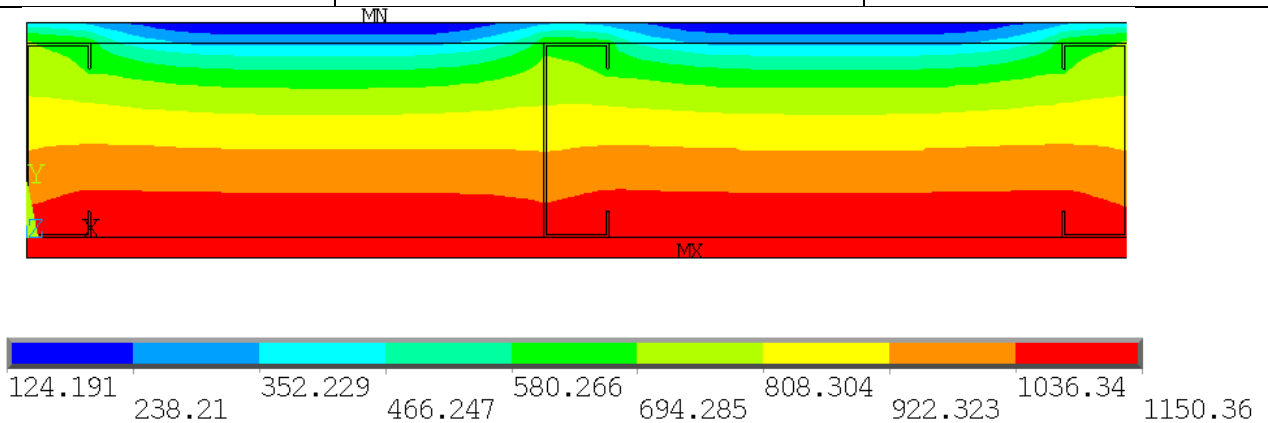


Unexposed curves

Ansys Fire Resistance(min)

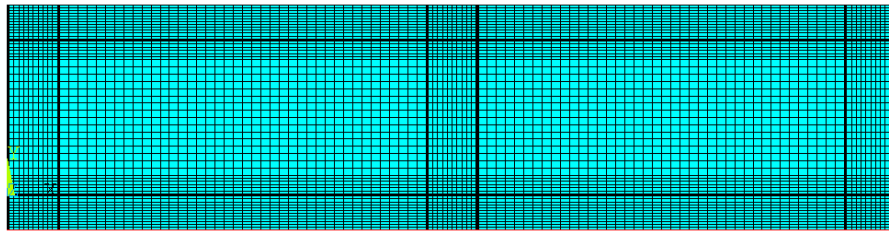
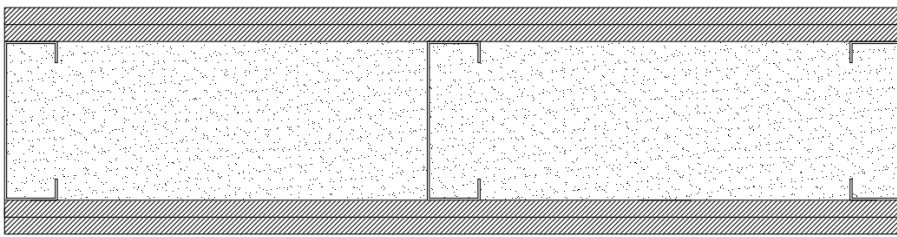
Avg : 178

Max : 153

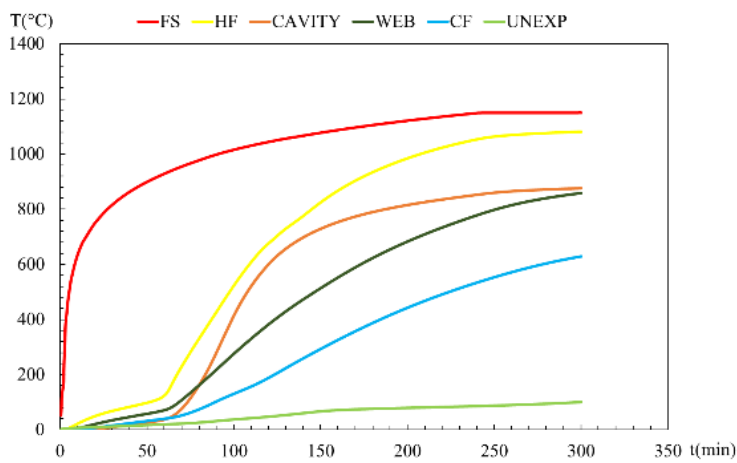


Ansys result in t= 300 min

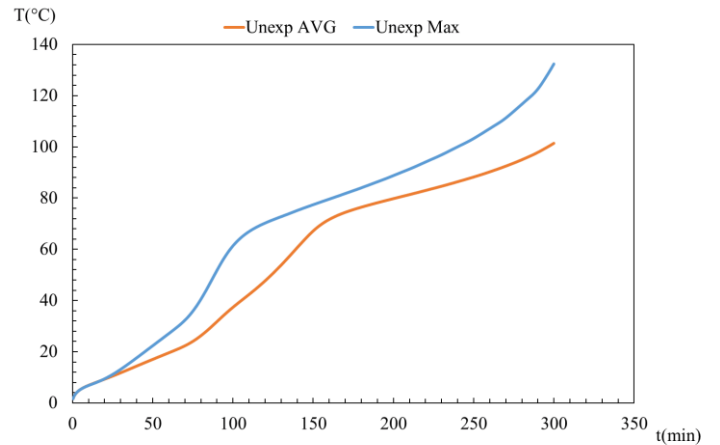
Specimen n°	Steel Section	Spacing between the studs (mm)	N° Layers gyps	Cavity insulation
47	C150x50x20x2.0	400	2Gypsum16	Rockwool



Mesh from Ansys

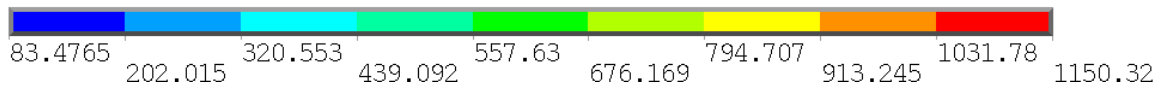
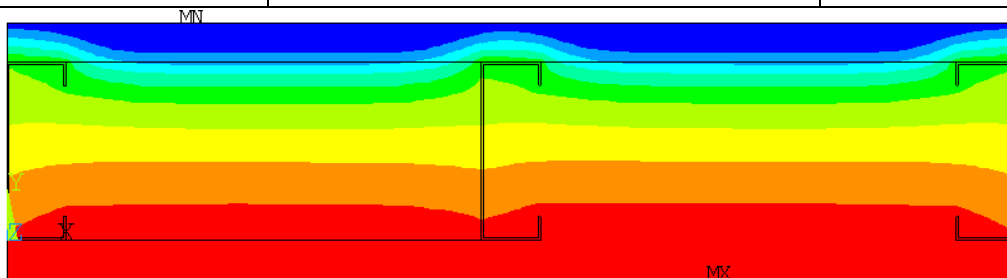


Average temperature results



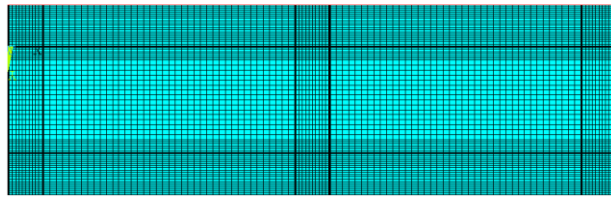
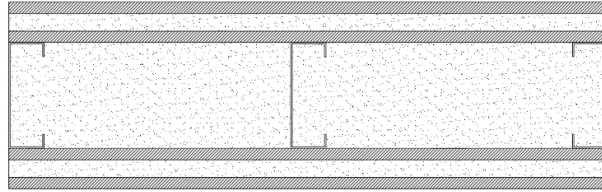
Unexposed curves

Ansys Fire Resistance(min)

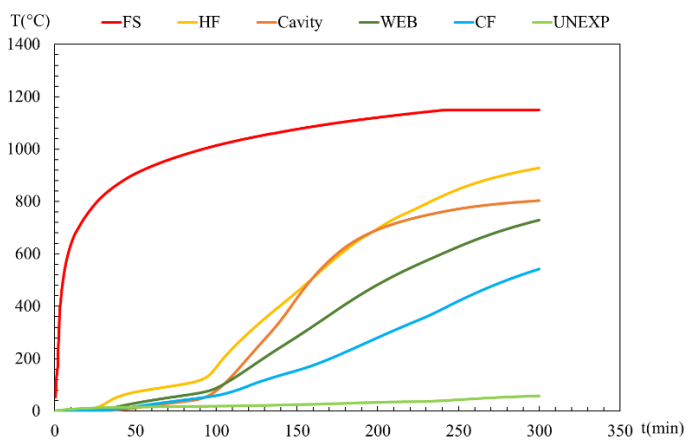


Ansys result in t= 300 min

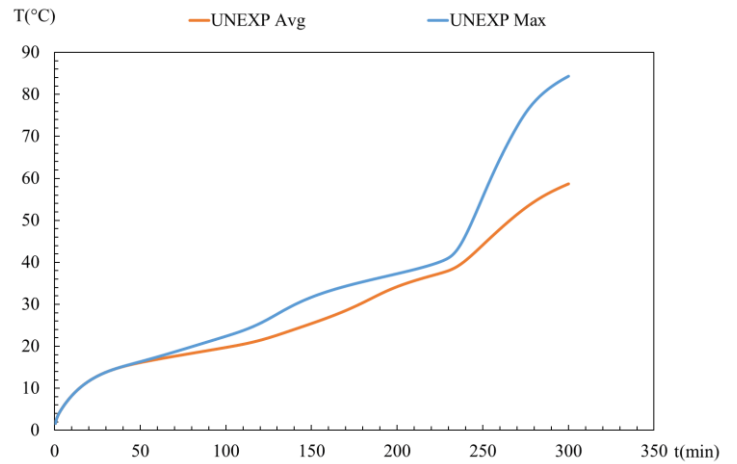
Specimen n°	Steel Section	Spacing between the studs (mm)	N° Layers gyps	Cavity insulation
48	C150x50x20x2.0	400	1Gypsum16 1Rockwool25 1Gypsum16	Rockwool



Mesh from Ansys

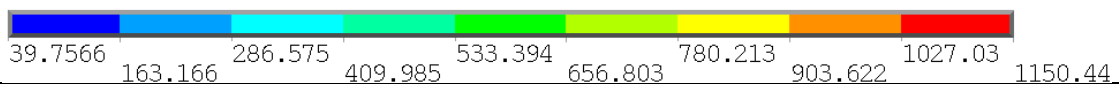
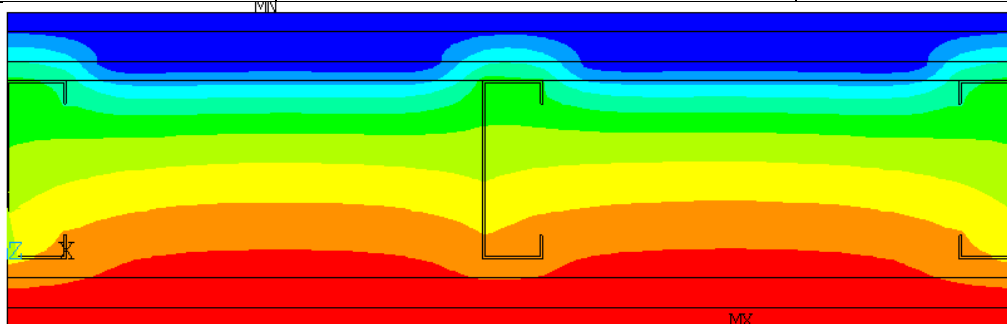


Average temperature results



Unexposed curves

Ansys Fire Resistance(min)



Ansys result in t= 300 min